Scuola Superiore Sant'Anna
di Studi Universitari e di Perfezionamento

ON THE DEVELOPMENT OF A CYBERNETIC PROSTHETIC HAND

by
Massimiliano Zecca

SUBMITTED IN PARTIAL FULFILLMENT OF THE
REQUIREMENTS FOR THE DEGREE OF
DOCTOR OF PHILOSOPHY

SCUOLA SUPERIORE SANT'ANNA
SETTORE DI INGEGNERIA

Date: **March 2003**

The undersigned hereby certify that they have read and recommend to the Classe di Scienze Sperimentali for acceptance a thesis entitled "**On the development of a cybernetic prosthetic hand**" by **Massimiliano Zecca** in partial fulfillment of the requirements for the degree of **Doctor of Philosophy**.

Committee in charge:

Prof. Paolo Dario

Prof. Angelo M. Sabatini

Prof. Maria Chiara Carrozza

SCUOLA SUPERIORE SANT'ANNA

Date: **March 2003**

Author: **Massimiliano Zecca**

Title: **On the development of a cybernetic prosthetic hand**

Dept.: **Settore di Ingegneria**

Degree: **Ph.D.**

Signature of Author

to my sister, Valentina

Contents

List of Figures

List of Tables

Abstract

The human hand is the end organ of the upper limb, which in humans serves the important function of prehension, as well as being an important organ for sensation and communication. It is a marvelous example of how a complex mechanism can be implemented, capable of realizing very complex and useful tasks using a very effective combination of mechanisms, sensing, actuation and control functions.

In this thesis, the road towards the realization of a cybernetic hand has been presented. After a detailed analysis of the model, the human hand, a deep review of the state of the art of artificial hands has been carried out. In particular, the performance of prosthetic hands used in clinical practice has been compared with the research prototypes, both for prosthetic and for robotic applications. By following a biomechatronic approach, i.e. by comparing the characteristics of these hands with the natural model, the human hand, the limitations of current artificial devices will be put in evidence, thus outlining the design goals for a new cybernetic device.

Three hand prototypes with a high number of degrees of freedom have been realized and tested: the first one uses microactuators embedded inside the structure of the fingers, and the second and third prototypes exploit the concept of microactuation in order to increase the dexterity of the hand while maintaining the semplicity for the control. In particular, a framework for the definition and realization of the closed-loop electromyografic control of these devices has been presented and implemented.

The results were quite promising, putting in evidence that, in the future, there could be two different approaches for the realization of artificial devices. On one side there could be the EMG-controlled hands, with compliant fingers but only one active degree of freedom. On the other side, more performing artificial hands could be directly interfaced with the peripheral nervous system, thus establishing a bi-directional communication with the human brain.

Acknowledgements

Like most things in life, a research project is made better by teamwork, and this thesis has come to the and thanks to the support of many people. I'm happily in their debt.

First of all, I want to thank my supervisors, Prof. Paolo Dario, Prof. Angelo M. Sabatini, and Prof. M. Chiara Carrozza for taking care of my scientific growth during these years. Without their patient guidance and their helpful suggestions this thesis would not have been even possible. I would also acknowledge Mr. Rinaldo Sacchetti for many helpful discussions and criticism based on his deep experience in the clinical application of hand prostheses.

I would like to thank all the persons I'm working or I worked with. In particular, I would like to thank Roberto for his valuable support in the realization and in the debugging of the electronic boards. Thanks to Fabrizio, Stefano, Bruno, and also to Luca, Giovanni, Francesco, Carlo, and Pierpaolo: I could not have been here without their support.

My gratitude also goes to Silvestro, an infinite and precious source of suggestions, ideas, and criticisms. He is a wonderful colleague, but also a wonderful friend. I am also grateful to all friends and colleagues at ARTS lab, Crim lab, and INAIL RTR Center, Giovanna, Lisa, Sara, Oliver, Carlo, and many many others, for all the time we spent together.

I should also thank several friends for the direct and indirect support they gave me in these years. The complete list would be too long, but a special thank should be given to Francesca and my master Stefano.

Last but not least, I would like to say thank you to my parents, for the understanding and help they have given me many times during these years.

One

Introduction

The human hand is the end organ of the upper limb, which in humans serves the important function of prehension, as well as being an important organ for sensation and communication. It is a marvelous example of how a complex mechanism can be implemented, capable of realizing very complex and useful tasks using a very effective combination of mechanisms, sensing, actuation and control functions [41, 43, 86].

In this thesis, the road towards the realization of a cybernetic hand will be presented. After a detailed analysis of the model, the human hand, in Chapter 2, a deep review of the state of the art of artificial hands will be carried out (Chapter 3). In particular, the performance of prosthetic hands used in clinical practice (§3.3) will be compared with the research prototypes (§3.4), both for prosthetic and for robotic applications.

The limitations of the current artificial devices, aimed at the functional substitution of the human hand, could be overcome by pursuing a "biomechatronic" design approach:

1. analysis of the model (the human hand) - Chapter 2;
2. analysis of the state of the art of prosthetic hands in clinical applications - §3.3;
3. analysis of the state of the art of prosthetic hands in research - §3.4.1;
4. analysis of the state of the art of robotic hands in research - §3.4.2;
5. analysis of the state of the art of the control techniques for the artificial hands - §3.5;
6. identification of the drawbacks of current artificial hands - §4.1;
7. identification of the specifications for the realization and the control of a truly cybernetic prosthetic hand - §4.2.

By comparing the characteristics of these hands with the natural model, the human hand (Chapter 2), the limitations of current artificial devices will be put in evidence, thus outlining the design goals for a new cybernetic device.

Three hand prototypes with a high number of degrees of freedom will be realized and tested:

- RTR 1 hand (Chapter 5);
- RTR 2 hand (Chapter 6);
- SPRING hand (Chapter 7).

The first one uses microactuators embedded inside the structure of the fingers, and the second and third prototypes exploit the concept of microactuation in order to increase the dexterity of the hand while maintaining the semplicity for the control.

A framework for the definition and realization of the closed-loop electromyografic control of these devices will be presented (§4.3) and implemented (§5.4, §6.4, and §7.5).

The results of the tests will be commented separately, and the general conclusions will be presented in Chapter 8. Then, a possible road map for the development and realization of prosthetic devices in the future will be traced (§8.2).

Two

Our model: the human hand

> The whole is more than the sum of the parts.
>
> *Metaphysica*
> Aristotele

The hand is the end organ of the upper limb, which in humans serves the important function of prehension, as well as being an important organ for sensation and communication. Pentadactyl organs are common in nature but the human hand is remarkable in that it has a versatility that is arguably unrivaled. Even in our evolutionarily close relatives, the primates, hands tend to be more specialized for suspensory (i.e., gorilla) or locomotive (i.e., baboon) function. In contrast, our hands tend to be well suited to, or some suggest evolved due to, tool-making. Several anatomical features specific to our hands suggest this, for example, the shorter opposable thumb to produce large grip forces to make and hold tools, opposed by the greater mobility of metacarpals of the ring and little fingers; the pronounced deviation of the wrist that allows aligning a tool, or weapon, with the longitudinal shaft of the forearm; and the flatter, ridged thumb and finger pads to hold and manipulate small objects [43].

In this chapter a brief overview of the human hand will be presented, in terms of anatomy, sensorization and performance, in order to determine the characteristics requested to an artificial device that could substitute the lost limb.

2.1 Overview of the human hand

The hand is the organ of the human body that is most well adapted to prehensile function [43, 86]. The hand is composed of the palm and digits and is articulated to the forearm by the wrist (carpus). The palm is a flat surface that serves as the central support surface to the hand created by five long metacarpal bones radiating from the wrist like the spokes of a wheel with the capitate bone serving as the axle (Figure 2.2).

Figure 2.1: Albrecht Dürer (1471–1528), "Studie zu den Händen eines Apostels", (Die betenden Hände), paper, white gehöht, 290 x 197 cm (1506).

The digits are composed of long bones called phalanges arranged in series continuing each metacarpal ray. The first digit, called the thumb, is composed of two phalanges; it is the most mobile of the digits and can oppose to the palm and the tips of the other fingers when these are flexed. The remaining four digits each contain 3 phalanges and are called fingers. Axial rotation (pronation-supination) of the hand occurs as the more mobile the two long bones of the forearm (the radius) rotates about the other relatively fixed bone (the ulna). The length, distribution and mobility of the digits with respect to the palm give the hand the ability to perform a wide variety of prehensile tasks [18].

The hand owes its structure to bones, its mobility to joints, and its force generation to muscles. Specialized sensory neurons provide tactile and kinesthetic information.

2.1.1 Muscles and tendons

Muscles are composed of tissue that can actively contract under the influence of the brain and spinal cord (central nervous system, CNS) to produce hand and finger motion and forces by pulling on bones via tendons. Muscle tissue is composed of muscle fibers that

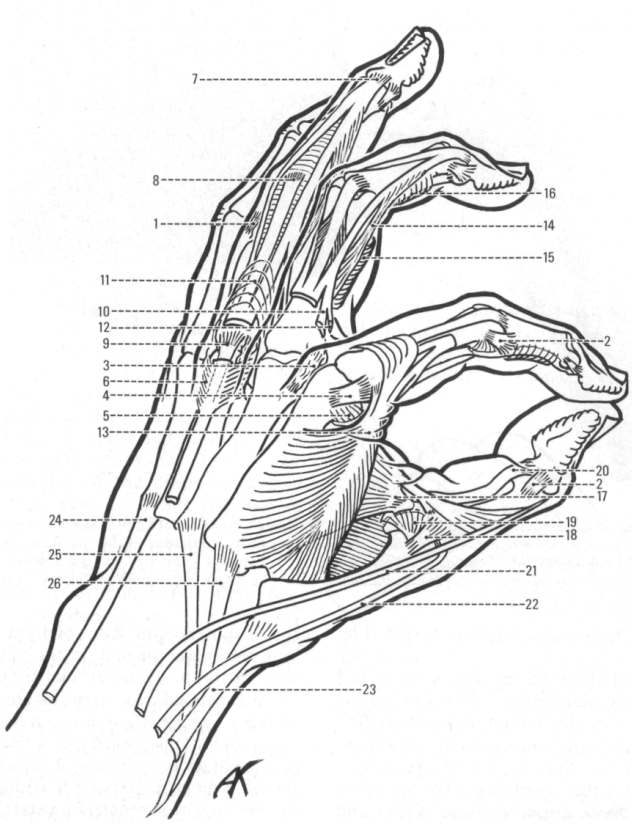

FIGURE 2.2: The hand with the skin removed. I: Collateral ligament (CL) of the proximal interphalangeal (PIP) joint slightly relaxed in complete extension; 2: CL of the PIP tightened in intermediate flexion; 3: CL of the metacarpophalangeal (MP) joint relaxed in extension; 4: CL of the MP tightened in flexion; 5: Accessory fibers of CL of the MP inserting on the volar plate; 6: Expansion of the common extensor on the interglenoid ligament (deep intermetacarpal); 7: Distal insertion of the extensor digitorum on P_3; 8, Insertion of the middle extensor tendon on P_2; 9: Deep expansion on P_1; IO: Expansion of the interosseous to the lateral band of the extensor digitorum; 11: Interosseous hood; 12: Lumbrical tendon; 13: First dorsal interosseous with its complete system of insertion and the tendon of the first lumbrical; 14: Retinacular ligament; 15: Flexor pulley on the first phalanx; 16: Distal pulley on the second phalanx; 17: Adductor pollicis with its insertions on the internal sesamoid, the base of P'_1 and the dorsal aponeurosis; 18: Medial CL of the MP joint of the thumb; 19: Accessory CLs inserted into the volar plate and the sesamoid; 20: Flexor pollicis longus; 21: Extensor pollicis longus; 22: Extensor pollicis brevis; 23: Abductor pollicis longus; 24: Extensor carpi ulnaris; 25: Extensor carpi radialis brevis; 26: Extensor carpi radialis longus.

can actively shorten and passively resist stretching, but cannot actively lengthen. The muscles of the hand anchor to bone at either end, typically by a short tendon at their origin (proximal end) and a long tendon at their insertion (distal end).

Muscle tissue is composed of muscle fibers that run along the length of the muscle attaching to tendon at either end. Tendons are stout parallel bundles of collagen fibers that often cross multiple joints of the hand before inserting into bone. Some tendons of the hand are atypical as they bifurcate or combine before inserting into bone to form the

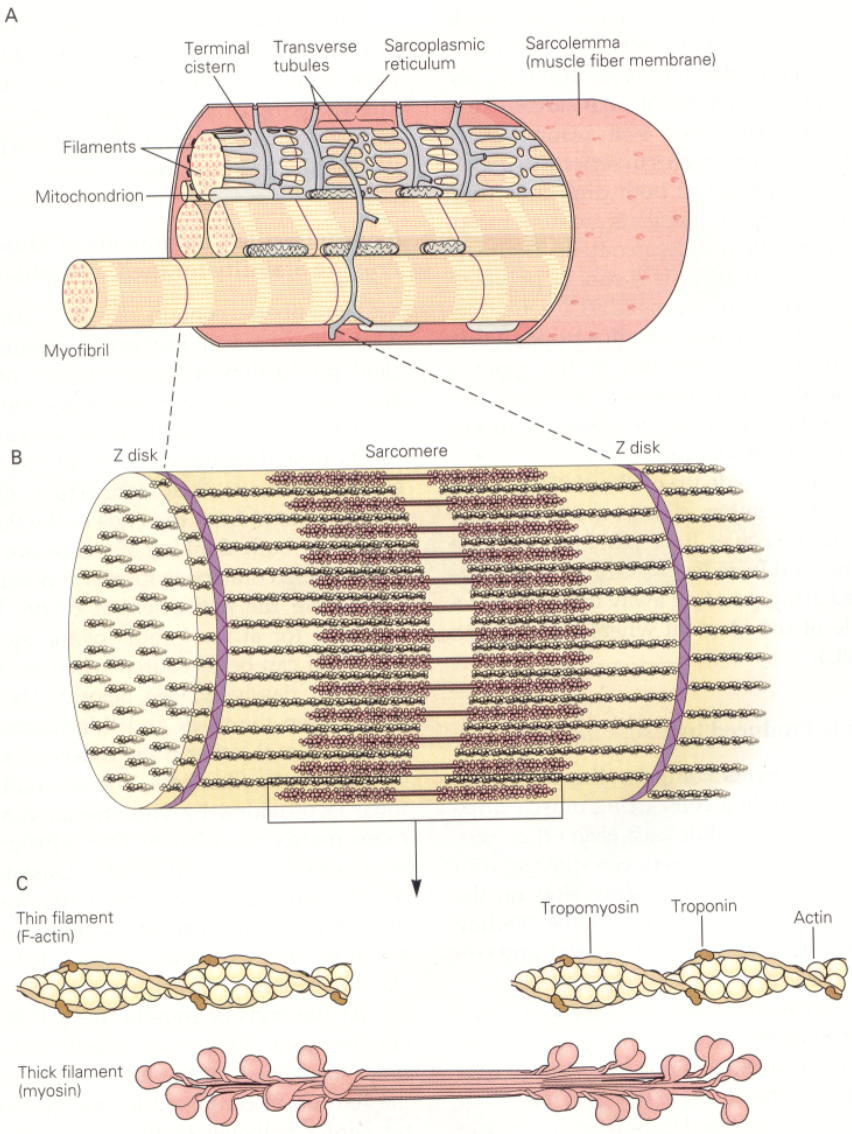

Figure 2.3: Anatomy of the muscle: (A) 3D reconstruction of a section of muscle fibers; (B) The sarcomere is the functional unit of the muscle; (C) Detail of the contractile proteins (myofilaments).

extensor mechanism (or extensor hood) of the fingers. The lumbrical muscle is atypical as it both originates from and inserts onto tendon (the flexor profundus tendon and the extensor hood, respectively) and has no direct bony attachment. Striated muscle fibers are themselves parallel assemblies of similarly long cells with multiple nuclei containing sarcomeres, the fundamental contractile unit of muscle tissue (Figure 2.3). At the biochemical level, sarcomeres are interdigitated filaments of f-actin and myosin. Muscle

activation and contraction occurs when a neural command releases calcium ions inside the muscle cell to cause myosin filaments to "ratchet" past the f-actin filaments to increase the overlap between them by metabolizing adenosine triphosphate, ATP, an important source of energy fueling cellular processes. Concentric contractions occur when the muscle fiber can shorten to induce tendon excursion and bone motion. Eccentric contractions occur when tendon forces overpower the contractile force of the muscle and the muscle lengthens during muscle activation. Isometric contractions occur when the muscle is not allowed to shorten. The structural and biochemical properties of the sarcomere make muscle force a function of activation level, length of the fibers, velocity at which fibers shorten or lengthen, and its previous activation history. Maximal muscle force is produced during eccentric contractions, drops rapidly with concentric contractions, scales with activation and increases linearly with the physiological cross sectional area (PCSA) of the muscle. Mammalian muscle tissue is considered to produce a maximal stress of 35 N/cm^2, which is a remarkable ratio of force per unit weight difficult to match artificially.

Excitation of muscle fibers is induced via frequency modulated electrochemical events (action potentials) that propagate from the motor neurons located in the CNS to the target muscle via the long output threadlike component of the motor neuron (axons). The numerous muscle fibers in a muscle are functionally grouped into motor units consisting of a subset of muscle fibers controlled by a single motor neuron. The force at the tendon is regulated by the sequential recruitment of motor units in a fixed order starting with the small, low force and fatigue resistant fibers, and ending with the large, high force and fatigue sensitive fibers.

Muscle fiber length and velocity are sensed by muscle spindles interdigitated with muscle fibers deep in the muscle. Golgi tendon organs are located on the tendon near the aponeurosis and sense tendon force, while sensors imbedded in the synovial capsule are thought to provide joint configuration information.

The human hand nominally has 40 muscles classified as those located in the hand distal to the wrist (*intrinsic muscles*), and those located in the forearm (*extrinsic muscles*). All the muscles of the hand can be considered multi-articular because their tendons cross a joint with at least two DOFs. Nominally, the wrist has five dedicated muscles, nine muscles act on the thumb (four extrinsic and five intrinsic), seven on the index and little fingers (four extrinsic and three intrinsic), and six on the middle and ring fingers (three intrinsic and three extrinsic). There exist numerous anatomical variations, the most common of are the absence of the palmaris longus (a flexor of the wrist), and the morphology of extrinsic flexor muscles [86].

2.1.2 Sensors

The somatic sensory system transmits information about four major modalities:

- touch sense;
- proprioception sense;

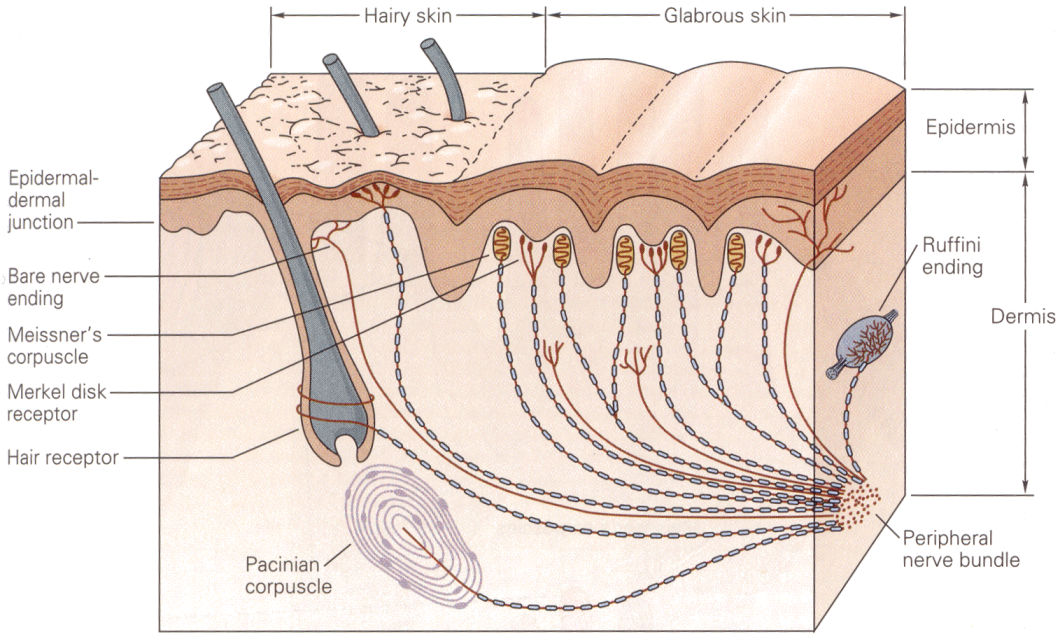

Figure 2.4: Mechanoreceptors in the human skin.

- pain sense;
- temperature sense;

Altough these modalities share the same type of sensory neuron, the receptors for each modality have distinct morphological and molecular specializations [41].

2.1.2.1 The sense of touch

Sensors of touch and position in humans represent a very sophisticated and thus inspiring model for mechano-reception in artificial machines [41, 87]. Humans skin, in fact, is an active sensory organ that is both highly sensitive and resistant. The glabrous skin has about 17,000 tactile units composed of five major types of receptors: free receptors, Meissner Corpuscles, Merkel's disks, Pacinian corpuscles, and Ruffini endings [90]. These receptors are found at all depths below the skin surface and can be described as follows (Figure 2.4):

Meissner's corpuscles: they are the 43% of the tactile units in the hand. The average size of these corpuscles for an adult is about 80 μm x 30 μm, with the long axis perpendicular to the surface of the skin. They are velocity detectors or touch receptors, since they move with the ridged skin of the fingers and the palm and provide the best reception of movement across the skin;

PROBABLE RECEPTOR	CLASS (STEP INDENTATION RESPONSE)	RECEPTIVE FIELD (mm^2) (MEDIAN)	SKIN TYPE *	FREQUENCY RANGE (MOST SENSITIVE)	THRESHOLD SKIN DEFORM ON HAND (MEDIAN)	PROBABLE SENSORY CORRELATE	RECEPTORS/cm^2 FINGERTIP (PALM)
PACINIAN CORPUSCLE	**FA II** (RA II, QA II, PC)	10-1000 (101)	G,H	40-800 Hz (200-300 Hz)	3-20 μm (9.2 μm)	VIBRATION TICKLE	21 (9)
MEISSNER'S CORPUSCLE	**FA I** (RA I, QA I, RA)	1-100 (12.6)	G	10-200 Hz (20-40 Hz)	4-500 μm (13.8 μm)	TOUCH TICKLE MOTION VIBR FLUTTER TAP	140 (25)
HAIR FOLLICLE RECEPTOR	**FA** (RA, QA)	?	H	?	?	TOUCH VIBRATION	–
RUFFINI ENDING	**SA II**	10-500 (59)	G,H	7 Hz	40-1500 μm (331 μm)	STRETCH SHEAR TENSION (?)	9 (15)
MERKEL'S CELLS	**SA I**	2-100 (11.0)	G	0.4-100 Hz (7 Hz)	7-600 μm (56.5 μm)	EDGE (?) PRESSURE	70 (8)

SA: SLOW ADAPTING FA: FAST ADAPTING
I: SMALL, DISTINCT FIELD II: LARGE, DIFFUSE FIELD
* G: GLABROUS SKIN H: HAIRY SKIN

TABLE 2.1: Characteristics and distributions of the different mechanoreceptors sensors in the human skin.

Pacinian corpuscles: they are from 1 to 4 mm in length and from 0.5 to 1 mm in diameter. There are about 2000 Pacinian corpuscles distributed all around the body, with one third of them localized in the digits. They are acceleration detectors and provide vibration reception. They cannot detect steady pressure, but they are responsible for the threshold detection of light touch;

Ruffini's endings: they are composed of a fusiform structure with a definite capsule in the subcutaneous tissue of the pulp of the human finger. They are the 19% of the tactile units in the hand, and they are detectors of intensity and pressure. They are also responsible of detecting shear on the skin;

Merkel's disks: they are 25% of the tactile units in the hand. They are composed of disk-like nerve ending and a specialized receptor cell, and they are about 70–90 nm in diameter. They provide excellent detection of intensity; however they provide tactile and vibration information;

Free receptors: they are the most important cutaneous receptors, as they permeate the entire thickness of the dermis. They have diameters ranging from 0.5 to 2.5 μm, and generally they form thermoreceptors and nociceptors (pain receptors).

Mechanoreceptors in the human skin detect pressure, touch, vibration, and tactile sensation. They are divided into three main classes: slowly adapting (SA), rapidly or fast adapting (RA or FA) and very rapidly adapting (VRA). Each adaptation class can be further divided into two types, namely, type I and type II, according to their receptive field:

small with sharp borders for the type I, large with obscure borders for the type II. Table 2.1 shows the classification of mechanoreceptors according to their rate of adaptation.

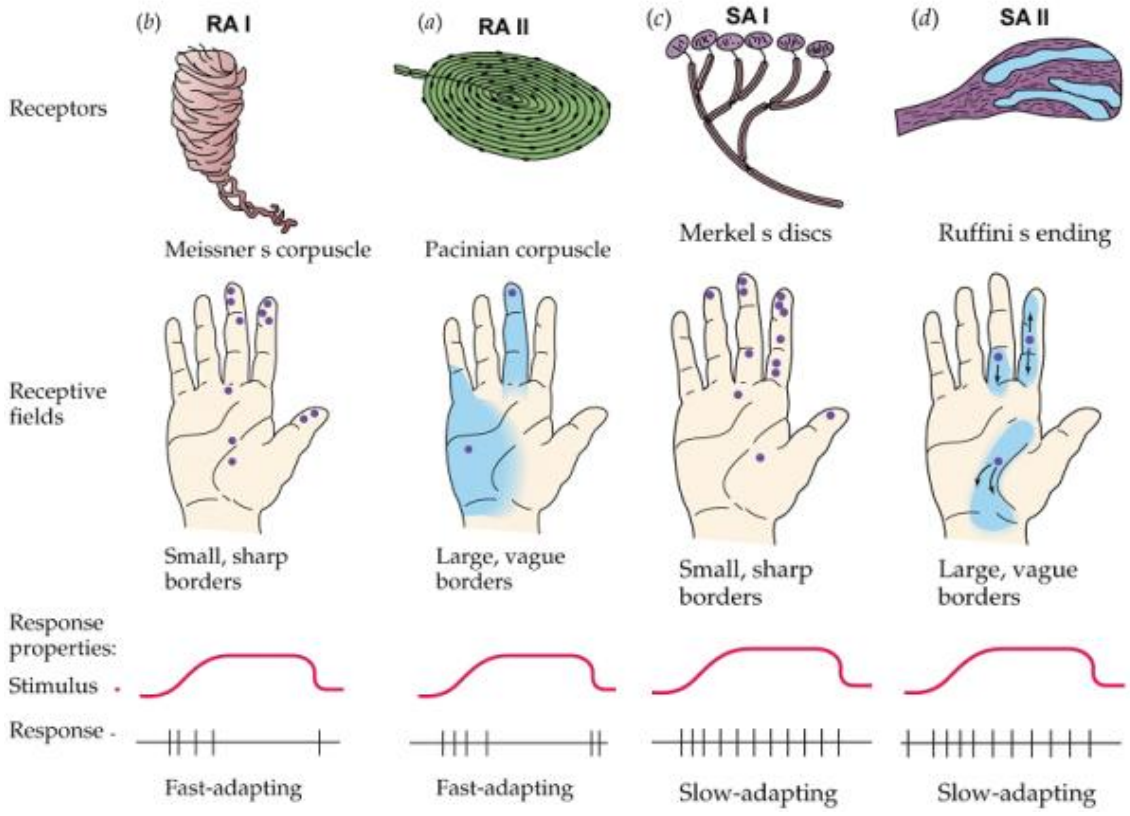

Figure 2.5: Comparison between the distribution, the receptive field and the stimulus response of the different mechanoceptors. SA: Slowly Adapting; RA: Rapidly (or Fast) Adapting; Type I: sharp borders; Type II: smooth borders.

2.1.2.2 The proprioception

Other important mechanoreceptors of the human body are the *proprioceptors*. They are sensory receptors that respond to stimuli arising within the body. Proprioception provides information on the orientation of our limbs with respect to one another. More generally, proprioception is the perception of the body's movement and its position in space, whether still or in motion. Proprioceptors generate the sense of position, the sense of movement, and the sense of force. The first let us know the position of our limbs without visual feedback; the second enable us to perceive the speed of retraction as well as controlled extension of our limbs; the latter is the ability to know how much force to use to push, pull, or lift.

The cutaneous receptors previously discussed could also be used as proprioceptors, since position and movement can be perceived from the deformation of the skin.

Joint receptors detect position, velocity, and acceleration occurring at the joint capsule. This is possible because whenever a joint is moved, the joint capsules are either compressed or stretched. Physiologically, the rate of change of impulse frequency yields the angular speed, and the magnitude of the impulse frequency yields the position of a joint.

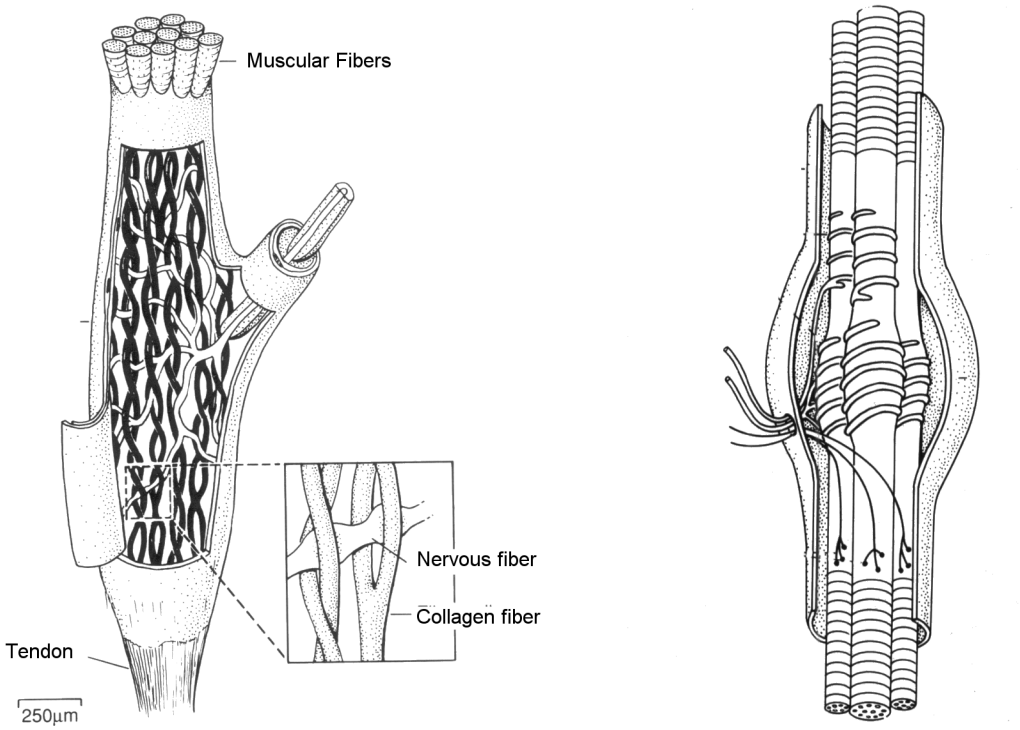

(a) Golgi organ. (b) Muscle spindle.

FIGURE 2.6: Schematic picture of the Golgi organ and of a muscle spindle.

Musculotendinous receptors are divided into *tendon receptors* and *muscle receptors*. Golgi tendon organs (Figure 2.6(a)) are located between the muscle and its tendon. Their function is to inhibit muscle contraction when the muscle's associated muscle is stretched. Golgi tendon organs are sensitive detectors of tension in distinct, localized regions of their host muscle. Probably they are important contributors to fine motor control. On the other hand, muscle spindles (Figure 2.6(b)) are located throughout the muscle between parallel individual muscle fibers. They detect the stretch of their adjacent muscle fibers. Their functional substructure provides constant monitoring and regulation of sensory-motor functions that enable appropriate body movement.

2.1.2.3 The sense of temperature

Although the mechanical properties of an object are also mediated by the vision, the thermal qualities are only somatosensory. Humans can recognize four different thermal sensations [41]: cold, cool, warm, and hot.

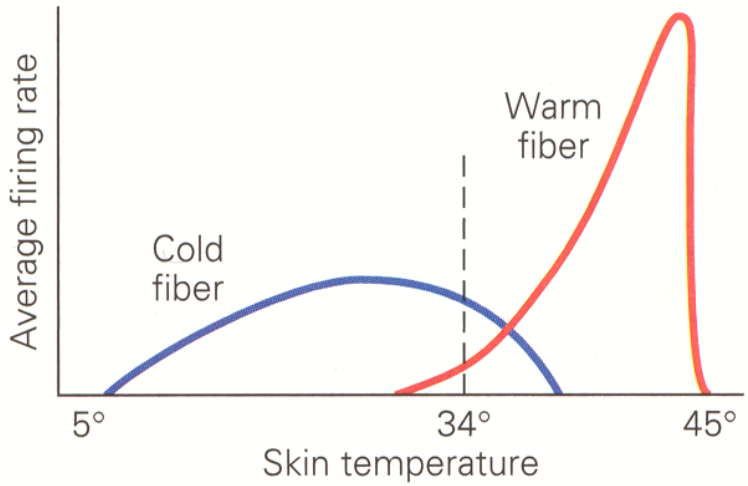

Figure 2.7: The average firing rate of cold receptors and warmth receptors is function of the temperature.

The firing of the thermal receptors is modulated as a function of the temperature (Figure 2.7). Both cold and warmth receptors fire continuosly at low rates at the normal temperature of 34°C. Cold receptors, however, are most active at skin temperature of about 25°C, while warmth receptors fire more vigorously at 45°C.

2.1.2.4 The sense of pain

The sense of pain is mediated by *nociceptors*. These sensors respond directly to some noxoius stimuli and indirectly to others by means of one or more chemical released from cells in the traumatized tissue. We can distinguish three classes of nociceptors:

Mechanical nociceptors: they require a strong tactile stimuli. They are also excited by sharp object that penetrate, squeeze, or pinch the skin (Figure 2.8);

Thermal nociceptors: they are excited by extremes of temperature. One group responds for temperature above 45°C, the second one for temperature below 5°C;

Polymodal nociceptors: they responds to a variety of destructive mechanical, thermal, and chemical stimuli.

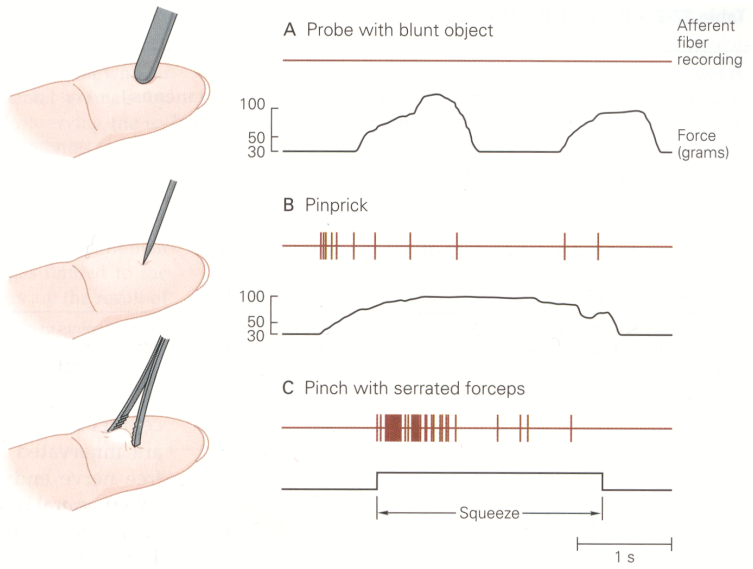

FIGURE 2.8: Response of the nociceptors.

An example of how the firing rate of mechanical nociceptors changes according to the type of the stimulus is showed in Figure 2.8.

2.2 Amputation of the hand

Amputation remains one of the oldest surgical procedures [60]. Archeologists have uncovered evidence of prehistoric people with amputations, both congenital and those acquired by surgery or trauma. While the procedure has evolved significantly since the days of quickly severing a limb from an unanesthetized patient and dipping the stump in boiling oil to achieve hemostasis, it was not until World Wars I and II that modern ideas of amputation and prosthetics developed. Particularly within the last 3 decades, prosthetic research and rehabilitation engineering centers have disseminated new information regarding biomechanics and prosthetic design. With the advent of physical and rehabilitative medicine, surgeons now realize that the care for the person with an amputation does not end with removal of sutures.

The surgeon faces many challenges over the course of treatment of the individual with an amputation. The following are major goals of amputation surgery in the upper extremity:

- preservation of functional length;
- durable coverage;
- preservation of useful sensation;

- prevention of symptomatic neuromas;
- prevention of adjacent joint contractures:
- short-term morbidity;
- early prosthetic fitting, when applicable;
- early return of the patient to work and play.

The true frequency of acquired amputation of the wrist and forearm is unknown. Published estimates of amputated limbs, including upper extremities, vary significantly, citing prevalences of 350,000-1,000,000 persons with amputations and annual incidence of 20,000-30,000 new amputations. Some statistics about the level of amputation in a rehabilitation center in Japan (Table 2.2) and in UK (Table 2.3) are showed.

	Male	(%)	Female	(%)	Total	(%)
Shoulder disarticulation	0	0%	1	6%	1	1%
Transhumeral amputation	9	18%	3	17%	12	18%
Transradial amputation	15	30%	9	50%	24	35%
Wrist disarticulation	11	22%	2	11%	13	19%
Partial hand amputation	15	30%	3	17%	18	26%
TOTALS	**50**	**100%**	**18**	**100%**	**68**	**100%**

Table 2.2: Statistics of the sites of upper limb amputation in 2001 in the KIBIKOGEN Rehabilitation Center For Employment, Japan.

2.2.1 Reasons for the amputation

Irreparable loss of the blood supply of a diseased or injured upper extremity is the only absolute indication for amputation regardless of all other circumstances. Severe peripheral vascular disease, traumatic injury, thermal and electrical injury, and frostbite commonly require amputation. Not only has the part been rendered useless, but it is also a threat to the life of the individual because the toxic products of tissue destruction are disseminated systemically. Likewise, in individuals with systemic sepsis, amputations are necessary to control an otherwise rampant infection. An indication for amputation after nerve injury is the development of uncontrolled trophic ulcers in an anesthetic upper extremity.

In general, amputations in the upper extremity also are indicated for persons with malignant tumors without evidence of metastases. Even after metastases, amputation

	Males							Females							NA	**Total**
Level	<16	16–54	55–64	65–74	>75	NA	All	<16	16–54	55–64	65–74	>75	NA	All		
FQ	1	3	1	2	-	-	7	-	2	1	1	1	-	5	-	**12**
SD	1	6	1	-	1	-	9	-	-	-	-	1	-	1	-	**10**
TH	4	39	7	3	3	1	57	1	6	5	3	1	-	16	-	**73**
ED	-	1	-	-	-	-	1	-	-	1	-	-	-	1	-	**2**
TR	7	32	3	7	4	-	53	2	6	3	2	7	-	20	1	**74**
WD	-	3	-	-	-	-	3	-	-	-	-	-	-	0	-	**3**
PH	4	19	4	4	2	-	33	4	10	2	2	1	-	19	1	**53**
UD	1	6	1	3	-	-	11	2	2	1	1	-	1	7	-	**18**
DU	3	4	-	1	-	-	8	1	-	-	-	-	-	1	-	**9**
Total	**21**	**113**	**17**	**20**	**10**	**1**	**182**	**10**	**26**	**13**	**9**	**11**	**1**	**70**	**2**	**254**

Table 2.3: Level of amputation for 254 referrals in 1999/2000 in UK divided by age and sex. The different levels of amputation are: FQ: Forequarter; SD: Shoulder disarticulation; TH: Transhumeral; ED: Elbow disarticulation; TR: Transradial; WD: Wrist disarticulation; PH: Partial hand; DG: Digits; DU: Double upper amputation. NA means that no data were available.

may be necessary to relieve pain when a neoplasm has become ulcerated and infected or has caused a pathologic fracture. In these oncologic cases, the indications for amputations versus limb salvage procedures are evolving constantly and require individual consideration beyond the scope of this article.

Of the 211 (83% of the total) referrals where a cause of limb loss was reported, trauma accounted for 57%, neoplasia for 11 per cent and dysvascularity for 13 per cent (Table 2.4). It should be noted that the completeness of cause of amputation data has improved, decreasing by 10 per cent from last year. In 1999/00 only 43/254 cases had no cause provided recorded compared with 70/257 cases in1998/99. Although it is possible to record more detailed information on the cause of amputation, in the majority of trauma cases (60/121) no additional detail was provided by centres.

2.2.2 Wrist and forearm amputation

Depending on the level of amputation, we can distinguish between:

Transcarpal amputation: At this level, supination and pronation of the forearm as well as flexion and extension of the wrist are preserved and can improve the patient's overall function. Furthermore, when compared to more proximal amputations, the long lever arm increases the ease and power with which a prosthesis can be used. However, prosthetic fitting is more difficult and requires a skilled prosthetist.

	Level of amputation									Total
Cause of amputation	FQ	SD	TH	ED	TR	WD	PH	DG	DU	
Trauma	4	5	29	1	34	2	32	11	3	121
Dysvascularity	-	-	11	-	14	-	2	1	-	28
Infection	-	-	4	-	3	-	-	1	-	8
Neoplasia	8	3	6	-	5	-	-	1	-	23
Other	-	2	5	1	9	1	9	4	-	31
No Cause Provided	-	-	18	-	9	-	10	-	6	43
All causes	12	10	73	2	74	3	53	18	9	254

Table 2.4: Causes of amputation for 254 referrals in 1999/2000 in UK divided by the level of amputation. The different levels of amputation are: FQ: Forequarter; SD: Shoulder disarticulation; TH: Transhumeral; ED: Elbow disarticulation; TR: Transradial; WD: Wrist disarticulation; PH: Partial hand; DG: Digits; DU: Double upper amputation.

Wrist disarticulation: Wrist disarticulation has many of the same advantages as transcarpal amputation with regard to providing a long lever arm and preserved supination and pronation. However, wrist flexion and extension are sacrificed. Because of their length, conventional wrist units are not used and myoelectric fitting is problematic, such as in persons with transcarpal amputations. However, recent wrist disarticulation prostheses can be fashioned with thin wrist units that minimize the length discrepancy between upper extremities.
Wrist disarticulation is the procedure of choice in children. In general, disarticulations are preferable to transactions through bone at a more proximal level because the distal physis is spared and, consequently, the growth of the distal stump continues at a normal rate. In addition, disarticulation prevents terminal overgrowth of the bone.

Distal forearm amputation: While maintaining length remains an important consideration in the upper extremity, the underlying soft tissues in the distal forearm consist of relatively avascular structures, such as fascia and tendon, and may not always offer adequate padding for the bony stump. Furthermore, the skin and subcutaneous tissue in this area are thin and may be predisposed to wound problems. A good compromise between adequate functional length and adequate wound healing appears to be at the junction of the distal and middle third of the forearm. Despite resection of the distal radioulnar joint, some degree of pronation and supination is preserved in persons with forearm amputations. The extent of motion is dependent on the length of residual forearm stump; the longer the stump, the greater the arc of motion.

Proximal forearm amputations: The technique for proximal forearm amputation is

similar to that a for more distal amputations. A short stump having as little as 4 cm of ulna is preferable to an above-elbow amputation.

Krukenberg procedure: More than 80 years ago, Krukenberg described a technique that converts a forearm stump into a pincer that is motorized by the pronator teres muscle (Figure 2.9). Indications for this procedure have been debated; however, they generally include bilateral upper-extremity amputations, especially in those who are also blind. The procedure also has been used successfully in persons in developing countries who lack the means to obtain expensive prostheses.
This procedure preserves proprioception and stereognosis in the functional stump to allow for effective maneuvering in the dark. It is important to note that this procedure is not recommended as a primary procedure at the time of an amputation, and the procedure must be preceded with appropriate counseling due to cosmetic concerns. Conversely, once this procedure is performed, it does not preclude the use of a functional prosthesis. Therefore, the patient is afforded the option to use either functional strategy.

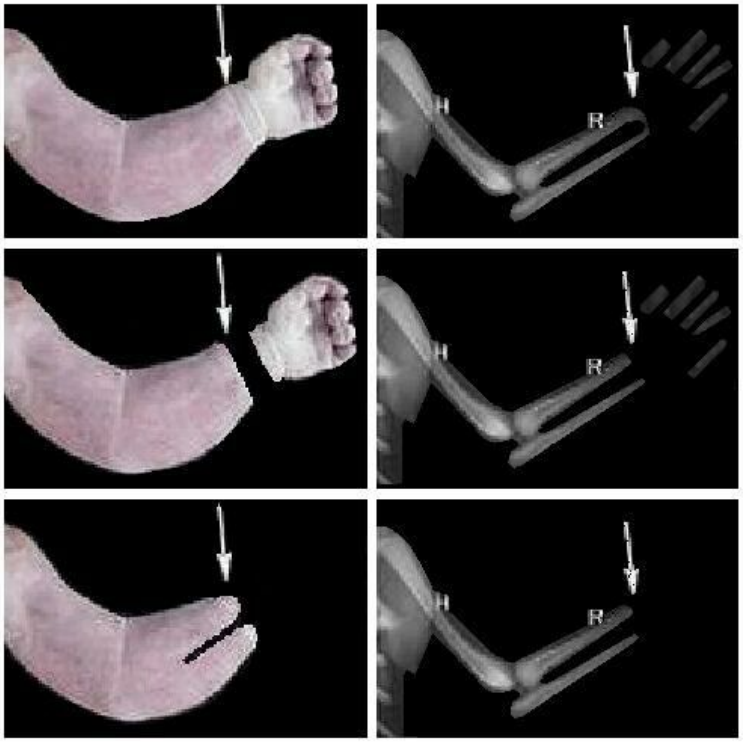

FIGURE 2.9: Schematic representation of the Krukenberg procedure.

According to the Statistical Database for the United Kingdom 1999/2000 [66], just over three quarters of upper limb amputee referrals occur in the 16-64 age range (200/254,

78.7%) with the majority of these being male (151/182, 82.9%). The three most common levels of amputation, trans-humeral, transradial and partial hand levels, together account for almost 80 per cent of these referrals. The more unusual levels of upper limb amputation tend to be referred to centres with special interests.

2.3 Specifications for the functional substitution of the hand

The function of the hand are multiple, though the most important are the sensory function of touch and the function of prehension. The hand has several other functions which play an essential role in our lives [86]:

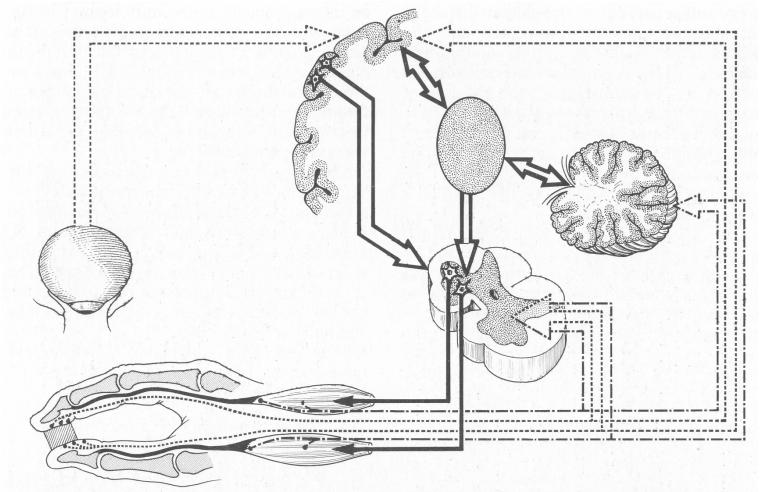

Figure 2.10: Schematic view of the sensory and motor neural pathways of the hand. In heavy lines, the motor pathways. Infine dotted lines, the superficial sensory or exteroceptive pathways. In dashes, the deep sensory or proprioceptive pathways. There are several synapses: (I) in the medulla; (2) in the cerebellum and in the subcortical region; (3) in the cortical region, thus permitting different medullary and subcortical reflex circuits as well as conscious control. Ocular control is necessary when sensation is absent or insufficient. The knowledge from sensory input or "tactile gnosis" demands cortical participation.

- expression through gesture;
- visceral function in carrying food to the mouth;
- emotional and sexual functions in caressing;

Natural Hand performance	
DoFs	22
Type of Grasps	Power Grasp and Precision Grasp
Tapping force	1-4 N
Force of power grasp	>500 N (age 20-25); >300 N (age 70-75)
Two fingers force	>100 N
Max. tapping frequency	4.5/sec.
Range of flexion	100^o depending on joint
Max. duration of grasp	Var. with energy
Number of sensors	$\simeq$ 17'000
Proprioceptive sensing	Position movement Force
Exteroceptive sensing	Pression Force Acceleration Temperature Pain
Proportional Control and Dexterity	Ability to regulate force and velocity according to the type of grasp
Stability	The grasp is stable against incipient slip or external load
Number of possible flexion	Limited only by muscular fatigue
Total volume	50 cc
Wrist mobility	2+1 DoFs
Weight	400 g

Table 2.5: Main characteristics of the human hand.

- aggressive function for both offense and defense;
- bodily hygiene;
- thermoregulatory role.

What confers on the hand an exceptional sensory value is not only the great number of sensitive corpuscles of its covering, but also the possibility of augmenting its capacity for information by means of voluntary maneuvers of exploration (manipulation and palpation). Thus, the hand can be considered as a *sensory organ* (Figure 2.10).

An artificial hand should be able to replicate as much as possible the characteristics of the human hand. In particular, as showed in Table 2.5, the artificial substitute should:

- possess a high number of degrees of freedom (DoFs);
- be capable of different types of power and precision grasps;
- exert a very high force during power grasping, but at the same time should be capable of fine movements;
- possess a high number of sensors, both proprioceptive and exteroceptive, for different measurements: force, position, speed, pain, temperature, and so on;
- be able to regulate force and velocity according to the tipe of grasping;
- be of the same size and weight of the natural hand.

In the following chapters a review of the state of the art in the realization of artificial hands will be presented, both for the prosthetic and for the robotic applications. The comparison of the performance of the human hand, the prosthetic hands and the robotic hands will give the design goals for an innovative cybernetic hand prosthesis.

Three

The problem of the functional substitution

One of the dreams of scientists and engineers is the creation of a humanoid, a robotic creature similar to the human being in its aspect, behaviors and functionalities. The realization of such a humanoid or, better, the realization of some of its parts, could be useful also in the rehabilitation field, in particular when we consider that - for various reasons - human beings could loss one of their functional organs, both internal and external.

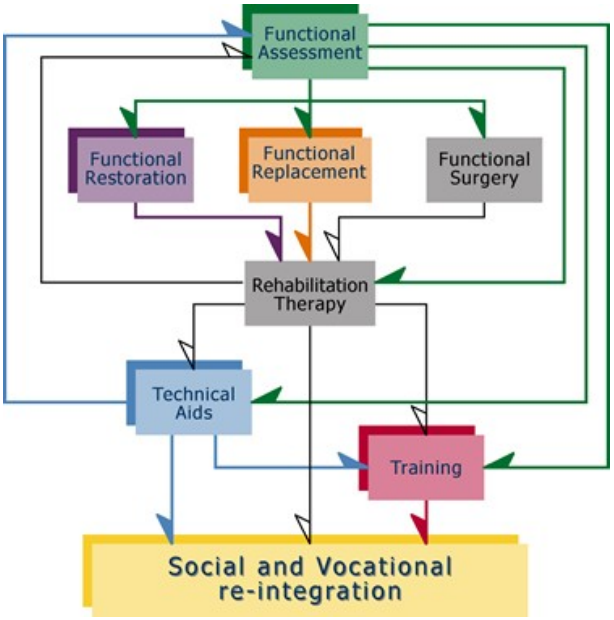

FIGURE 3.1: Ideal rehabilitation process.

Generally speaking, an ideal rehabilitation process presents a looping structure (Figure 3.1). After an initial assessment of the functional capabilities of the patient, the most

appropriate rehabilitative solution is chosen among:

- functional restoration;
- functional replacement;
- functional surgery.

Then, a period of rehabilitation follows, in order to led the patient to the social and vocational re-integration by means of (when needed) technical aids and training. Each of these treatments (prosthesis implantation, surgery, functional restoration, motor rehabilitation, functional integration by Technological aids) is followed in the model by one or more evaluation phases.

3.1 The substitution of the human hand

The human hand is a marvelous example of how a complex mechanism can be implemented, capable of realizing very complex and useful tasks using a very effective combination of mechanisms, sensing, actuation and control functions [41, 43, 86]. The human hand is not only an effective tool but also an ideal instrument to acquire information from the external environment. Imitating the capabilities of the human manipulation systems has been for centuries the dream of scientists and engineers. In fact, developing a truly human-like artificial hand is probably one of the most widely known paradigm of "bionics".

In the next sections, the state of the art in the realization of artificial hands, both for prosthetic and robotic applications, will be reviewed.

3.2 The amputation of the hand

Based on information available from the National Center for Health Statistics there are approximately 50,000 new amputations every year in the United States of America [51]. The ratio of upper limb to lower limb amputation estimated from this information is 1:4.9. The most frequent causes of upper limb amputation are trauma and cancer, followed by vascular complications of disease. Transradial level accounts for 57% and transhumeral for 23% of all arm amputations with the right arm more frequently involved in work related injuries. Sixty percent of arm amputees are between the ages of 21 and 64 years and ten percent are under 21 years of age. Congenital upper limb deficiency has an incidence of approximately 4.1 per 10000 live births (Table 2.4).

The viability of the soft tissues and skin coverage with adequate sensation will usually determine the most distal possible functional level for amputation, whenever possible transradial amputation level is preferred. Preserving length of the residual limb to improve prosthetic suspension and force transmission from the residual limb to the socket is a principal responsibility and goal of the surgeon.

FIGURE 3.2: A drawing of a man donning a hand prosthesis (ca. 1903).

The residual limb must be surgically constructed with care to optimize the intimacy of fit, maintain muscle balance, and to allow it to assume the stresses necessary to meet its new function. Bony prominences, skin scars, soft tissue traction, shear and perspiration can complicate this function. After surgery ideally the patient with an upper limb amputation should be able to use prosthesis, be it body or externally powered, during most of the day through a newly created man-machine interface (the socket/ residual limb). In the upper limb amputee, fitting of the first prosthesis should be implemented as soon as possible after wound healing. There is a direct relationship between the time of fitting and long-term prosthetic use, a three to six months window of opportunity when there is a much greater rate of acceptance and functional integration of the artificial arm for the unilateral upper limb amputee.

Upper limb prostheses choices have increased greatly over the past several years, with improvements in components (prosthetic terminal devices, wrist, elbows and shoulders), socket fabrication materials (carbon graphite or high temperature thermoplastics) and fitting techniques, suspension systems (silicone, etc.), and power sources and electronic controls. The more traditional levels of amputation have greatly benefited from the technological advances including the incorporation of myoelectric and proportional controlled terminal devices and slip sensors. The higher levels of upper limb amputation can now be fitted with functional prosthesis, which allow more patients to achieve independent life styles. This is of particular importance for the bilateral upper limb amputee, particularly the very high levels of amputation.

The prosthetic prescription should be carefully prepared to satisfy the needs and desires of the patient. A team approach to prescription writing should be used whenever possible. Appropriate training to be accomplished by a specialized team of professionals in close communication with the patient should follow the provision of a prosthetic device. The device will have a terminal device, socket, suspension system and if appropriate and elbow mechanism.

3.3 What the user can receive

The human hand is a very complex anatomical and physiological structure [43, 86] that cannot be replaced with the current level of prosthetic technology. The functional activities of the hand are extensive but can be grouped into non prehensile (touching, feeling, tapping, etc.) and prehensile activities (three-jaw, and lateral or key grip, power grip, hook grip and spherical grip). A variety of prosthetic terminal devices are available and include passive, body and external powered hooks and hands. They all lack sensory feedback and have limited mobility and dexterity. Prosthetic hands provide a three-jaw chuck pinch and hooks provide the equivalent of lateral or tip pinch. Electric devices can have digital (on/off) or proportional (stronger signal = faster action) control systems.

There are six basic prosthetic options to consider for the upper extremity amputee. Some may be more appropriate than others based on many factors, including level of amputation, condition of residual limb, individual goals and work requirements. In addition, more than one option may be necessary for an individual to maximize his or her rehabilitation potential. These options are:

1. no prosthesis (§3.3.1);
2. cosmetic prosthesis (§3.3.2);
3. body-powered prosthesis (§3.3.3);
4. myoelectric prosthesis (§3.3.4);
5. hybrid prosthesis (§3.3.5);
6. activity-specific prosthesis (§3.3.6).

Each patient has her/his own needs, so each possibility should be explored for all the patients. In the next subsections these options will be briefly reviewed, and some example will be given.

3.3.1 No prosthesis

For many amputees, their level of function is not enhanced by the use of a prosthesis. Some either cannot obtain funding, or are provided with a prosthesis that does not address their individual needs. Others had a poor first experience that may have included pain, discomfort, and poor function, and thereafter choose not to pursue further prosthetic care. Of course, this choice depends also on the level of the amputation, as there is more need for a prosthesis as amputation become more severe.

3.3.2 Cosmetic prosthesis

Cosmetic restoration, or duplication of the contralateral arm or hand, is a popular prosthetic option. This involves replacing what was lost from amputation or congenital deficiency with a prosthesis that is similar in appearance to the non-affected arm or hand and provides simple aid in balancing and carrying. An example of cosmetic restoration of an amputated finger is showed in Figure 3.3, and an example of the duplication of the contralateral arm is given in Figure 3.4.

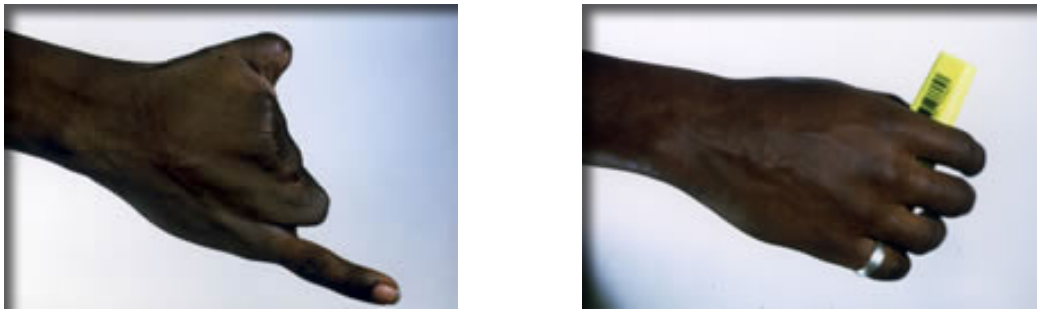

(a) Before. (b) After.

FIGURE 3.3: An example of cosmetic prosthesis for the restoration of an amputated finger.

A cosmetic prosthesis is sometimes called *passive prosthesis* because the prosthetic hand is non-functional. That is, it rarely provides the ability to grasp items. The main advantages and drawbacks of the cosmetic prostheses are summarized in Table 3.1. Cosmetic restoration is typically achieved using one of three materials: rigid PVC, flexible latex, or

FIGURE 3.4: An example of a cosmetic prosthesis which replicates the contralateral arm.

▲ Lightweight;	▼ Difficult to perform activities that require bilateral grasping;
▲ Minimal harnessing;	
▲ Low maintenance;	
▲ No control cables.	▼ Only passive support

(a) Advantages (b) Drawbacks

Table 3.1: Advantage and disavantages in the use of cosmetic prosthesis.

silicone. These types of prostheses are often lighter weight than other prosthetic options and require less maintenance because they have fewer moving parts than other prosthetic options.

3.3.2.1 Latex Covering

This is the most common material utilized for cosmetic restorations. Latex is usually a thin material that comes in pre-made sizes called gloves to fit over most available prosthetic hands. These hands may be passive, body-powered or electrically-powered. A latex glove is most often provided in a solid color that can be enhanced by custom painted details such as freckles, nails, age spots, and knuckles. Partial hand restorations can be made with this material and often utilize a zipper in the palmar surface to allow the patient to easily don and doff but still have the stability and confidence that the prosthesis is firmly attached.
Advantages:

- it is fairly lightweight and inexpensive.

Drawbacks:

- latex easily stains, often permanently;
- most wearers replace a latex glove 3-12 times a year due to wear and staining;
- some patients also say that it lacks the realism (aesthetic and sensory) offered by other materials.

3.3.2.2 Rigid PVC

This material is most often used on individuals with amputations or deficiencies above the wrist disarticulation level. There are good results using this material especially on individuals who have short residual limbs (a common congenital deficiency) that cannot tolerate the weight of a standard cosmetic prosthesis.
Advantages:

- these gloves are solid color core which is advantageous because if scratched the color is retained.

Drawbacks:

- it is rigid.

3.3.2.3 Silicone

Silicone has been around for many years, but only recently has it been refined for utilization in upper extremity restorations. The process to receive a silicone restoration is more complex than with the other two materials due to its customized nature, but often provides the most realistic and long-lasting restorations. Realism is achieved by the varied texture of silicone, size and shape matching through custom molding, and color duplication utilizing multiple photographs of the non-affected hand. The final product is a cosmetic restoration that often goes unnoticed because it so closely resembles the non- affected hand.
Advantages:

- it does not stain like latex;
- it provides the highest cosmetic restoration quality;
- it has a longevity of 3 to 5 years.

Drawbacks:

- it is heavier than latex;
- it can only be used with certain types of prosthetic hands, specifically those that utilize an endoskeletal design;
- it is also more expensive;
- it takes longer to fabricate.

3.3.3 Body-powered prosthesis

A body-powered prosthesis (Figure 3.5(a)), sometimes called a conventional prosthesis, is powered and controlled by gross body movements. These movements, usually of the shoulder, upper arm, or chest are captured by a harness system which is attached to a cable that is connected to a terminal device (hook or hand). For some levels of amputation or deficiency an elbow system can be added to provide the patient additional function. The main advantages and drawbacks of body-powered prostheses are summarized in Table 3.2(a) and Table 3.2(b), respectively.

For a patient to be able to control a body-powered prosthesis he or she must possess at least one or more of the following gross body movements:

- glenohumeral flexion;
- scapular abduction or adduction;

▲ Because of its simple design, it is highly durable and can be used for tasks that involve water and dust and in other potentially damaging environments	▼ Uncomfortable and restrictive control harness
▲ Increased control due to proprioception	▼ The tight harness can also restrict range of motion and the functional envelope
▲ Reduced maintenance cost, as most repairs are related to broken control cables, replacement harnesses, and realignment of terminal devices.	▼ Significant control reduction when attempting to operate the prosthesis out to the side, down by the feet, and above the head
	▼ Some patients dislike the look of the hook and control cables and request a prosthesis that is more "lifelike"
(a) Advantages	(b) Drawbacks

Table 3.2: Advantage and disavantages in the use of body-powered prosthesis.

(a) An example of body-powered prosthesis.

(b) An example of hybrid prosthesis.

Figure 3.5: An example of a body-powered prosthesis a of a hybrid prosthesis, with a body-powered elbow and a myoelectrically-controlled hook.

- shoulder depression and elevation;
- chest expansion.

There are several basic requirements that are generally necessary for a patient to be a candidate for a body powered prosthesis:

- sufficient residual limb length;

- sufficient musculature;
- sufficient range of motion.

There are two types of controls for body-powered hands and hooks, *voluntary opening* and *voluntary closing*. Voluntary opening gives the patient grasping control even when the patient is relaxed. The trade-off for this is limited grip force, often less than 3 kilograms. Voluntary closing allows the patient to have substantially greater grip force, often over 25 kilos, but does not allow the patient to relax without losing grasp.

3.3.4 Myoelectric prosthesis

Myoelectric prosthesis uses small electrical motors to provide function. These motors can be found in the terminal device (hand or hook), wrist, and elbow. An electrically-powered prosthesis utilizes a rechargeable battery system to power the motors. Because electric motors are used to operate hand function, grip force of the hand is significantly increased, often in excess of 10-15 kilos.

There are several ways to control this type of prosthesis (control schemes):

- Myoelectric Control;
- Servo Control;
- Push Button Control;
- Harness Switch Control.

In most cases a single control scheme is chosen. For the more advanced/higher level fittings, several control schemes may be used on the same prosthesis to provide enhanced function.

The "state of the art" of current prosthetic devices is the Otto Bock™ SUVA[1] hand (Figure 3.6) [70]. This hand has only one DoF, and is present in three standard adult size ($7\,^1/_4$, $7\,^3/_4$, $8\,^1/_4$). The difference respect to the other myoelectric hands in the market is that the SUVA hand is equipped with a slippage sensor which should automatically increase the gripping force until the object is held securely. Unfortunately, this sensor does not work very well. Some technical data about the SUVA hand are presented in Table 3.3.

3.3.4.1 Advantages

Unlike a body-powered prosthesis that requires gross body movement to operate it, a myoelectrically-controlled prosthesis only requires the wearer to flex his muscles. This eliminates the need for a tight, often uncomfortable control harness. Another advantage of a myoelectric prosthesis is that because it does not require a control cable or harness, a cosmetic skin can be applied in either latex or silicone, greatly enhancing the cosmetic restoration.

[1]SUVA: Schweizerische Unfall Versicherungs Anstalt SUVA (Swiss Insurance Agency).

The patient can also operate the prosthesis over his head, down by his feet, and out to his side, all of which are difficult to do with a body-powered prosthesis. A myoelectrically-controlled prosthesis also eliminates the suspension harness by using one of two suspension techniques: Skeletal/soft tissue lock or suction.

A Skeletal/soft tissue lock is a technique that involves designing the socket, or patient interface, in such a way that it compresses in areas around the elbow or wrist to provide suspension. Suction suspension is achieved by fabricating the socket with a valve. Once the patient has donned the socket, the valve creates negative pressure inside the socket, providing adequate suspension.

3.3.4.2 Drawbacks

Unlike the other prosthetic options, the electrically-powered prosthesis uses a battery system that requires a certain amount of maintenance which includes charging, discharging, eventual disposal, and replacement. Because of the battery system and the electrical motors, the electrically-powered prosthesis tends to be heavier than other prosthetic options, although advanced suspension techniques can minimize this sensation.

When properly fit and fabricated, electrically-powered prostheses require no more maintenance than other prosthetic options. However, when repairs are required they are often more expensive than other options due to their sophistication. An electrically-powered prosthesis provides a higher level of technology but at a higher cost. An electrically-powered prosthesis is susceptible to damage when introduced to moisture. If you are

(a) The SUVA hand. (b) The transcarpal hand.

Figure 3.6: The SUVA prosthetic hand (left) and the transcarpal hand (right).

Technical Data		
Sizes		$7\,^{1}/_{4}$, $7\,^{3}/_{4}$, $8\,^{1}/_{4}$
Number of fingers		1
Number of active DoFs		1
Operating voltage	V	6
Opening width	mm	100
Proportional speed	mm/sec	15-130
Proportional grip force	N	0-100
Weight (with System Inner Hand)	g	460

TABLE 3.3: Technical data of the Otto Bock SUVA prosthetic hand.

▲ only requires the wearer to flex his muscles	▼ it uses a battery system that requires a certain amount of maintenance
▲ The patient can operate the prosthesis over his head, down by his feet, and out to his side	▼ it is heavier than other prosthetic options
▲ it eliminates the suspension harness	▼ An electrically-powered prosthesis provides a higher level of technology, but at a higher cost
(a) Advantages	(b) Drawbacks

TABLE 3.4: Advantage and drawbacks in the use of myoelectric prosthesis.

considering this option and work in or around heavy moisture this should probably not be your primary work prosthesis.

3.3.5 Hybrid prosthesis

A hybrid prosthesis combines body power and electrical power in a single prosthesis. Most commonly, hybrid prostheses are used for individuals with transhumeral (above the elbow) amputations or deficiencies.

The hybrid prosthesis (Figure 3.5(b)) often utilizes a body-powered elbow and a myoelectrically-controlled terminal device (hook or hand). If desired by the wearer, a myoelectrically-controlled wrist and a cosmetic restoration of the forearm and hand may also be included. Another type of hybrid prosthesis combines an electrically-powered elbow with a body-powered hook or hand. While shoulder disarticulation level amputations or deficiencies have been fit with hybrid prostheses, these cases should be carefully considered because of of the amount of gross body movement needed to operate this type of prosthesis and the EMG signal interference created during such movement.

There are several unique advantages to a hybrid prosthesis. Most important is the ability to simultaneously control elbow flexion and extension while opening or closing the electric hand/hook or while rotating the wrist. The other prosthetic options generally require the wearer to control one function at a time (flex the elbow, lock the elbow, open or close the terminal device). The hybrid prosthesis weighs less and is less expensive than a similar prosthesis with an electrically-powered elbow and hand. The same drawbacks apply to the hybrid as to the prosthetic options it incorporates.

3.3.6 Activity-specific prostheses

This prosthetic option is designed specifically for an activity in which the use of a passive, body-powered, electrically-powered or hybrid prosthesis would place unacceptable limitations on function or durability.

Often this type of prosthesis is recreational in nature, but several prostheses have been created for such activities as music and work-related tasks. Most common are the prostheses designed for fishing, swimming, golfing, hunting, bicycle riding and weight-lifting. The only real drawback to this prosthetic option is that its specificity limits what other activities can be performed outside of its intended use.

(a) Free climbing. (b) Golf.

Figure 3.7: Two examples of activity-specific prosthesis.

3.4 Research on artificial hands

It is evident that the SUVA hand has good reliability and robustness, but its grasping capability is quite far from the capabilities of the human hand. Several research groups are trying to fill the gap between the prosthetic devices and the human hand, and some examples are presented in the following sections (§3.4.1 and §3.4.2). In addition to these research efforts for the realization of a closer replication of the human hand, several groups are working on the development of new techniques for the control of such multifunctional devices, in particular by using the electromyographic signal. These activities are summarized in §3.5.

3.4.1 Hand prosthesis

3.4.1.1 MARCUS hand

The MARCUS hand was intended as an evolution of the Otto Bock Prosthetic hand. It consists of three fingers: a thumb, an index, and a middle finger. The MARCUS hand has two DoFs and it is equipped with two separate motors: the first one driving the thumb movement and the second one driving the movement of the index and middle fingers, which are mechanically coupled [49]. A photograph of the hand is showed in Figure 3.8. The hand was equipped with Hall-effect sensors for finger position information and with a tactile sensor on the thumb for force information.

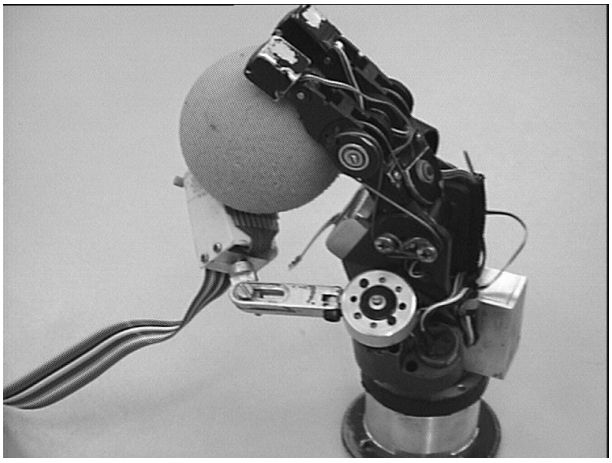

FIGURE 3.8: A picture of the MARCUS hand.

(a) Cylindrical Grasping

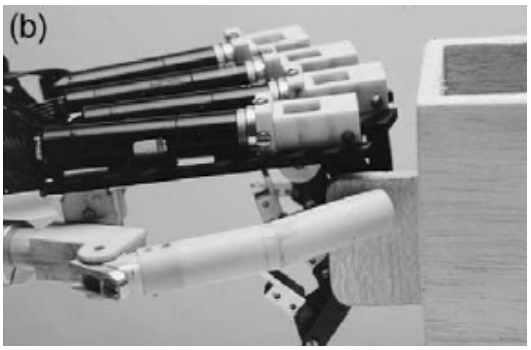

(b) Lateral grasping

Figure 3.9: The Southampton-remedi hand in cylindrical (left) and lateral (right) grasping.

3.4.1.2 Southampton-Remedi hand

The first example of advanced prosthetic hand is the Southampton-Remedi[2] hand (Figure 3.9), which tries to address these objectives [52, 53].
The hand is composed by four digits, each driven by a Maxon DC motor (13 mm diameter), and an opposable thumb, powered by a Maxon DC motorgearbox combination (13 mm diameter) for the circumduction axis, and a Minimotor (10 mm diameter) for the thumb flexion, giving a total weight of 400g. Thanks to the adaptability of the fingers (due to a 6-bar linkage design) the hand should be capable of stable active prehension with a cumulative grip force of 38 N (Table 3.5). The total flexion of the thumb is achieved in 2.5 seconds, and the average curl time (from fully extended to fully flexed) of the fingers is about 0.84 s.

3.4.1.3 A prosthetic hand by the Hokkaido University

An interesting mechanism has been proposed by the Autonomous Systems Engineering Lab of the Hokkaido University [31, 94]. They proposed an adjustable power transmitting mechanism in which the course of the wire changes dependent on the size of load. Thanks to this mechanism, the fingers move fast under a light load, and slowly with high torque under heavy one. Some pictures of the prototype of the hand are showed in Figure 3.10.

A tendon driven method has been choosed in order to locate actuators outside the driven elements. The hand has 7 DoFs, one for each finger plus thumb abduction/adduction and wrist pronosupination Table 3.6. The hand is made by aluminum, and each finger weights 25 grams. However, all the actuators are external to the hand, thus, increasing the total size of the hand, making it impossible to use this hand as a prosthesis.

[2]REMEDI = Rehabilitation and Medical Research Trust.

Technical Data		
Size		$7\,^{3}/_{4}$
Number of fingers		5
Number of active DoF		6
Thumb flexion	sec	2.5
Curl	sec	0.84
Stable grip force	N	38
Weight	g	400

TABLE 3.5: Technical data of the Southampton-Remedi hand.

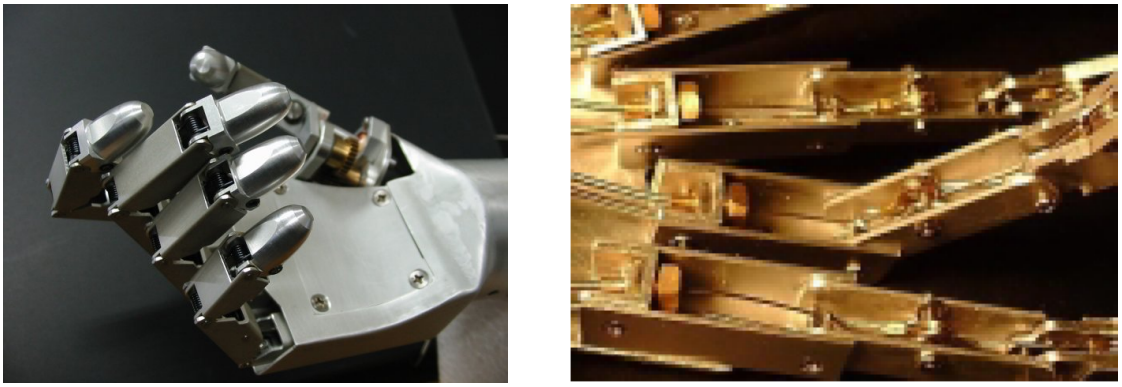

(a) The hand.

(b) Detailed view of the fingers.

FIGURE 3.10: Some pictures of the prosthetic hand developed at the Autonomous Systems Engineering Lab of the Hokkaido University.

3.4.1.4 An ultralight anthropomorphic hand

A different approach has been used to realize a very lightweight artificial hand that approximates the manipulation abilities of a human hand very well [78]. Instead of DC motors, this hand uses 18 miniaturized flexible fluidic actuators, which actuates 5 fingers. Each finger contains the flexible fluidic actuators that lead to a flexion of the finger, flex sensors and touch sensors The metacarpus provides enough space to house a microcontroller, microvalves, the energy source and a micropump. An optional wrist contains the flexible fluidic actuators that bend the wrist (Figure 3.11).

Technical Data		
Size		> adult hand
Number of fingers		5
Number of active DoF		7
Actuation		external
Weight	g	125 (without actuation)

Table 3.6: Technical data of the Hokkaido hand.

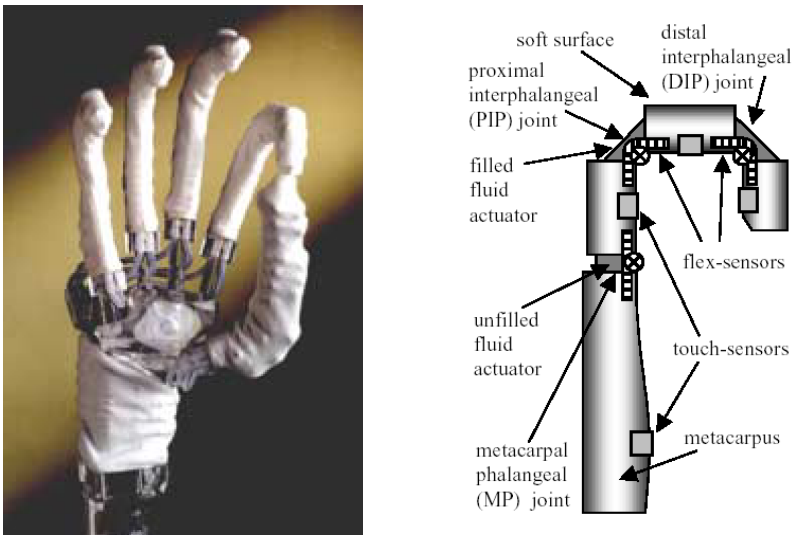

(a) The Karlsruhe hand.

(b) Details of the finger.

Figure 3.11: A picture of the Karlsruhe hand (left) and a schematic drawing of the finger (right).

The flexible fingers are able to wrap around objects of different sizes and shapes, spreading the contact force over a greater contact area. Thus, thanks to this self-adaptability, a large variety of different objects can be grasped reliably without any sensory information, and the movements of the hand appear to be quite natural. Some data about this hand are presented in Table 3.7.

Technical Data		
Size		adult hand
Number of fingers		5
Number of active DoF		17
Flexion/extension	sec	0.1
Weight	g	20 (each finger)
Maximun force (at fingertips)	N	12

TABLE 3.7: Technical data of the Karlsruhe hand.

3.4.2 Robotic hands

During the last two decades several robotic and anthropomorphic hands has been developed. All these hands have a high number of DoFs (up to 16), and have a dexterity and a grasp force comparable to that of the human hand. Unfortunately, all these hands cannot be used as prostheses, because their actuation and control systems are quite heavy and bulky, and thus they cannot be embedded within the hand. Some examples of this kind of hand are given in the following subsections.

3.4.2.1 NTU Hand

The NTU hand (Figure 3.12(a)), developed at the National Taiwan University, is a prosthetic hand with 5 fingers, each of them equipped with sensors, and 17 DoFs in total [54]. Both thumb and the first finger have four DoFs, while other fingers have three active joints. Each finger is equipped with tactile sensors (18 sensor pads in total) to detect grasping force, and 17 position sensors for the position control. A detailed drawing of the assembly of each finger is showed in Figure 3.12(b). Although the authors refer to the hand as a prosthetic device, its weight is much more appropriate for robotics application (Table 3.8).

A discrimination system has been developed [38] (further details will be provided in the following chapters). Two electrodes, placed on the *flexor digitorum superficialis* muscle and on the *extensor pollicis brevis* muscle, are used in order to distcriminate among 8 different movements. Unfortunately, the results showed poor performance (success rate lower than 71% in the best case for online testing).

3.4.2.2 Utah/MIT hand

The Utah/MIT hand [75, 84] was developed to perform laboratory research on grasping and finger manipulation (Figure 3.13). The Utah/MIT Dexterous Hand has 4 DoFs in each of the three fingers, and a 4 DoFs thumb. The geometry of the hand is roughly anthropomorphic. The thumb is, however, permanently in opposition, and the phalange

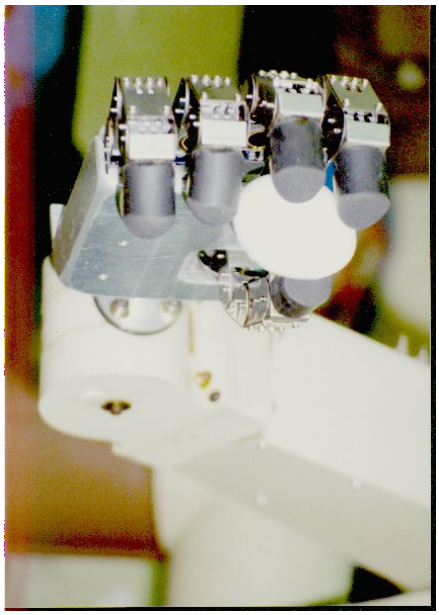

(a) The NTU hand.

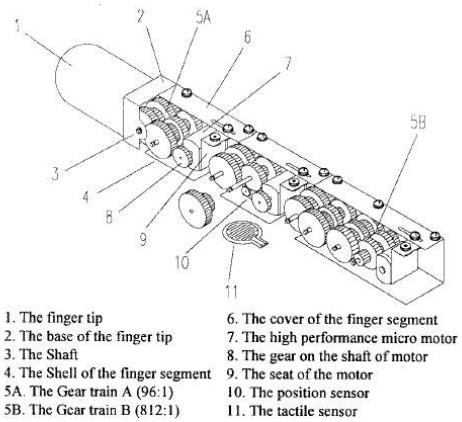

(b) Details of the finger

Figure 3.12: A picture of the NTU hand (left) and the detailed drawing of the assembly of its fingers.

Technical Data		
Size		≈ adult hand
Number of fingers		5
Number of active DoF		17
Weight	Kg	1.57

Table 3.8: Technical data of the NTU hand.

lengths and joint positions have been altered to facilitate the routing of tendons. The 16 DoFs hand is actuated using an antagonistic tendon approach, which requires a system of 32 independent polymeric tendons and pneumatic actuators (Figure 3.13(b)). The pneumatic actuators are fast, low friction, and can generate relatively high forces. The lowest level of control for the Utah/MIT Hand includes an analog controller for each of the 16 DoFs which executes position control and tendon management.

The Utah/MIT Hand closely copies the outward appearance of the human hand and is

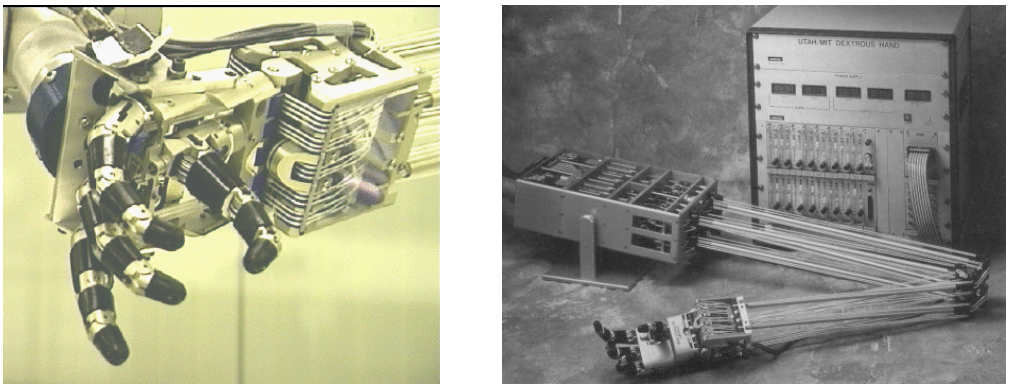

(a) (b)

FIGURE 3.13: The Utah/MIT hand.

Technical Data	
Size	≈ 2
Number of fingers	4
Number of active DoF	16
Number of actuators	32

TABLE 3.9: Technical data of the Utah/MIT hand.

modular in design; each finger is identical. However, cabling is very complex and requires a separate, articulated arm-like frame because each joint is controlled by a pair of antagonistic tendons.

The hand is powered by by 32 50-to-100 psi pneumatic double acting glass cylinders, obtaining a tip force of about 31.8 N. Inside each knuckle is a linear Hall effect sensor that provides joint angle information. Hall effect sensors also monitor tendon tension in the wrist and are used in the finger knuckle joints for position sensing. Design allowances were made for tactile sensor wiring. The wrist is a conventional unpowered U-joint design. Range of motion is less than that of the human wrist with pitch 90 degrees, yaw 30 degrees, roll 270 degrees.

The tendon drive system was an obvious short term design convenience that cascaded negative effects into the design. Control is difficult because the tendons are compliant, while wrist range and finger kinematics are compromised. Tendons made the design nightmarishly complicated; friction requires an elaborate system of 288 pulleys.

Some technical data about the Utah/MIT hand are presented in Table 3.9.

3.4.2.3 Belgrade/UCS hand

Among the earliest underactuated hands driven by rigid links was the Belgrade/USC robot hand by G. A. Bekey and R. Tomovic [4]. This hand has 4 fingers with 3 joints each (Figure 3.14), each finger pair being driven by one motor. The motion of the 2 joints is not independent, but embodied a built-in synergy modeled on observations of human hands. The articulated thumb moves in an arc into opposition to one or more fingers; another motor flexes and extends is at its 2nd joint. Finger, thumb, and palm surfaces are covered with 23 pressure sensors. The driving motors are equipped with encoders for sensing finger rotation with respect to the palm (Table 3.10).

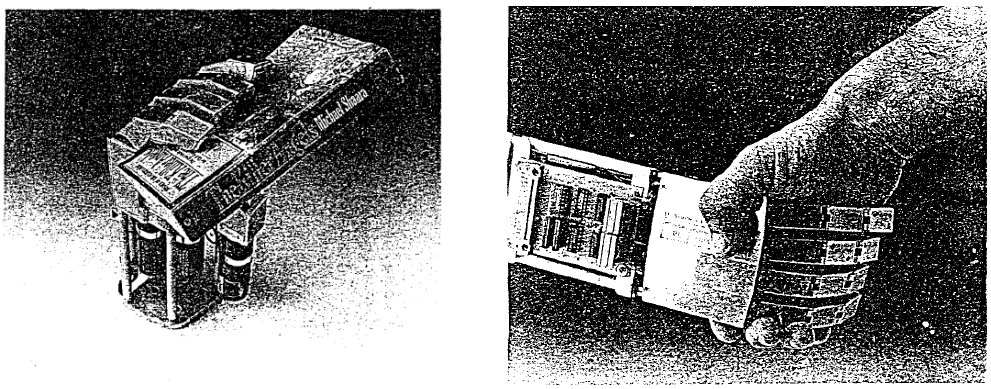

(a) (b)

Figure 3.14: The Belgrade/USC hand.

Technical Data	
Size	≈ 1.1
Number of fingers	5
Number of active DoF	4
Number of actuators	4
Number of sensors	23+4

Table 3.10: Technical data of the Belgrade/USC hand.

These authors believed that robotic systems should use local autonomy as much as possible and that grasp control should reside within the hand itself, using positioning, pressure, contact slippage sensors [40]. After an accurate study of a theory of grasping, they provided a parametric description of a hand that allows for an analytic determination of the appropriate match between the hand properties and task requirements [5].

Some technical data about the Belgrade/USC hand are presented in Table 3.10.

3.4.2.4 Stanford/JPL (Salisbury) hand

Originally called the Stanford/JPL (Jet Propulsion Laboratory) Hand, the Salisbury Hand weights 1.1 Kg. and the drive assembly weights 5.5 Kg. Output force is 45 N for up to two minutes. It is a 9 DoFs Hand with two fingers and an opposing thumb [58, 75]

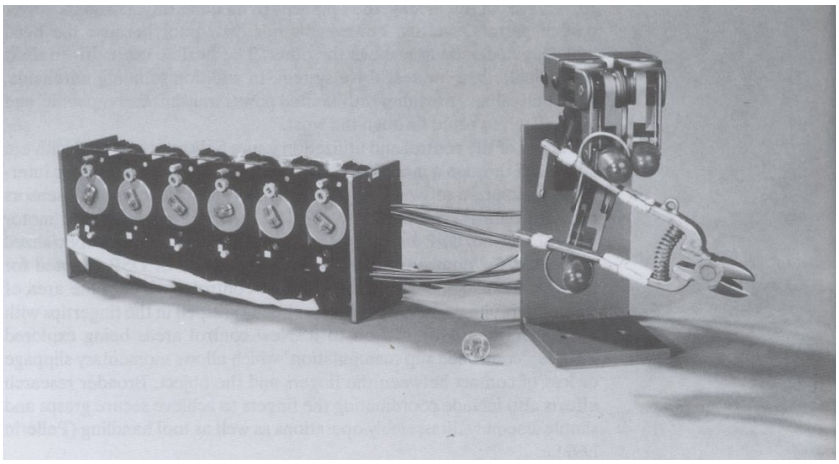

FIGURE 3.15: Salisbury hand.

The unit has been sold primarily to university and corporate research departments for laboratory demonstrations. In an ironic conflict of complexity versus simplicity, each three DoFs finger has no less than four Teflon coated control cables that slide in Teflon lined conduits, yet the fingers are modular to reduce the number of parts. Finger position information is produced by strain gauge sensors and motor position sensors located behind each proximal joint. The tension signal is translated into a joint torque signal used to close the servo loop. Fingertips feature a highly compliant rubber-like material that provides friction and "give" for a secure grip.

An actuator pack of 12 samarium-cobalt LO-COG DC servo motors with 25:1 speed reducers power cables that drive the fingers. Each of the three fingers is composed of a double jointed head knuckle that provides the joint with plus or minus 90 degrees of pitch and yaw motion. An additional knuckle above the head knuckle has a range of plus or

Technical Data	
Size	≈ 1.2
Number of fingers	3
Number of active DoF	9
Number of actuators	12

Table 3.11: Technical data of the Stanford/JPL (Salisbury) hand.

minus 135 degrees. This increased range compensates for the absence of the third knuckle found in the human finger, but unlike the human head knuckle, the pitch and yaw axes do not intersect in the head knuckle. Advantages of this include the simplicity of modular fingers and the lower cost of parts.

Dexterity, however, is relatively poor because the head knuckles stack one axis above the other. The flexible cable drivetrain is less reliable than a direct drive system. In addition to being unreliable, push/pull cables have inherently limited power transmission capability and are difficult to route through the wrist.

Some of the control and utilization issues Salisbury grappled with are addressed through a modified PUMA controller for the electronic interface. Customized software for driving fingers and interacting with sensors provides data fusion. Salisbury predicts the next generation of motor control will be DSP based (digital signal processor), with specialized processors for number crunching, with some form of DSP adopted for motor control.

3.4.2.5 DLR hands

In 1997 DLR developed one of the first articulated hands with completely integrated actuators and electronics (Figure 3.16(a)). The DLR I hand has been used for several years and it is the first version of a new hand according to a fully integrated mechatronics concept which yielded a reasonably better performance in grasping and manipulation applications.

In order to achieve the goal of maximum flexibility and performance, the philosophy is the miniaturization and complete integration of all components of the hand and also the massive reduction of cabling. As on DLR's Hand I the main aspects in developing the new hand have been the maximum performance to improve autonomous grasping and fine manipulation possibilities and the use of fully integrated actuators and electronics without a forearm. For this reason the size of DLR hand is approximately 1.5 times the size of a human hand.

Due to maintenance problems with Hand I and in order to reduce weight and production costs the fingers and base joints of Hand II [7] have been developed as an open skeleton structure (Figure 3.16(a)). The open structure is covered by 4 semi shells and one 2-component fingertip housing implemented in stereolitography and vacuum mold. This

(a) DLR I Hand

(b) DLR II Hand

FIGURE 3.16: Pictures of the DLR I hand and of the DLR II hand.

Technical Data		
Size		≈ 1.5
Number of fingers		4
Number of active DoF		13
Number of actuators		13
Number of sensors		64
Weight	g	320
Maximum force	N	30

TABLE 3.12: Technical data of the DLR II hand.

enables to test the influence of different shapes of the outer surfaces on grasping tasks without redesigning finger parts. An overall number of 13 DoFs was found.

The three independent joints (there is one additional coupled joint) of each finger are equipped with appropriate actuators. The actuation systems essentially consist of brushless dc-motors, tooth belts, harmonic drive gears and bevel gears in the base joint. The configuration differs among the different joints.

The actuation system in the medial joint is designed to meet the conditions in the base joint when the finger is in stretched position and can apply a force of up to 30 N on the fingertip.

Each joint is equipped with strain gauges based joint torque sensors and specially designed potentiometers based on conductive plastic. Beside the torque sensors in each joint there is a tiny six dimensional force torque sensor for each finger tip. The potentiometers are not absolutely necessary, since one may calculate the joint position from the motor position, however they provide a more accurate information of joint position, and they can be the solution to eliminate the necessity of referencing the fingers after power up. Moreover each finger integrates 6 temperature sensors.

A summary of the technical data of the DLR II hand are presented in Table 3.12.

3.4.2.6 Robonaut Hand

The Robonaut hand is one of the first hand under development for space EVA use characterised by the size and capability close to a suited astronaut's hand [55]. The Robonaut Hand has a total of 14 DoFs. It consists of:

- a forearm which houses the motors and drive electronics;
- a 2 DoFs wrist;
- a 5 fingers, 12 DoFs hand.

The forearm houses all fourteen motors, 12 separate circuit boards, and all of the wiring for the hand.

In order to match the size of an astronaut's gloved hand, the motors are mounted outside the hand (inside the forearm), and mechanical power is transmitted through a flexible drive train.

The finger drive consists of a brushless DC motor equipped with an encoder and a 14 to 1 planetary gear head. Coupled to the motors are stainless steel high flexibility flexshafts. At the distal end of the flex shaft is a small modular leadscrew assembly. The assembly converts the rotary motion of the flexshaft to linear motion. The top of the lead screw assemblies are clamped into the palm of the hand to allow the shell to stretch or compress under load, thereby giving a direct reading of force acting on the fingers. The result is a compact yet rugged drive train.

Overall the hand is equipped with forty-three sensors not including tactile sensing. Each joint is equipped with embedded absolute position sensors and each motor is equipped with incremental encoders. Each of the leadscrew assemblies as well as the wrist ball joint links are instrumented as load cells to provide force feedback.

The hand itself is broken down into two sections:

- a dexterous work set which is used for manipulation;
- a grasping set which allows the hand to maintain a stable grasp while manipulating or actuating a given object.

(a)

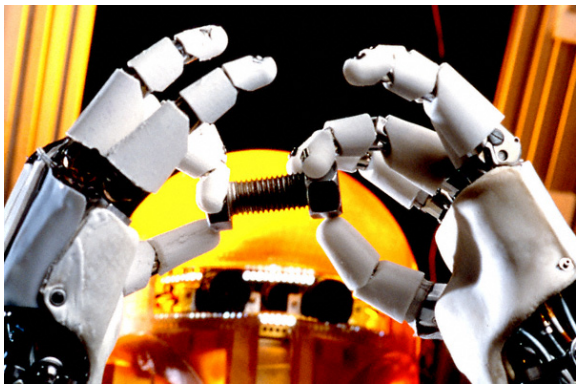

(b)

FIGURE 3.17: The Robonaut hand.

Technical Data	
Size	≈ 1.5
Number of fingers	5
Number of active DoF	12+2
Number of actuators	14
Number of sensors	43 + tactile

TABLE 3.13: Technical data of the Robonaut hand.

The dexterous set consists of two fingers with 3 DoFs (middle and index) and a opposable thumb with 3 DoFs. The grasping set consists of two 1-DoF fingers (ring and pinkie) and a palm degree of freedom. A summary of the technical data of the Robonaut hand are presented in Table 3.13.

3.5 Control of multifunctional prosthetic hands using EMG

In Figure **??** the schematic diagram of a multifunctional hand prosthesis is illustrated. Even if we could increase the number of DoFs of the prosthesis, the main limitation would remain the control of the artificial device [95]. In fact, many DoFs cannot be controlled directly by the subject, unless using complicate coding of movements which, in turn, requires high level

of training. The user interface, on the contrary, should be as intuitive and non-fatiguing as possible to enable practical long-term use of the device, as the user cannot be productive if she/he must spend a large portion of her/his energy and concentration controlling the artificial hand [30].

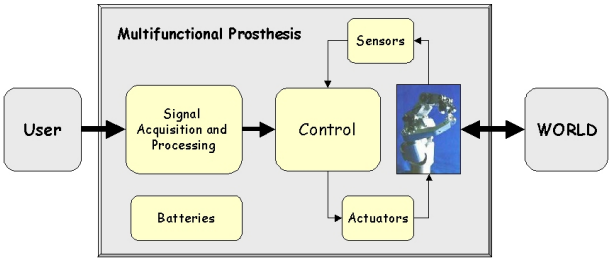

Figure 3.18: Scheme of a multifunctional hand prosthesis. A multifunctional hand prosthesis is a mechatronic device composed by several modules: Signal acquisition and processing; Control; Sensors; Actuators; Batteries.

Several possibilities were exploited during last years. For examples, hand prosthesis could be controlled by harness (*body-powered*), by Tendon Activated Pneumatic (TAP) foam sensors [12, 16], or by Hall effect sensors [45]. Another approach uses direct tunnel muscle cineplasties [11, 92], in an extension of the Extended Physical Proprioception (EPP) concept [82].

Electromyographic signal (EMG) is a simple and easy to obtain source of information on what the user of a prosthesis would like to do with her/his artificial hand [95]. Surface electrodes are easy to use and manage, and they do not require any surgery. Moreover, there are no harness that could limit the movements of the forearm. It is possible to control an active device with just one differential electrode placed on the residual limb, even in infants[93]. The technology of EMG signal processing is making steady progress. The evolution of the use of the EMG signal in order to actively control a prosthetic hand is showed in Figure 3.19.

Reiter [73] in 1948 was the first who used the EMG signal to control a simple prosthetic device. Nowadays, all prosthetic devices used in clinical practice have one ore two active DoFs, directly controlled by a couple of electrodes placed on two antagonist muscles, either in proportional or on/off mode [79]. The use of a larger number of electrodes in order to control more active DoFs has several drawbacks, because the coding of the movements and the number of electrodes would greatly increment the problems in fabricating and using the socket.

Starting from 1975, some research groups [34, 35, 77] realized that a correct modelling of the EMG signal could make it possible to control a device with more than just one DoF. Unfortunately the hardware and software resources available at that time were not sufficient to realize a device that could be used in clinical practice. In particular, Graupe *et al*

[35] with AR modelling and Bayesian discrimination were able to successfully discriminate between 6 different classes of movement, with a success rate up to 99%. Unfortunately, these results were obtained only after 12 hours of user training, and performance significantly degraded with time, because of the modification of EMG generated by the user. The use of Artificial Neural Networks (ANNs) [44] could reduce the time needed for the user training, but the problems of the modification related to signal variation with time and from person to person still remain.

In all these works EMG signal was used in its stationary phase, and users were trained to contract their residual muscles in order to obtain constant levels of EMG. In this way the control of the prosthetic device was simplified (it could be a simple proportional control, as showed in Dorcas and Scott [25]) but a lot of information was ignored.

In 1993 Hudgins *et al* [39] firstly proposed a new control strategy for artificial devices. In fact, they observed that there is considerable structure in the myoelectric signal during the onset of a contraction. This structure is distinct for different limb movements and could be used as source of information for the classification of the EMG signal. They were able to discriminate between 4 different movements with just one bipolar electrode by extracting Mean Absolute Value (MAV), Mean Absolute Value Slope (MAVSLP), Zero Crossing (ZC), Slope Sign Changes (SSC), and Waveform Length (WL) from the measured signal, with a 2-layer ANN. However, the discrimination error was still quite high (more than 10%).

In recent years EMG signal has been largely investigated, both for the realization of multifunctional myoelectric prostheses [27, 63, 67] and for the improvement of teleoperation of robotic devices [30], but yet all these systems are not capable of successfully controlling a multifunctional hand. The major problem is the time-variant characteristics of the EMG signal, due to physiological changes in the muscles and to the changes in the coupling between skin and the electrodes. An equally important problem is the stochastic nature of the EMG, thus resulting in parameter estimation errors which, in turn, cause classification and/or control difficulties. Moreover, some control errors are generally introduced by the inability of the patient to reliably generate and reproduce the target contraction signals (operator errors). A possible solution is the realization of an *On-line Learning Module*, either supervised [67, 68, 68] or unsupervised [32], in order to continuously adapt the parameters of the classifier. For example, Nishikawa and colleagues [69] were able to discriminate among ten different movements of the forearm on three normal subjects with two channels EMG signals by using Gabor Transform, MAV, and feed-forward ANN, but the success rate was lower than 90%.

Some of the problems of the myoelectric control could be overcome by automating some grasping functions [47–49]. Some attempts of controlling multifunctional devices by using more than a couple of electrodes [29] have been made, and the use of nerve-muscle graft technique [46] have been proposed, but increasing the number of electrodes is not useful in clinical practice, as it introduces additional discomfort in using the prosthesis.

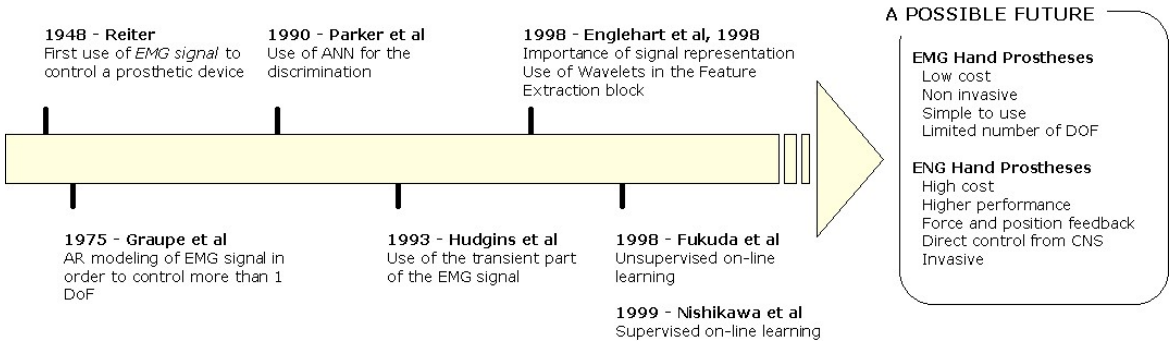

Figure 3.19: Evolution and possible future of the use of the EMG signal in the control of hand prosthetic devices.

3.6 Discussion

The performance of the hand prostheses are quite far from the performance of the human hand. In clinical practice, simple grippers with just one active DoF are used. In the research field, instead, several prosthetic hands with a greater number of active DoFs have been presented. Each of them has its advantages and its drawbacks, but none of them seem to be usable in clinical practice. Moreover, in the last decades several robotic hands have been presented. They present a number of active DoFs similar to the one of the natural hand, but their weight and their size make their application as prostheses impossible. Moreover, at present prosthetic users have not so much reliable opportunities to control more than one DoF.

A comparison of the performance of the human hand, prosthetic devices and robotic hands is presented in Table 3.14. This table will be used in the next chapter in order to define the design goals for a new artificial hand.

	Size (norm.)	# of fingers	DoFs	Actuators (type)	Control	# of sensors	Weight (gr)	Force (N)	Speed (sec)
Human hand [41]	1	5	22	38 (I+E)	E	$\simeq$17'000	$\simeq 400$	> 300	0.25
Ottobock SUVA [70]	1	3	1	1 (E)	I	2	600	$\simeq 100$	< 1
MARCUS Hand [49]	$\simeq 1.1$	3	2	2 (I)	I	3	-	-	-
Southampton hand [53]	$\simeq 1$	5	6	6 (E)	E	-	400	38	2.5 [a]
Hokkaido hand [31]	> 1	5	7	7 (E)	E	-	125	-	-
Karlsruhe [78]	$\simeq 1$	5	17	17 (E)	E	-	20[b]	12	0.1
NTU Hand [54]	$\simeq 1$	5	17	17 (E)	E	35	1570	-	-
Utah/MIT [84]	$\simeq 2$	4	16	32 (E)	E	16	-	31.8	-
Belgrade/USC [4]	$\simeq 1.1$	4	4	4 (E)	E	23+4	-	-	-
Stanford/JPL Hand [58]	$\simeq 1.2$	3	9	12 (E)	E	-	1100[c]	-45	-
DLR Hand II [7]	$\simeq 1.5$	4	13	13 (E)	E	64	320	30	-
Robonaut Hand [55]	$\simeq 1.5$	5	12 + 2	14 (E)	E	43 + tactile	-	-	-

TABLE 3.14: Comparison among several types of artificial hands. In the Actuator type and in the Control rows, 'I' means 'internal', and 'E' means 'external'. The size of the hand is normalized recpect to the adult human hand.

[a] Only for the flexion movement.
[b] 20 grams is just the weigth of the mechanical structure of a single finger.
[c] Plus gr. 5500 for the forearm.

Four

The biomechatronic approach

A continuous challenge for scientists and engineers is to replicate the sensory-motor function of the human hand, a complex and adaptable system, capable of both delicate and precise manipulation and power grasping of heavy objects [10, 43]. This result is achieved by a combination of a large number of Degrees of Freedom (DoFs), proprioceptive and exteroceptive sensors, and a complex hierarchical architecture control [41]. However, despite of this complexity, the efforts required to the user during the daily activities are very small, even if this ability is achieved only after several years of unconscious and conscious training.

During the last two decades several robotic and anthropomorphic hands has been developed. All these hands have a high number of DoFs (up to 16), and have a dexterity comparable to that of the human hand (§3.4.2). Unfortunately, all these hands cannot be used as prostheses, because their actuation and control systems are quite heavy and bulky, and thus they cannot be embedded within the hand nor donned by the user (Table 3.14).

On the contrary, current commercial prosthetic hands, aimed at replicating the natural system, are unable to provide enough grasping functionality and to deliver sensory-motor information to the user [1, 15, 49]. Commercially available prosthetic devices (§3.3), such as Otto Bock SensorHand [70], as well as multifunctional hand designs (§3.4) are far from providing the manipulation capabilities of the human hand [17]. Moreover, they require a great deal of training and of concentration in order to be effectively used. This is due to many different reasons. For example, in prosthetic hands active bending is restricted to two or three joints, actuated by a single motor drive acting simultaneously on the metacarpophalangeal (MP) joints of the thumb, of the index and of the middle finger, while other joints are fixed (Table 3.14).

Some of limitations of the current artificial devices, aimed at the functional substitution of the human hand, could be overcome by pursuing a "biomechatronic" design approach:

1. analysis of the model (the human hand) - Chapter 2;

2. analysis of the state of the art of prosthetic hands in clinical applications - §3.3;

3. analysis of the state of the art of prosthetic hands in research - §3.4.1;
4. analysis of the state of the art of robotic hands in research - §3.4.2;
5. analysis of the state of the art of the control techniques for the artificial hands - §3.5;
6. identification of the drawbacks of current artificial hands - §4.1;
7. identification of the specifications for the realization and the control of a truly cybernetic prosthetic hand - §4.2.

In any case, it should be considered that biological structures are still superior to any artificial device.

4.1 Drawbacks of the current prosthetic devices

As we have seen in the Chapter 3, prosthetic hands, nowadays, have optimal reliability and robustness, but at present many limitations which can be summarized as follows [9]:

1. the low grasping capabilities, because current prosthetic hands have no more than two active DoFs (and act like a simple gripper);
2. the non cosmetic and unnatural appearance of the grasping movement due to the low number of DoFs. On the other hand, cosmetic devices have no active functionality, and can be used only as a passive support;
3. the lack of a "natural", intuitive and non-fatiguing, command interface, to enable practical long-term use of a multifunctional prosthetic hand.
4. the lack of sensory information given to the user. There is no feedback except visual outside, so the user has to judge by sight when to stop moving the hand. Otto Bock HealthCare GmbH recently introduced in the market the SUVA Hand (§3.3.4), which uses a force sensor in order to optimize the grip strength, but there is still no sensory feedback besides direct visualization and such subtle clues as the sound of the speed changes of the motor and transmission;

The first two points could be overcome by a complete redesign of the hand prosthesis [8, 9]. Anyhow, even if we could increase the number of DoFs of the prosthesis, the main limitation would remain the control of the artificial device. In fact, many DoFs cannot be controlled directly by the subject, unless using complicate coding of movements which, in turn, requires high level of training [95]. The user interface, on the contrary, should be as intuitive and non-fatiguing as possible to enable practical long-term use of the device, as the user cannot be productive if she/he must spend a large portion of her/his energy and concentration controlling the artificial hand [30].

4.2 Specifications for the artificial device

According to the analysis of the human hand and of its artificial counterparts, some guidelines could be defined for the realization of a new artificial device (Table 4.1). In particular, these aspects should be considered:

- Mechanism;
- Actuators;
- Control;
- Sensors;
- Human-machine interface.

In the next subsections some general consideration and some specification for each module of the hand will be provided.

4.2.1 Mechanism

The mechanical part of the artificial device should be kept as simple and as reliable as possible, in order to be used during normal activities in daily living (ADLs). A high number of DoFs is desirable, but it should be obtained without increasing the complexity of the Human-Machine Interface (henceforth HMI) and of the control.

Moreover, the system should be unbackdrivable, in order to save the charge of the batteries during grasping. Once the desired level of force is reached, the power supply to the motor is cut off, but the grasp remains stable.

4.2.2 Actuators

Current prosthetic devices have only one bulky DC-motor that allows the control of only one DoF. More DoFs, both passive or active, are advisable. Another design aspect that should be considered is the dimension of the motors. A smaller motor means a smaller hand, thus increasing the possibilities of application of the hand in more distal amputation (wrist disarticulation or partial hand amputation, for example).

4.2.3 Control

The control scheme should be designed in order to make the user feel the prosthetic device as an extension of his arm, or better like her/his lost hand, instead of an external tool [82]. Ideally, the HMI should be able to decode the user intentions, and the control unit should control directly the prosthesis, without requiring any additional user effort.

4.2.4 Sensors

Current prosthetic hand have a few sensors on board, or no sensor at all. In this way, the user is forced to keep the attention on the hand continuously, thus increasing the discomfort during ADLs. Some proprioceptive and exteroceptive sensors, similar to the human sensory system, are advisable in order to let the hand automatically grasp the objects.

4.2.5 Human-machine interface

The Human-machine interface HMI should be kept as simple as possible. An ideal interface should be able to acquire the user intentions without causing any discomfort or fatigue to the user.

Specifications for a new hand prosthesis	
DoFs	$\geq 1, \leq 22$
Type of Grasps	Power Grasp and Precision Grasp
Force of power grasp	$\simeq$ 100 N
Range of flexion	100^o depending on joint
Max. duration of grasp	Variable with energy
Proprioceptive sensing	Position
	Movement
	Force
Exteroceptive sensing	Pression
	Force
	Acceleration
	Temperature
	Pain
Proportional Control and Dexterity	Ability to regulate force and velocity according to the type of grasp
Stability	The grasp is stable against incipient slip or external load
Duration of the batteries	$\simeq$ 8 hours
Total volume	50 cc
Weight	$\simeq$ 400 g

Table 4.1: Technical specifications for .

4.3 The formal control scheme of a multifunctional artificial hand

In Figure 4.1 the control scheme for a multifunctional hand prosthesis is illustrated. As seen in §3.5, the main limitation in the use of an artificial prosthesis is the control system [95], that should be as intuitive and non-fatiguing as possible to enable practical long-term use of the device.

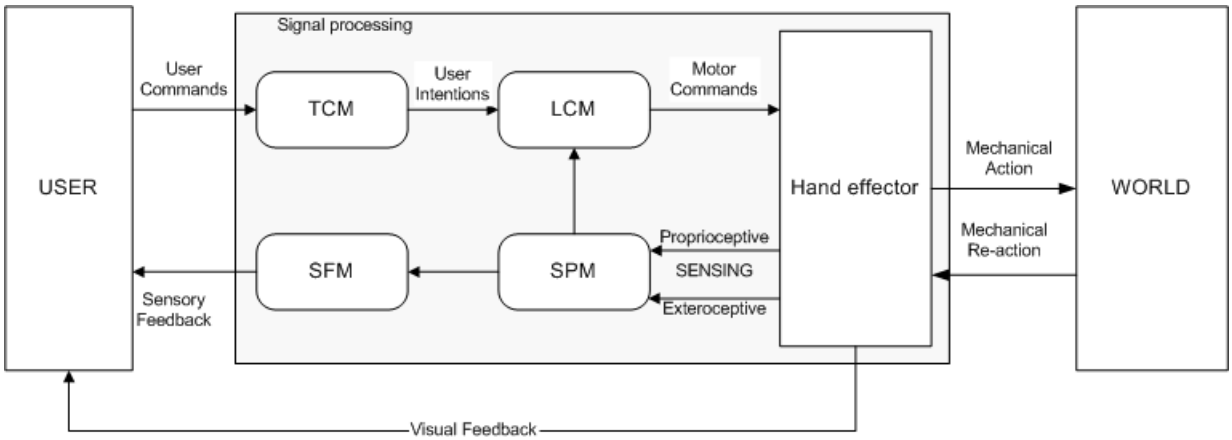

FIGURE 4.1: The formal scheme of an artificial prosthetic device.

The prosthetic hand could be seen as the interface between the user and the real world (Figure 4.1). The control system of the hand is composed by several modules:

Top-Level Controlling Module (TCM): this module acquires the input signals from the users and then generates the commands for the Low-Level Controlling Module (§4.3.1).

Low-Level Controlling Module (LCM): this module receives as input the signals generated by the TCM, and uses the signals coming from the Sensory Processing Module (SPM) to control the movement of the hand and the grasping force (§4.3.2).

Sensory Processing Module (SPM): this module acquires the signals coming from the sensors in the hand and converts them to information useful for the closed loop control of the hand (§4.3.3).

Sensory Feedback Module (SFM): this module acquires the information generated by the SPM and bring them to the user using an appropriate coding (§4.3.4).

These modules could be present or not in a particular prosthetic device according to its complexity.

In the next sections the behavior of each module will be explained in details, outlining their main characteristics. Then, in the next chapters these modules will be developed and realized for three different hand prostheses.

4.3.1 The Top-Level Controlling Module (TCM)

A prosthetic device could be controlled in several different ways. Simple mechanical devices could be controlled by harness (*body-powered prostheses*), with the movement of the shoulders that controls the opening and closing of the prosthetic device. Active prostheses requires different kinds of input. For example, some researchers are trying to use Tendon Activated Pneumatic (TAP) foam sensors [12, 16], or Hall effect sensors [45] in order to detect the movement of the residual muscles of the stump. Another approach uses direct tunnel muscle cineplasties [11, 92], in an extension of the Extended Physical Proprioception (EPP) concept [82].

The most common solution (both in clinical practice and in the research field) is the use of Electromyographic (EMG) signals, because they provide an easy and non-invasive access to physiological processes that cause the contraction of the muscles. Anyhow, the myoelectric signal permits the control of no more than one or two active DoFs (generally, 1 DoF for the gripper and 1 DoF for the wrist). Limitations in the mechanics of the prosthetic device and in the processing of EMG data make it impossible to control more [79]. In the past decades, and especially during the last years, many efforts have been carried out in order to implement effective control algorithms based on the processing of EMG signals. Starting from the first attempts in the late '40 [73], several EMG-based algorithms have been developed and used in order to enhance the functionality and the usability of prosthetic hands [95]. However, despite of all these efforts, EMG signal analysis seems to be quite limited in the number of possible functions that could be restored by using a few electrodes. Moreover, the EMG signal cannot provide any feedback to the user.

A possible solution to overcome the limits of the EMG-based approach could be the realization of an interface between the Peripheral Nervous System (PNS) and the artificial device (i.e., a "natural" Neural Interface (NI)) to record and stimulate the PNS in a selective way [19, 21, 62, 74, 88].

Indipendently from the input signals, the formal scheme for the acquisition and analysis of the inputs for the control of prosthetic devices is composed of several modules (Figure 4.2):

1. signal conditioning and preprocessing;
2. feature extraction;
3. dimensionality reduction;
4. pattern recognition;
5. off-line and on-line learning.

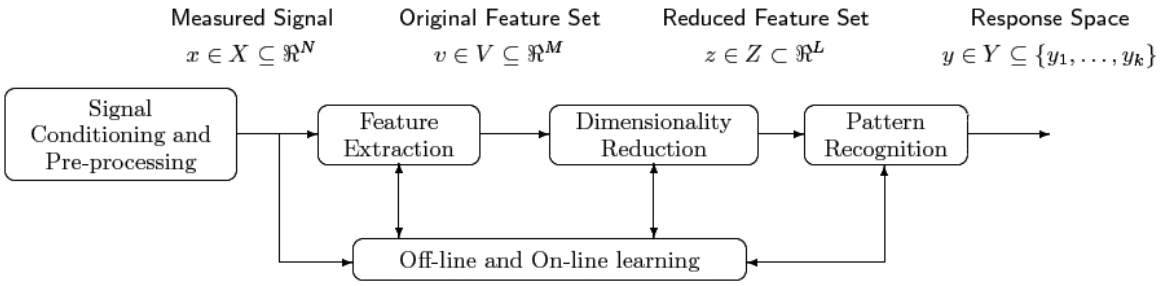

FIGURE 4.2: The formal scheme for the acquisition and analysis of input signals for the control of prosthetic devices.

The first module preprocesses the input signals in order to reduce noise artifacts and/or enhance spectral components which contain important information for data analysis. Moreover, it detects the onset of the movement, and activates all the following modules. During the feature extraction phase, the measured EMG signal $x \in X \subseteq \Re^N$ is processed in order to emphasize the relevant structures in the data, while rejecting noise and irrelevant data, producing the so called "Original Feature Set" $v \in V \subseteq \Re^M$. Sometimes a reduction of the dimensionality is needed, to simplify the task of the classifier. In this case, a pattern recognition algorithm is used on the (reduced) feature set $z \in Z \subseteq \Re^L$ and the measured signal is classified into the output space $y \in Y = \{y_1, \ldots, y_k\}$. The learning modules are used to adapt the device to the input signals generated by the users, because they are (in general) subject to several fluctuations, depending on a wide range of external conditions [95].

4.3.2 The Low-Level Controlling Module (LCM)

The LCM is dedicated to the control of the motors of the hand by using as inputs the user intensions (detected by the TCM) and the informatiomn coming from the SPM (figure 4.3). The LCM uses part of the sensory data according to its internal state.
In general, for each of the internal state of the LCM the desired value (coming from the TCM) is compared with the measured value (coming from the SPM), thus generating an error signal. This error, then, is used to control the motors of the prosthetic device in the appropriate way.

The type of the control used could be, for example [70]:

- simple on-off control: in this case the user sends all the commands as TTL digital inputs $(0 - 5\text{V})$ to the LCM.

- proportional opening and closing: the inputs to the LCM are analogic signals, ranging from $0V$ to $+5V$;

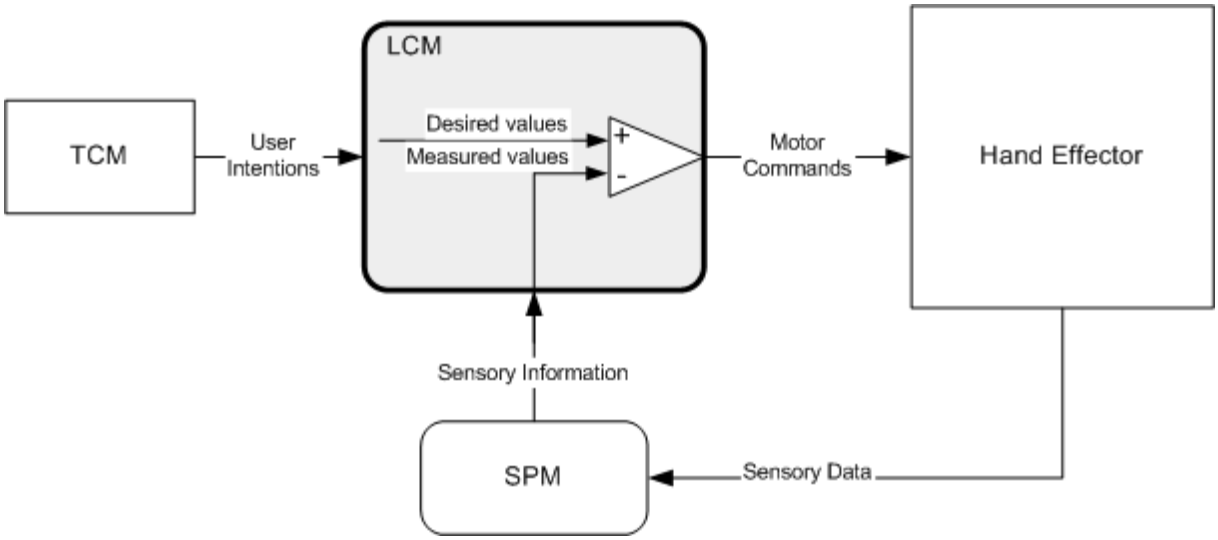

Figure 4.3: The formal scheme of the Low level Control Module.

Moreover, depending on the sensors of the prosthetic hand, the low level control could be *open loop* or *closed loop*.

4.3.3 The Sensory Processing Module (SPM)

The SPM converts the transduction of some physical quantity (i.e., dispacement of a slider, deformation of a cantilever, and so on) into a suitable analogic signal. In general, for each transduced signal $s \in S \subseteq \Re$ the following operations are carried out (figure 4.4):

1. the signal $s \in S \subseteq \Re$ is acquired from the hand by an appropriate electronic interface;
2. this signal is then conditioned (i.e., prefiltered ($s_f \in S \subseteq \Re$) and amplified ($s_{fa} \in S \subseteq \Re$)) in order to respect the Nyquist's theorem and in order to maximize the output;
3. the conditioned signal is then sampled at an appropriate frequency ($\hat{s} \in S \subseteq Z$), typically twice the maximum frequency present in the conditioned signal.
4. After the digitalization, the signal $\hat{s}$ is ready to be used for the closed loop control of the hand prosthis and for the sensosy feedback.

4.3.4 The Sensory Feedback Module (SFM)

In general, current prosthetic devices do not provide any direct feedback to the user. In particular this is true with myoelectric devices, in which the user must control the hand

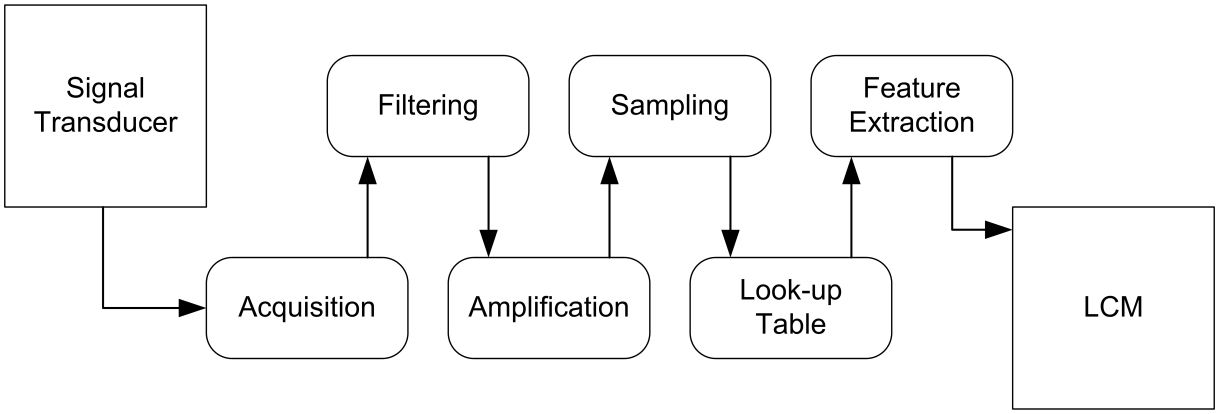

FIGURE 4.4: The formal scheme of the Sensory Processing Module.

with her/his eyes during operations. On the contrary, Body-powered devices provide a natural proprioception of the hand because they use the movement of the shoulders to open and close the hand.

In literature there are several examples of Cognitive Feedback applied to prosthetic devices, by which the data coming from sensors are delivered to the user by stimulating the skin, either with mechanical, electrical or thermal stimuli [57], or by using auditory signals [56]. All these systems, however, even if promising are not successful, because the sensation that is felt is not a natural one, and the device results quite uncomfortable.

Five

The RTR1 prosthetic hand

5.1 Introduction

We have seen in the previous chapters that commercially available prosthetic devices, as well as multifunctional hand designs [1, 2, 15, 26, 49, 81, 89] have good (sometimes excellent) reliability and robustness, but their grasping capabilities are far to be similar to the capabilities of the human hand [17].

The objective of this work is to develop an artificial hand aimed at replicating appearance and performance of the natural hand. The ultimate goal of this research is to obtain a complete functional substitution of the natural hand. This means that the artificial hand should be felt by the user as a part of the own body (Extended Physiological Proprioception – EPP [82]), and it should provide the user with the same functions of natural hand: tactile exploration, grasping and manipulation ("cybernetic" prosthesis [24]).

In fact, the artificial hands for prosthetic applications pose challenging specifications and problems, as is usually the case for devices to be used for functional replacement in clinical practice. These problems have forced the development of simple, robust and reliable commercial prosthetic hands, as the Otto Bock SensorHand [70] prosthesis which is widely implanted and appreciated by users. The Otto Bock hand has only one degree of freedom (DoF), it can move the fingers at proportional speed from 15 to 130 mm/sec and can generate a grip force up to 100 N.

But, as already said in Chapter 3, these kind of hands have some major drawback:

1. lack of sensory information given to the amputee;
2. lack of a "natural" command interface;
3. limited grasping capabilities;
4. unnatural movements of fingers during grasping.

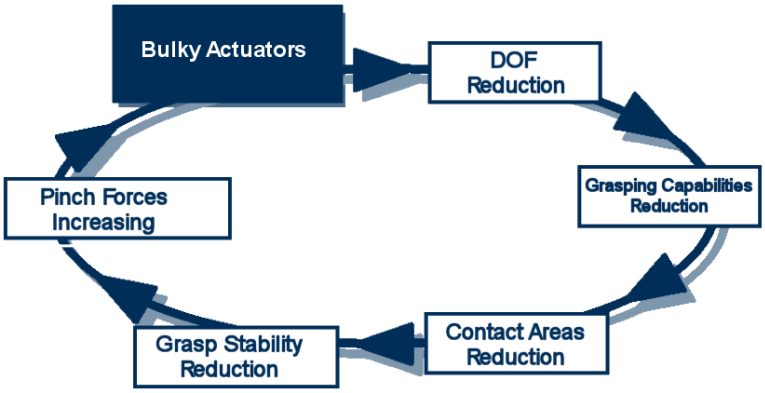

Figure 5.1: The standard approach to grasp based on traditional actuators.

The first and second problems can be addressed by developing a "natural" interface between the Peripheral Nervous System (PNS) and the artificial device (i.e., a "natural" Neural Interface (NI)) to record and stimulate the PNS in a selective way. The neural interface is the enabling technology for achieving ENG-based control of the prosthesis, i.e. for providing the sensory connection between the artificial hand and the amputee. Sensory feedback can be restored by stimulating in an appropriate way user's afferent nerves after characterisation of afferent PNS signals in response to mechanical and proprioceptive stimuli.

In general, cosmetics requirements force to incorporate the entire device in a glove, and to keep size and mass of the entire device comparable to that of the human hand. It turns out that the combination of robust design goals, cosmetics and limitations of available components, can be matched only with a drastic reduction of DoFs, as compared to those of the natural hand. In fact, in prosthetic hands active bending of joints is restricted only to two or three joints (metacarpo-phalangeal joints of the thumb, of the index and of the middle finger), while other joints are fixed.

Due to the lack of DoFs, prostheses are characterized by low grasping functionality, and thus they do not allow adequate encirclement of objects in comparison to the human hand; low flexibility and low adaptability of artificial fingers lead to instability of the grasp in presence of an external perturbation, as illustrated in [76]. In conclusion, commercial prostheses have been designed to be simple, robust, and low cost, at the expense of their grasping ability.

The adoption of bulky and heavy actuators in the design of commercial upper limb prostheses, leads to an extreme reduction of DoFs. The goal is to achieve stable grasp by means of high grip forces. This design philosophy (the so called "standard approach") can be represented as a loop (Figure 5.1).

The above schematization shows how this approach leads to design hands with a maximum of two DoFs and able to obtain stable grasps using high pinch force (up to 100 N).

Even if they are simple to implement and control, mechanical grippers, such as state of the art prosthetic hands, are not adaptable and may cause problems of low grasping stability [50].

5.2 Biomechatronic design

In order to try to solve this problem a new approach to the design of the prosthetic device should be followed. The main requirements that should be considered since the very beginning of prosthetic hand design are the following:

- cosmetics;
- controllability;
- noiselessness;
- lightness;
- low energy consumption.

These requirements can be fulfilled by an integrated design approach aimed at embedding different functions (mechanisms, actuation, sensing and control) within a housing closely replicating the shape, size and appearance of the human hand [8]. This approach can be synthesized with the term: "*biomechatronic*" design [22].

5.2.1 Architecture of the biomechatronic hand

The design goal of the biomechatronic hand is to improve to some extent one of the most important limitations of current prosthetic hands (no dexterity and no adaptability), while preserving the main advantages of such hands, that is lightness and simplicity. This objective has been pursued by using small actuators (two for each finger) instead of one single large actuator (as in most current prosthetic hands), and by designing a kinematic architecture able to provide better adaptation to object shape during grasping. It turns out that the use of micro-motors allows to augment functionality in grasping objects by means of "human-like" compliant movements of fingers. This result addresses the very basic requirements of "cosmetic" appearance of the hand in static and dynamic conditions [22].

The biomechatronic hand has three fingers to provide a tripod grasp: two identical fingers (index and middle fingers) and the thumb (see Fig. 5.2). In fact, as explained in [58], at least three fingers (nonrolling and nonsliding contact) are necessary to completely restrain an object. The hand performs two grasping tasks:

1. Cylindrical grasp;
2. Tripod grasp.

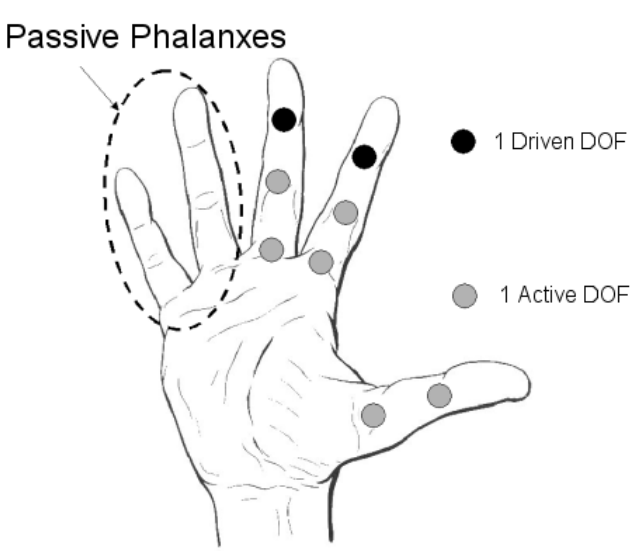

(a) Architecture of the first prototype

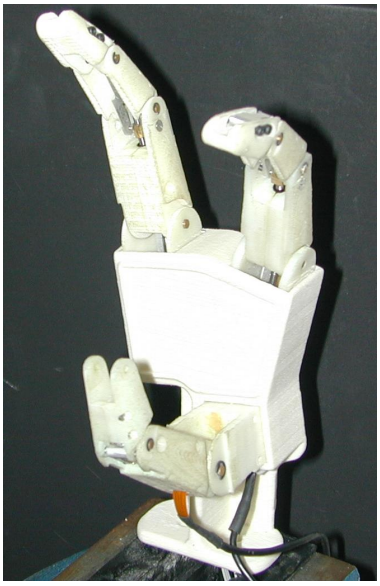

(b) Photograph of the first prototype

Figure 5.2: Architecture (left) and photograph of the first prototype (right) of the biomechatronic hand.

The finger actuation system is based on two micro-actuators, which drive the metacarpophalangeal (MP) and the proximal interphalangeal (PIP) joints, respectively; for cosmetic reasons, both actuators are fully integrated in the hand structure: the first in the palm and the second within the proximal phalange. The distal interphalangeal (DIP) joint is passively driven by a four-bars link connected to the PIP joint. The thumb actuation system is based on micro-actuators and has two active DoFs at the MP and at the interphalangeal (IP) joint, respectively.

5.2.2 The actuation system

In order to overcome the limitations of the standard approach to the realization of hand prosthesis, a new approach has been proposed: the loop of Figure 5.1 could be inverted by using micro-actuators and by exploiting the advantage of increasing DoFs (Figure 5.3).

According to this design philosophy, an artificial hand actuated by a plurality of microdrives would have enhanced mobility and thus larger contact areas between phalanges and grasped object. Therefore, a reduction of power actuation could be accepted and compensated by increasing contact areas in order to augment grasp stability. In fact, according to [22] a hand with independently movable fingers and multiple phalanges can encircle the object much better than a hand with rigid fingers. In addition, the contact area between an object and the finger can be larger and thus grasping stability is enhanced.

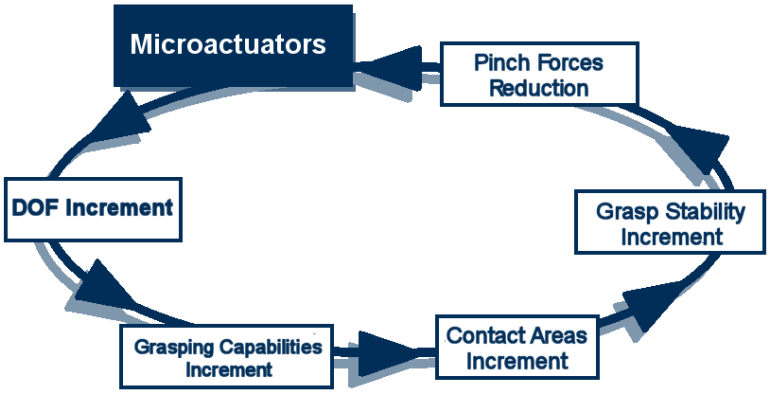

FIGURE 5.3: The proposed approach to grasp based on microactuators.

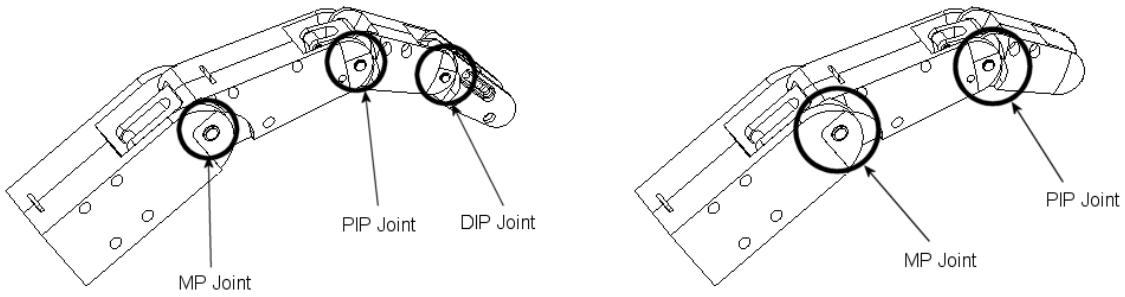

(a) Index/Middle finger (b) Thumb finger

FIGURE 5.4: Detail drawing of Index/Middle finger (left) and of the thumb (right).

5.3 Design of hand prototype

In order to demonstrate the feasibility of the described biomechatronic approach, a three fingered hand prototype with two identical fingers (index and middle) and thumb has been developed. Actuators, position sensors and 2D force sensors are integrated in the hand structure.

The index/middle finger has been designed by reproducing, as closely as possible, the size and kinematics of a human finger. Each finger consists of three phalanges and a palm housing, which is the part of the palm needed to house the proximal actuator (Figure 5.4(a)).

Smoovy brusheless DC motor	
Nominal force	12 N
Maximum speed	20 mm/s
Weight	3.2 g
Maximum load (axial)	40 N
Maximum load (radial)	25 N
Transmission rate	1:125
Gear stages	3

Table 5.1: Summary of the main characteristics of the Smoovy™(RMB, Eckweg, CH) micro drivers (5 mm diameter).

5.3.1 Actuator system architecture

In order to match the size of a human finger, two micro-motors have been integrated within the palm housing and the proximal phalange of each finger.

The selected micro-motors are Smoovy™ (RMB, Eckweg, CH) micro-drivers (5 mm diameter) high precision linear actuators, based on DC brushless motors with planetary gears. The rotary motion of the shaft is converted to linear motion using lead screw transmission.

The main mechanical characteristics of the linear actuators are listed below (Table 5.1).

The selected actuator fulfills almost all the specifications for application in the prosthetic finger: small size and low weight. The main problem encountered is related to noise, which turns out to be relatively high, at least in the current implementation. Despite of this limitation, we decided to proceed with the application of the linear actuator in order to investigate integration problems and global performance.

The shell housing provides mechanical resistance of the shaft to both axial and radial loads. This is very important during grasping tasks, when the forces generated from the thumb opposition act on the whole finger structure.

5.3.2 Kinematics architecture

The kinematics of each finger joint is described in the following subsections.

5.3.2.1 MP Joint

The proximal actuator is integrated in the palm and transmits the mechanical power through a slider crank mechanism to the proximal phalange providing flexion/extension

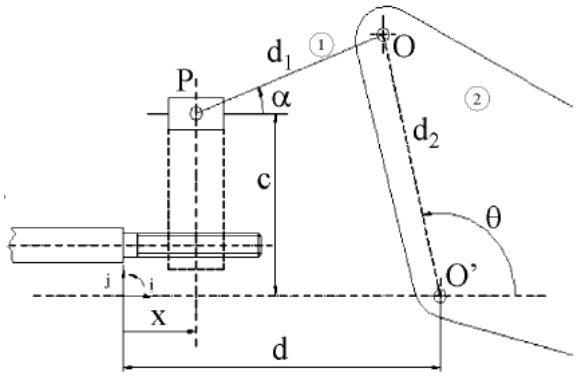

FIGURE 5.5: Detailed drawing of the slider crank mechanism in the MP joint.

movement (Figure 5.5). The slider is driven by the lead screw transmission directly mounted on the motor shaft. Member 1 is the connecting linkage and member 2 represents the proximal phalange.

Geometrical relations of the slider crank mechanism are:

$$\begin{cases} d_1 \ \sin\alpha + c = d_2 \sin\theta \Rightarrow \alpha = \alpha(\theta) \\ d - x = d_1 \ \cos\alpha - d_2 \cos\theta \Rightarrow \theta = \theta\,(x) \end{cases} \tag{5.1}$$

Symbols $c,\ d,\ d_1,\ d_2,\ \alpha$ and x refer to geometrical features of the slider crank mechanism and are defined according to Figure 5.5. In particular, θ represent the MP angular position with respect to an horizontal plane (30 [deg]: full extension and 120 [deg]: full flexion).

In order to obtain flexion velocity $\dot{\theta}$ of the proximal phalange as a function of translation velocity of the slider $\dot{x}$ we can write:

$$\begin{cases} \underline{v}_P = \dot{x}\ \underline{i} \\ \underline{v}_P = \underline{v}_O + \underline{\omega}_1 \wedge OP = \underline{v}_O + \dot{\alpha}\ \underline{k} \wedge OP \\ \underline{v}_O = \underline{\omega}_2 \wedge O'O = \dot{\theta}\ \underline{k} \wedge O'O \\ \dot{x}\ \underline{i} = \dot{\theta}\ \underline{k} \wedge O'O + \dot{\alpha}\ \underline{k} \wedge OP = -d_2\ \dot{\theta}\ \sin\theta\ \underline{i} + d_2\ \dot{\theta}\ \cos\theta \underline{j} + \\ \qquad\qquad + d_1\ \dot{\alpha}\ \sin\alpha\ \underline{i} - d_1\ \dot{\alpha}\ \cos\alpha\ \underline{j} \end{cases} \tag{5.2}$$

where $\underline{i}$, $\underline{j}$and $\underline{k}$are the three orthogonal versors, $\underline{v}_O$ and $\underline{v}_P$ are the velocities of points O and P, respectively and $\underline{\omega}_1$ and $\underline{\omega}_2$ are the angular velocities of the OP and of the OO' link, respectively.

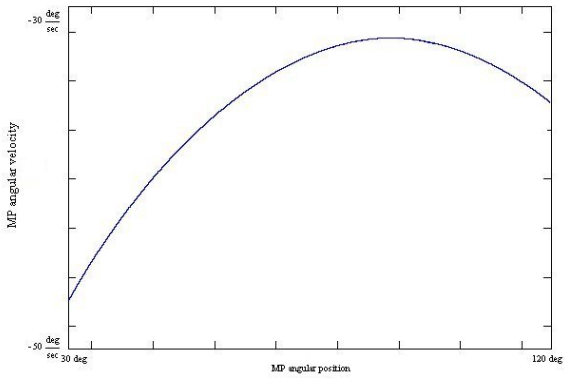

Figure 5.6: MP angular velocity $\dot{\theta}$ vs. MP angular position θ expected from calculations (see Figure 5.5 for variable definitions).

Projecting along the horizontal and vertical axes (described by versors $\underline{i}$and $\underline{j}$), we obtain:

$$\begin{cases} \dot{x} = -d_2\ \dot{\theta}\ \sin\theta + d_1\ \dot{\alpha}\ \sin\alpha \\ 0 = d_2\ \dot{\theta}\ \cos\theta - d_1\ \dot{\alpha}\ \cos\alpha \end{cases} \tag{5.3}$$

Substituting the second equation in the first equation we find the solution:

$$\begin{cases} \dot{\alpha} = \dfrac{d_2}{d_1}\ \dfrac{\cos\theta}{\cos\alpha}\ \dot{\theta} \\ \dot{x} = d_2\,(\cos\theta\ \tan\alpha - \sin\theta)\ \dot{\theta} \Rightarrow \dot{\theta} = \dot{\theta}(\theta, \dot{x}) \end{cases} \tag{5.4}$$

In Figure 5.6, the function $\dot{\theta} = \dot{\theta}\ (\theta, \dot{x})$ for the MP joint is showed. Where $\dot{x}$ is the maximum linear velocity of the micro-actuators (200 [mm/min]), $\dot{\theta}$ is the MP angular velocity.

5.3.2.2 PIP joint

The same mechanism used for the MP moves the PIP joint. Only the geometrical features are varied in order that the size mechanism fits within the space available according to the strict specifications of the biomechatronic hand (Table 5.2).

5.3.2.3 DIP joint

A four-bars link has been adopted for the DIP joint and its geometrical features have been designed in order to reproduce as closely as possible the natural DIP joint flexion. The mechanism has been synthesized according to the three prescribed positions method [28]. The lenght of the links A-D is showed in Table 5.3

Dimension	PIP joint	MP joint
d1	9 mm	18 mm
d2	4 mm	6 mm
C	5 mm	6 mm

TABLE 5.2: Geometrical features of the slider crank mechanism of the MP and of the PIP joints.

Link	Length
A	5.2 mm
B	28.7 mm
C	3.6 mm
D	25.1 mm

TABLE 5.3: Geometrical features of the four bars link mechanism.

PIP joint angle	DIP joint angle	Position
$\beta = 180$	$\chi = 180$	Full extension
$\beta = 150$	$\chi = 168.5$	Intermidiate position
$\beta = 100$	$\chi = 102$	Full flection

TABLE 5.4: Prescribed positions for four bars linkage synthesis.

The selected positions were the extended position, the flexed position and the intermediate position of the DIP joint, according to position assumed by the natural finger. These positions are illustrated in Table 5.4, where β and χ represent the PIP joint angular position and the DIP joint angular position, respectively.

Due to the high transmission rate (planetary gears and lead screw transmission), friction is high and thus the joints are not back-drivable. This causes problems in controlling accurately the hand. However, a positive side effect of friction is that grasping forces can be exerted even when power supply is off, a very important function for hand prostheses.

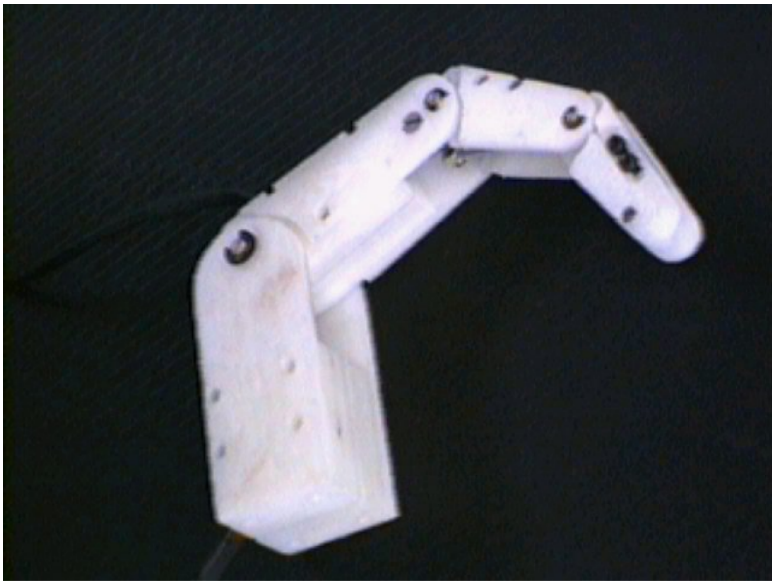

Figure 5.7: Picture of the first prototype of the finger.

5.3.2.4 Fabrication of the finger prototype

A first prototype of the finger was fabricated using the Fused Deposition Modeling [FDM] process (Figure **??**). This process allows the fabrication in a single process of three-dimensional objects, made out of acrylonitrile/butadiene/styrene [ABS] resin, directly from CAD-generated solid models. This rapid prototyping technique allows to make devices in order to make preliminary tests of different design solutions without the cost and time constraints typical of traditional prototyping technologies.

5.3.2.5 Fingertip force analysis

A first set of experimental tests has been performed in order to evaluate the force that the index/middle finger is able to exert on an external object [65, 72]. To this aim we have measured the force resulting when the finger is pressing directly on a high accuracy piezoelectric load cell (9251 A, PiezoInstrumentation KISTLER, Kiwag, CH), corresponding to different configurations of the joints.

The finger prototype was mounted on a four DoF manipulator (X, Y, Z translation plus one DoF for tilting) as depicted in Figure 5.8(a) and Figure 5.8(b). The force sensor was a 3-axial piezoelectric load cell (9251 A, PiezoInstrumentation KISTLER, Kiwag, CH); the sensor was mounted on a steel plate and covered by an aluminum plate in order to provide to the finger a contact area to apply the force. The load cell was connected to charge amplifier (PiezoInstrumentation KISTLER, Kiwag, CH); the analog signal was converted by a digital oscilloscope (TDS 220, Tektronix, Beaverton, US) and acquired through a PC

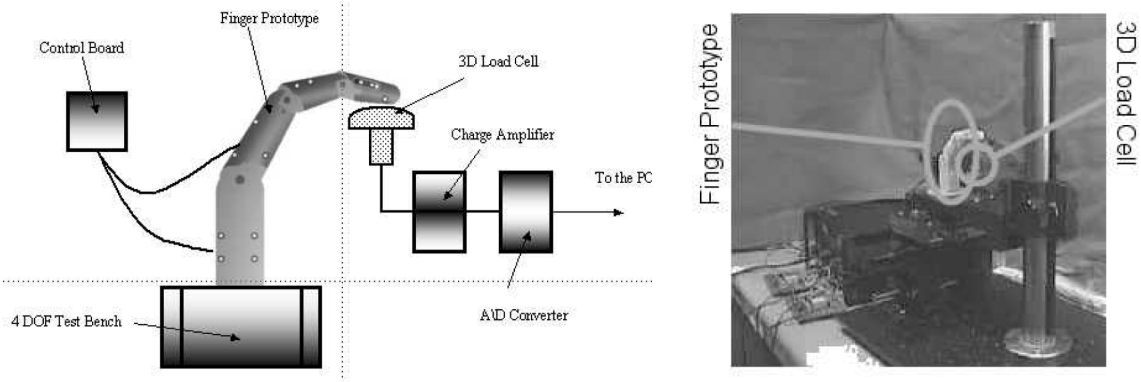

(a) Schematic drawing (b) Photograph

FIGURE 5.8: Schematic drawing and photograph of the experimental set-up

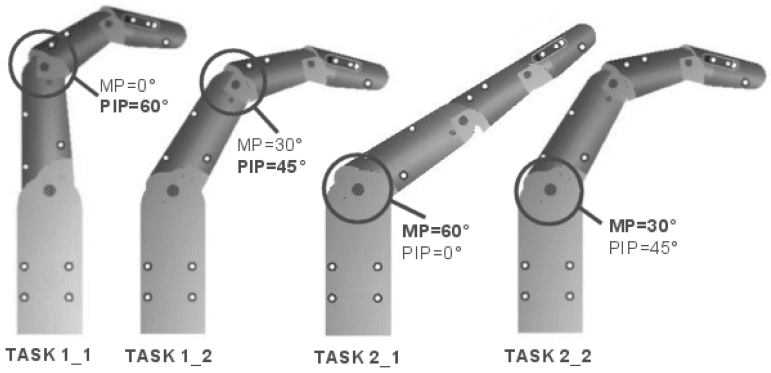

FIGURE 5.9: Different positions of finger joints for each task. The active joint for each task and position is indicated by a small circle.

(Figure 5.8(a) and Figure 5.8(b)) using WaveStar (Tektronix). Each Smoovy^{TM} actuator is controlled by a CCS00001 controller (RMB).

The finger position was adjusted in order to obtain an exerted force parallel to the Z axis of the load cell. Two "pressing" tasks were identified in order to evaluate separately and independently the force obtained by the two actuators incorporated in the finger:

TASK 1: the pushing action is exerted only by the distal actuator;

TASK 2: the pushing action is exerted only by the proximal actuator.

Corresponding to each task, two subtasks were identified according to the position of the nonactive joint (extended, flexed). The different values of joint rotation angles

	Task 1.1	Task 1.2	Task 2.1	Task 2.2
MP Joint [deg]	0	30	60	30
PIP Joint [deg]	60	45	0	45

Table 5.5: Pressing positions (see also Figure 5.9).

corresponding to each subtask are illustrated in Table 5.5 and Figure 5.9. These movements are widely used during ADLs, in particular during the first phase of the grasping, i.e. the positioning and shape adapting, where only low forces are required.

During the force characterization the fingertip pushed on the force sensor. The Z force component was recorded, the X and Y outputs of the load cell were monitored and led to zero. This was obtained by adjusting the finger position for obtaining a force parallel to the Z-axis of the load cell. A first set of experimental tests was done on the finger prototype, with the aim of evaluating how much force the finger is able to apply on an object.

5.3.3 Results of the characterization

Ten tests were performed for each subtask. The obtained results are summarized in Table 5.6 and illustrated in Figure 5.10. Table 5.6 also reports the expected values (without taking into account power losses) of the fingertip force, according to the calculations previously illustrated (see §5.3.2). During Tasks 1.1 and 1.2 the PIP motor exerted a force of 586 and 624 mN, respectively; 848 and 990 mN was obtained by the MP motor during Tasks 2.1 and 2.2. These levels are comparable with forces exerted by "natural" human fingers during fine manipulation [28].

We noticed a higher discrepancy between theoretical and measured force values during the different trials implementing Task 1 (more than 1,000 mN (theoretical) versus about 600 mN (experimental)) than during Task 2 (1,141 mN versus 990 mN). These differences are possibly related to the friction forces acting during the movement of the finger; in particular during Task 1 these losses are greater because of the action of the 4-bars link driving the DIP joint.

It is important to point out that all the values showed a quite narrow standard deviation (less than 3.3%) among each set, proving a good repeatability of the force developed by the biomechatronic finger.

Despite of their relatively low value, these force levels are sufficient to accomplish the first phase of the grasping task (reaching and shape adapting). For the second phase (grasping with thumb opposition) a different actuating solution should be found.

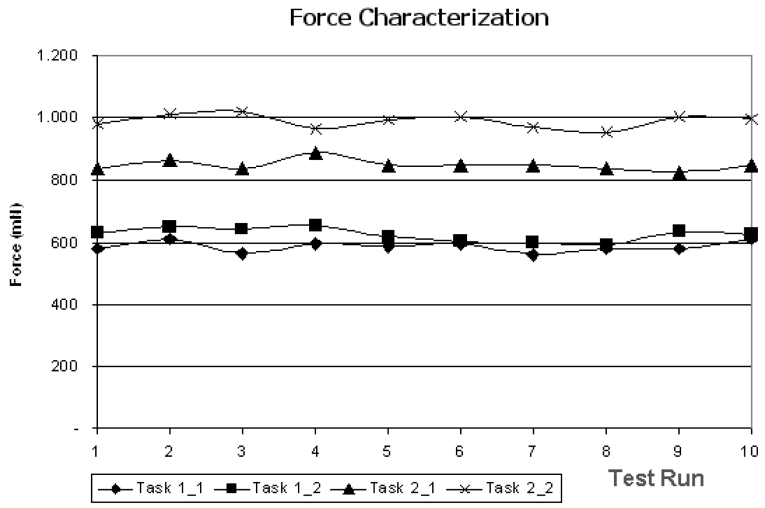

FIGURE 5.10: Experimental results of tests aimed at evaluating force performance of the biomechatronic fingers (force exerted in different runs). The number of the task is chosen according to Table 5.5.

	Task 1.1	Task 1.2	Task 2.1	Task 2.2
Mean Force (mN)	586	624	848	990
Standard Deviation (%)	2,84	3,29	2,00	2,07
Expected Value (mN)	1057	1059	951	1143

TABLE 5.6: Mean values and standard deviation of force exerted by the finger prototype during test run in different tasks. Tasks correspond to specific joint positions as defined Table 5.5.

5.3.4 Thumb design

The thumb has been designed to perform grasping tasks by thumb opposition. The thumb has been obtained by simply removing the distal phalanx from the index/middle finger (Figure 5.4(b)).

5.3.5 Hand fabrication

The hand prototype (Figure 5.11) comprises three fingers (index, middle and thumb), each with two DoFs actuated by micro-motors, and sensorized by Hall-effect position sensors and by strain gage-based force sensors. The characteristics of the position sensors and of the force sensors are illustrated in the following sections.

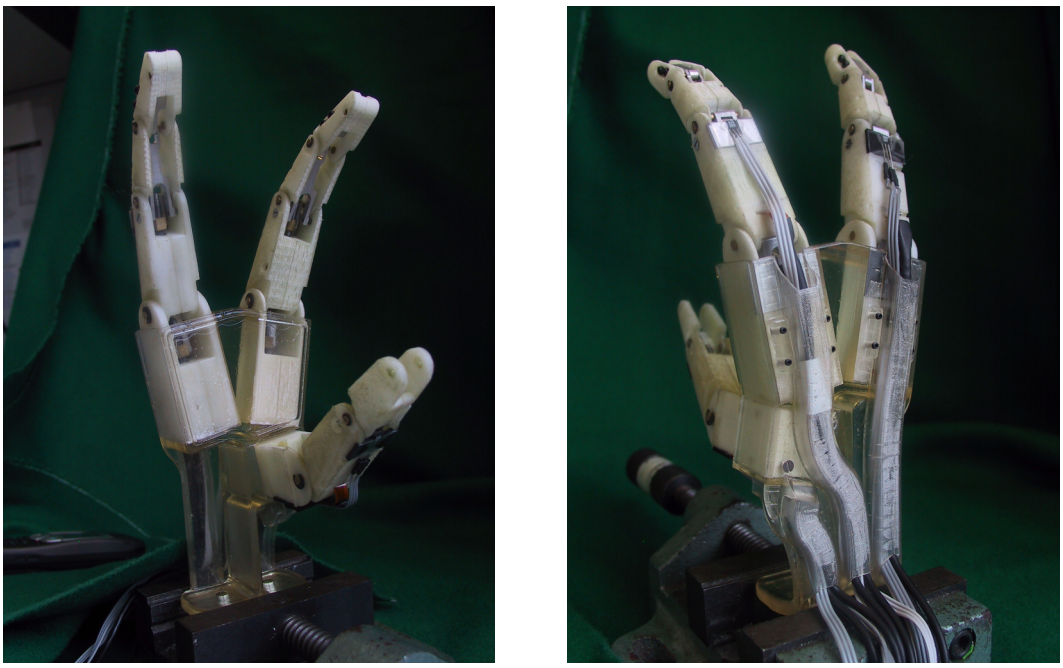

(a) Frontal View (b) Dorsal View

Figure 5.11: Frontal and dorsal photographs of the prosthetic hand.

The three fingers have been fabricated using the Fused Deposition Modeling (FDM) process. This process allows to obtain 3D complex shapes from CAD models easily, quickly and cheaply. The main limitation of the FDM process resides in the poor mechanical characteristics of the material that must be used, which is acrylonitrile/butadiene/styrene (ABS). However, this is acceptable for a prototype.

5.4 Control of the RTR1 hand

The description of the RTR1 prosthetic hand, according to the formal scheme presented in §4.3, is showed in Figure 5.12. In the next subsections, the 4 modules will be described in details. The National Instrument NI6025E has been used as interface between the user and the prosthesis. The configuration of the acquisition board is showed in Table 5.7(a) and Table 5.7(b).

5.4.1 TCM - Top Level Control Module

As previously pointed out, the user interface should be kept as simple as possible, in order to minimize the problems in the control of the hand due to muscle fatigue or to the misunderstanding of some user command.

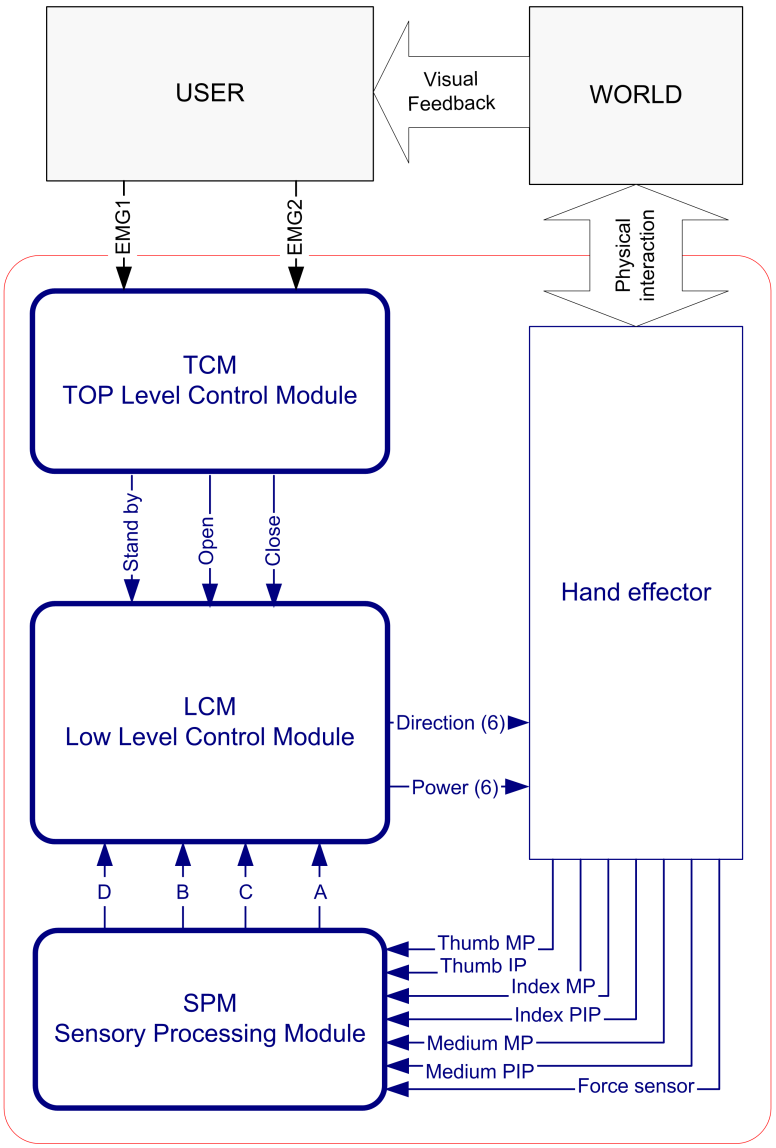

FIGURE 5.12: The control scheme of the RTR1 prosthetic hand.

Two EMG electrodes (Delsys DE2.3) have been used to acquire two EMG signals from the user, in order to control the opening and the closing of the hand. The first electrode is placed on the *extensor carpii radialis*, and the second on the *flexor carpii radialis*.

5.4.1.1 Signal Processing

The two EMG signals are sampled at 1000 Hz (channels 0 and 1 of the National Instruments NI6025E acquisition board), and the variance of the EMG is extracted by using the

Ch. #	type	Signal
0	A	EMG 1
1	A	EMG 2
2	A	Thumb Position (MP)
3	A	Thumb Position (IP)
4	A	Index Position (MP)
5	A	Index Position (PIP)
6	A	Middle Position (MP)
7	A	Middle Position (PIP)
8	A	Force sensor
9	A	-
10	A	-
11	A	-
12	A	-
13	A	-
14	A	-
15	A	-

(a) Analog inputs

Port #	Channel #	Type	Signal
0	0	D	MOT 1 - Pow
0	1	D	MOT 1 - Dir
0	2	D	MOT 2 - Pow
0	3	D	MOT 2 - Dir
0	4	D	MOT 3 - Pow
0	5	D	MOT 3 - Dir
0	6	D	MOT 4 - Pow
0	7	D	MOT 4 - Dir
1	0	D	MOT 5 - Pow
1	1	D	MOT 5 - Dir
1	2	D	MOT 6 - Pow
1	3	D	MOT 6 - Dir
1	4	D	-
1	5	D	-
1	6	D	-
1	7	D	Reset

(b) Digital outputs

Table 5.7: The configuration of the analog inputs and of the digital outputs of the NI6025E for the control of the RTR1 prosthetic hand. MP = metacarpophalangeal joint; IP = interphalangeal joint; PIP = proximal interphalangeal; DIP = distal interphalangeal joint; Pow = power signal; Dir = direction signal.

following equation:

$$VAR = \sigma^2 = \frac{1}{N-1}\sum_{k=1}^{N} x(k)^2 \tag{5.5}$$

Then a simple threshold classification has been chosen in order to discriminate among closing and opening of the hand.

5.4.1.1.1 Delsys DE2.3 EMG electrodes The Delsys DE2.3 EMG electrodes have been chosen for the acquisition of the EMG signal in order to control the prosthetic hands. The electrical and mechanical properties of these electrodes are summarized in tables 5.8(b) and 5.8(a), respectively. In particular, these EMG electrodes are designed with a built-in gain of 1000 V/V and a built-in filter from 20-450 Hz.

5.4.1.2 User training

A software for the training of the user has been developed by using LabVIEW (Figure 5.13). By using this software, the user is trained to contract the *extensor carpii radialis* and *flexor carpii radialis*, in order to generate the control signals. The visual representation of the EMG signal and its variance help the user to learn how to control the hand.

The following training protocol has been chosen:

Mechanical properties	
Number of Contacts	2
Contact Dimension (mm)	10.0x1.0
Contact Spacing (mm)	10.0
Contact Material	99.9% Ag
Case Dimensions (mm)	41x20x5
Cable Length (m)	1.5
Connector	Hypertronics
Temperature Range	0-40°C

(a) Mechanical properties

Electrical properties	
Gain (V/V)	1000± 2%
Bandwidth	20 ± 5Hz - 450 ± 50Hz
Bandwidth Rolloff	12dB/Oct
Noise (RMS, R.T.I.)	1.2μV
CMRR@60Hz (dB)	>80dB
Supply Voltage	±4.5–±9V
Supply Current	± 2.7mA
Input Impedance (Ω//pF)	>1015//0.2

(b) Electrical properties

TABLE 5.8: Mechanical and electrical properties of the Delsys DE-2.3 EMG electrodes.

1. the user is asked to contract the two antagonist muscles, in random sequence, for a variable period of time, ranging from $t_{\text{training}_0} = 2$ minutes (experienced user) to $t_{\text{training}_0} = 10$ minutes (new user). During this training period the position of the electrodes is adjusted in order to get the best signals;

2. in order to determine the dynamic range of the EMG signals, the user is asked to contract the *extensor carpii radialis* for $t_{\text{ext}} = 5$ seconds at maximum contraction level. The variance of the signal in the last part of this contraction (100 ms) is the signal the the user could reproduce without problems for the whole day during normal activities.
   This value σ_{ext} is normalized to 1, thus setting the gain of Channel 1 ($G_{\text{extension}}$).

3. the user is asked to contract the *flexor carpii radialis* for $t_{\text{flex}} = 5$ seconds at maximum contraction level. The variance of the signal in the last part of this contraction is the signal the the user could reproduce without problems for the whole day during normal activities.
   This value σ_{flex} is normalized to 1, thus setting the gain of Channel 2 (G_{flexion}).

4. the user is then asked to move the arm with the electrodes for $t_{\text{baseline}} = 5$ seconds *without* without commanding the opening or the closure of the hand. In this way the baselines of the 2 EMG channels are recorded, thus setting the 2 thresholds. The variance of the 2 channels are recorded, and the 2 thresholds are set as the mean value μ of the variance of the EMG signal during t_{baseline} plus its variance, i.e. $\tau_{\text{ext}} = \mu(\sigma_{\text{ext}}) + \sigma(\sigma_{\text{ext}})$, $\tau_{\text{flex}} = \mu(\sigma_{\text{flex}}) + \sigma(\sigma_{\text{flex}})$.

5. the uses is asked to move the hand and to contract the muscles and generate control commands, in order to verify that the above parameters suit the user needs.

6. the above steps are repeated until the user reaches a satisfactory ability in generating the commands to the hand.

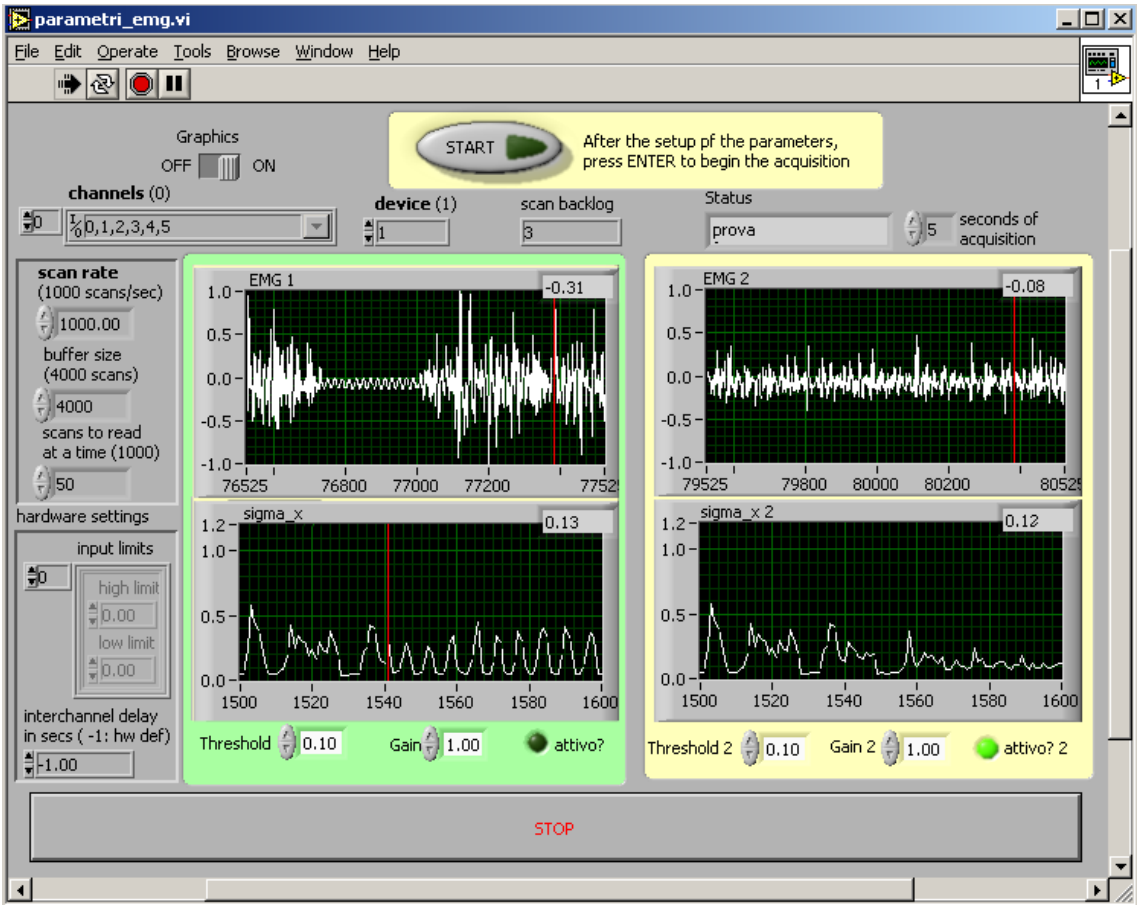

Figure 5.13: Screen capture of the software used for the user training and for the set up of the gain and threshold parameters for the 2 EMG channels.

5.4.2 LCM - Low Level Control Module

The control of the six brushell DC motor is demanded to six CCS00001 controller (RMB). An interface device have been realized in order to command these controllers through a LabVIEW interface (Figure 5.14). By using this interface, the following commands are sent to the hand:

- 6 direction commands (boolean);
- 6 on/off commands (boolean);
- 1 switch to read alternatively the 2 dimensions of the force sensor;

The hand operates as follows (Figure 5.15):

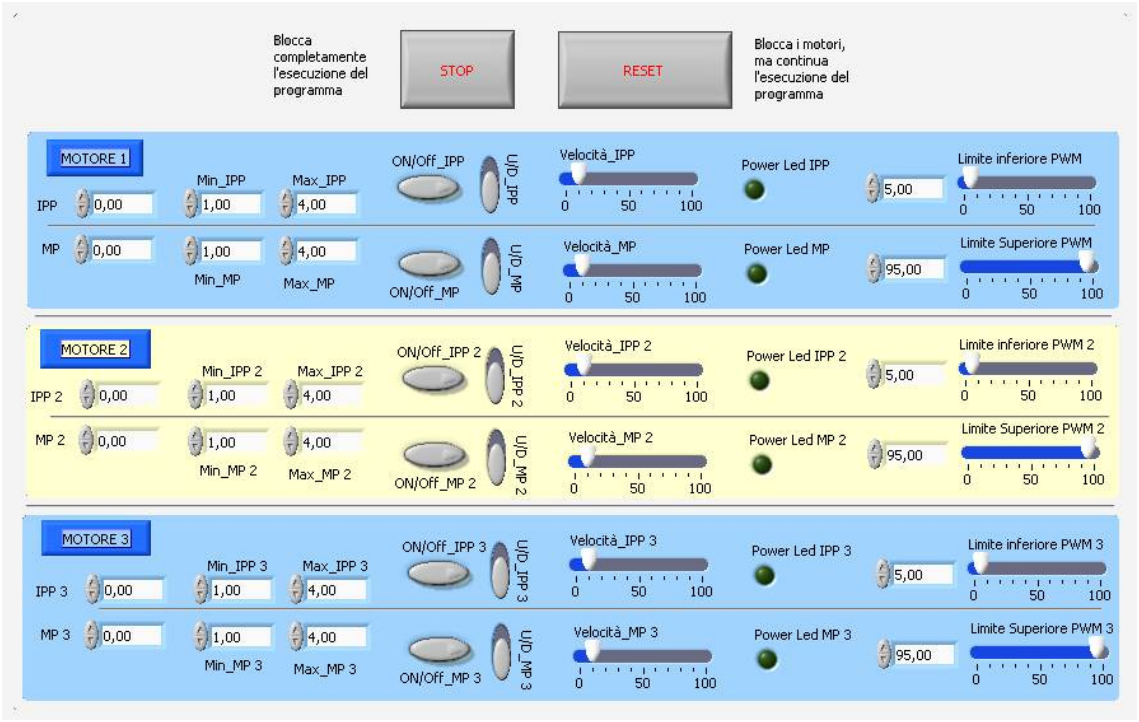

FIGURE 5.14: The control interface for the RTR1 prosthetic hand.

- When the system is turned on, it goes in the **Stand By** state, waiting for any command coming from the TCM.

- Once a command is generated from the TCM, the LCM reads its internal state, and goes into **S0: wait**, in which the hand executes the command arrived from the TCM. As said before, the possible commands coming from the TCM are:

  hand opening: the hand opens until it receives a STOP command (i.e., no more commands) or it reaches the maximum extension (determined by the slider sensor). The speed of the movement depends on the amplitude of the OPEN command

  hand closing: the hand closes until it receives a STOP command (i.e., no more commands), or if it reaches the maximum flexion/extension, or if a contact with an object is detected. The speed of the movement depends on the amplitude of the CLOSE command.
  In case a contact is detected, the hand goes into the **Grasp state**, in which it grasp the object with a force determined by the amplitude of the CLOSE command.

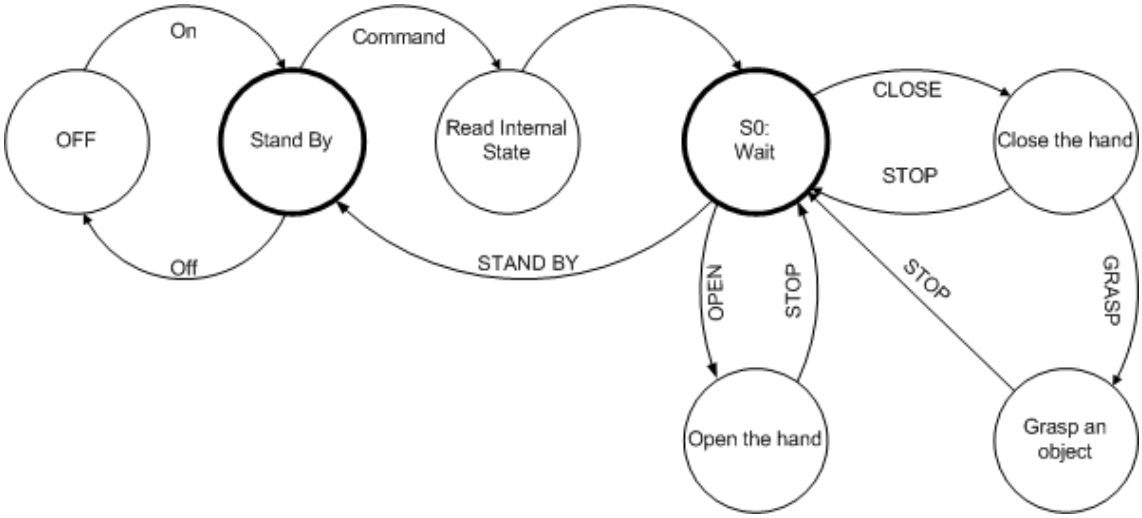

Figure 5.15: The control scheme for the RTR1 prosthetic hand.

STOP: the STOP command is issued both by the user (if s/he wants to stop the current movement) or automatically by the LCM (in case the hand has reached the desired level of grasping force, or the end of the active stroke of the slider or of the thumb, or there is an obstacle).

- In case no commands arrive to the hand within $t_{\text{stand-by}}$ the hand goes to the **Stand by** state.

5.4.3 SPM - Sensory Processing Module

As said in the previous sections, the hand is provided with the following sensors:

- six position sensors, made with Honeywell Hall Effect sensors SS495A and 103MG5 magnets;
- one two-dimensional force sensor, made with Entran ESA–25–1000 strain gauges.

5.4.3.1 Position sensors

In order to control the prosthetic hand, a position sensor, based on Hall-effect sensor (SS495A, Honeywell, USA) and Rare Earth Pressed Bar Magnets (103MG5, Honeywell, USA), is mounted on each active joint of the hand (6 sensors in total). The main advantages of Hall-effect sensors are their small size and their contactless working principle (§5.4.3.1.1). In each finger, the Hall sensors are fixed respectively to the palm and to the proximal

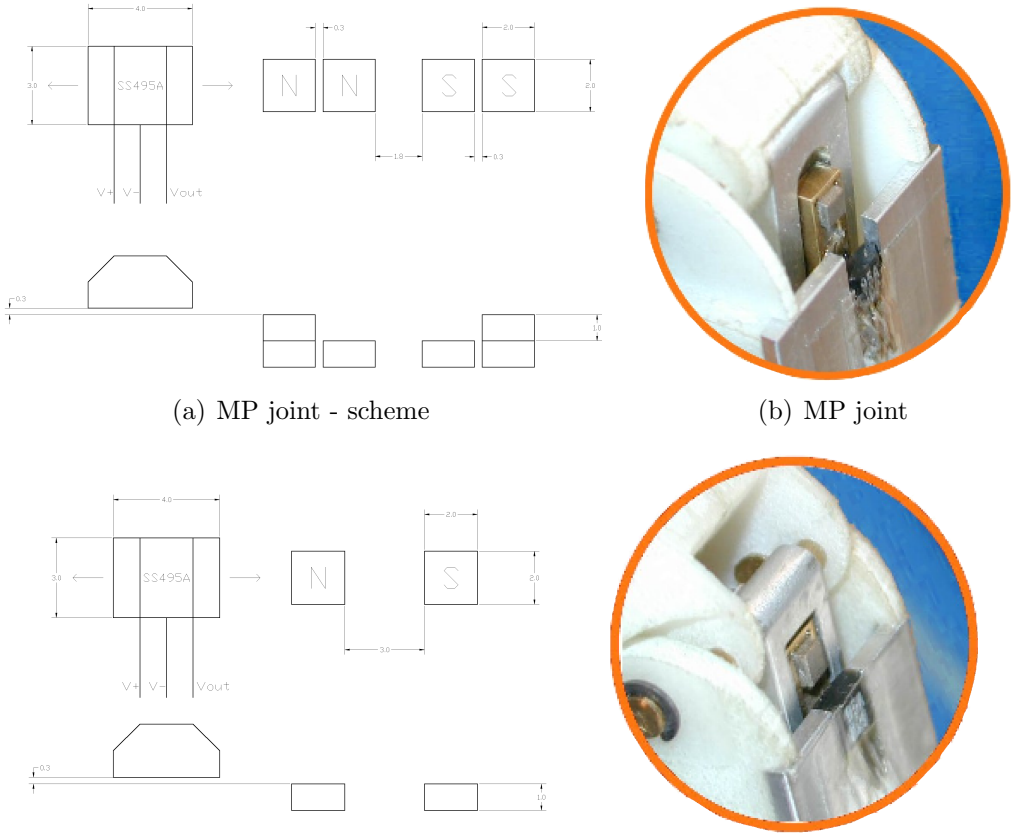

(a) MP joint - scheme

(b) MP joint

(c) PIP joint - scheme

(d) PIP joint

FIGURE 5.16: Configuration of the magnets for the MP and PIP joints (on the left, dimensions are in millimiters), and their photographs.

phalanxes, whereas the magnets are mounted directly on the sliders of each active joint. These sensors need only a stable power supply (ground, +5V) obtained by using a voltage regulator (MC7805). The output voltage is proportional to the magnetic field under the sensible area of the sensor.

In this configuration the sensor measures the linear movement of the slider, which is related to the angular position of the joint. In each MP joint, the linear range of the sensor is 5.2 mm, whereas in the PIP joint the linear range is 8 mm.

Using a micrometric translator stage we found two optimal configurations for the position sensors (Figure 5.16). In the first optimal configuration two magnets are used at a distance of 3.5 mm. This configuration (used for the PIP joints) has a working range of 5.4 mm with a linearity of 5.34%. The second optimal configuration (suitable for MP joints) has six magnets, and a working range of 8.4 mm with a linearity of 3.81%.

Product Specifications	
Supply Voltage	4.5 Vdc to 10.5 Vdc
Output Type	Sink/Source
Magnetic Actuation Type	Ratiometric
Operating Temperature Range	-40 °C to 150 °C
Output Voltage (typ,)	0.2 Vdc to (Vs - 0.2 Vdc) typ.
Output Voltage (min)	0.4 Vdc to (Vs - 0.4 Vdc) min.
Linearity (% of Span)	-1.0 % typ., -1.5 % max.
Output Voltage Span (min.)	0.4 Vdc to (Vs - 0.4 Vdc)
Supply Current (max. @ 25 °C)	8.7 mA @ 5 Vdc
Sensitivity @ 25 °C	2.500 mV ± 0.200 mV/G
Output Voltage Swing (Negative G)	0.4 Vdc
Output Voltage Swing (Positive G)	Vs - 0.4 Vdc
Temperature Error (@ 25 °C) Null Shift (%/°C)	-0.064 % min., 0.064 % max.
Temperature Error (@ 25 °C) Sensitivity (%/°C)	-0.02 % min., 0.08 % max.
Output Current Typ. Source (Vs > 4.5 Vdc)	1.5 mA
Output Current Min. Source (Vs > 4.5 Vdc)	1 mA
Output Current Min. Sink (Vs > 4.5 Vdc)	0.6 mA
Output Current Min. Sink (Vs > 5.0 Vdc)	1 mA
Magnetic Range (typ.)	-84 mT to 84 mT [-840 G to 840 G]
Magnetic Range (min.)	-75 mT to 75 mT [-750 G to 750 G]
Output Voltage Span (typ.)	0.2 Vdc to (Vs - 0.2 Vdc)
Null (Output @ 0 G)	2.50 Vdc ± 0.150 Vdc
Response Time (μs)	3 μs

Table 5.9: SS49x Series Miniature Hall-Effect Linear Position Sensor

5.4.3.1.1 Honeywell SS49x Hall-effect sensors The Hall effect is an ideal sensing technology for prosthetic applications. The Hall element is constructed from a thin sheet of conductive material with output connections perpendicular to the direction of current flow. When subjected to a magnetic field, it responds with an output voltage proportional to the magnetic field strength [80].

The Hall effect was discovered by Dr. Edwin Hall in 1879 while he was a doctoral candidate at Johns Hopkins University in Baltimore. Dr. Hall found when a magnet was placed so that its field was perpendicular to one face of a thin rectangle of gold through which current was flowing, a difference in potential appeared at the opposite edges. He found that this voltage was proportional to the current flowing through the conductor, and the flux density or magnetic induction perpendicular to the conductor.

The SS49x Series MRL (Miniature Ratiometric Linear) sensors are versatile linear Hall effect devices operated by the magnetic field from a permanent magnet or an electromagnet. The ratiometric output voltage is set by the supply voltage. It varies in proportion to the strength of the magnetic field. The integrated circuitry provides increased temperature stability and sensitivity. Laser trimmed thin film resistors on the chip provide high accuracy (null to ± 3%, sensitivity up to ±3%) and temperature compensation. The

Product Specifications	
0,25 Gap Distance/Gauss Level @ 25 °C	1110
0,76 Gap Distance/Gauss Level @ 25 °C	630
1,27 Gap Distance/Gauss Level @ 25 °C	365
2,54 Gap Distance/Gauss Level @ 25 °C	120
3,81 Gap Distance/Gauss Level @ 25 °C	55
5,08 Gap Distance/Gauss Level @ 25 °C	25
Outside Diameter, mm	2.0
Length, mm	2.0
Magnetic Shock Resistance	Good
Resistance to Demagnetization	Excellent
Operating Temperature Range	-40 °C to 250 °C
Magnet Shape	Bar
Magnet Material/Process	Rare Earth/Pressed

TABLE 5.10: Characteristics of the 103MG5 magnets.

positive temperature coefficient of the sensitivity (+0.02 %/°C typical) compensates for the negative temperature coefficients of low cost magnets.

The typical characteristics of the SS49x Hall-effect sensors family are showed in table 5.9. The mechanical drawings and a picture of the SS49x Hall-effect sensor are showed in figure **??** and **??**, respectively.

5.4.3.1.2 Honeywell 103MG5 Rare Earth Pressed Bar Magnet In prosthetic applications the dimension of the components is a critical factor. So, each component should be as small as possible, in order to reduce the total encumbrance and the total weight of the prosthesis. In order to obtain very reliable and very small sensible structures, the Honeywell 103MG5 Rare Earth Pressed Bar Magnets have been chosen, which guarantee very high magnetic induction while maintaining very small dimensions (2mm×2mm×1mm). The characteristics of these magnets are summarized in table 5.10, and the mechanical drawings are showed in figure 5.17.

5.4.3.1.3 Characterization of position sensors We found that the best and simplest way to characterize these sensors is to use an optical method. We used a Nikon Coolpix 950 digital camera mounted on a tripod in order to record the movement of the finger. The movement of each Smoovy actuator was driven by a CCS00001 Controller (RMB, CH). Each controller has a power supply of 11V, while each sensor was supplied with 6V.

For each active joint 100 different frames, 50 for flexion and 50 for extension movements, were acquired. For each frame the output value of the sensor was measured with a digital multimeter and recorded, whereas the relative position of the joint was measured using the module Measure Tool of Adobe PhotoShop 5.5, with a precision of 0.1 $^{\circ}$.

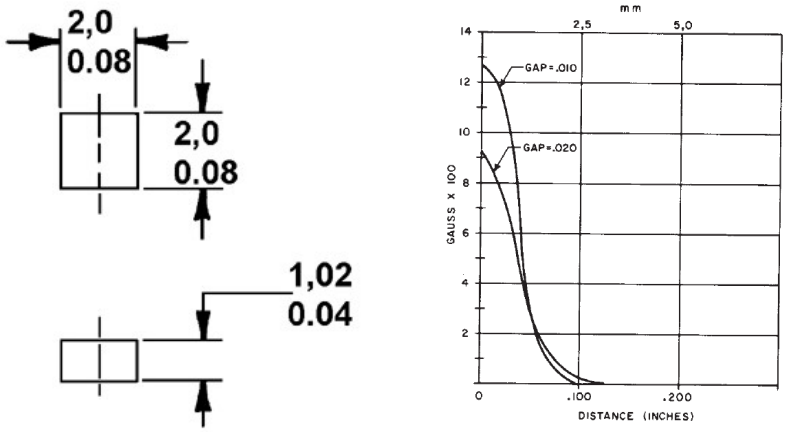

(a) Drawing.

(b) Typical plots of induction (gauss) versus distance.

Figure 5.17: Drawings and characteristic curve for the 103MG5 magnet.

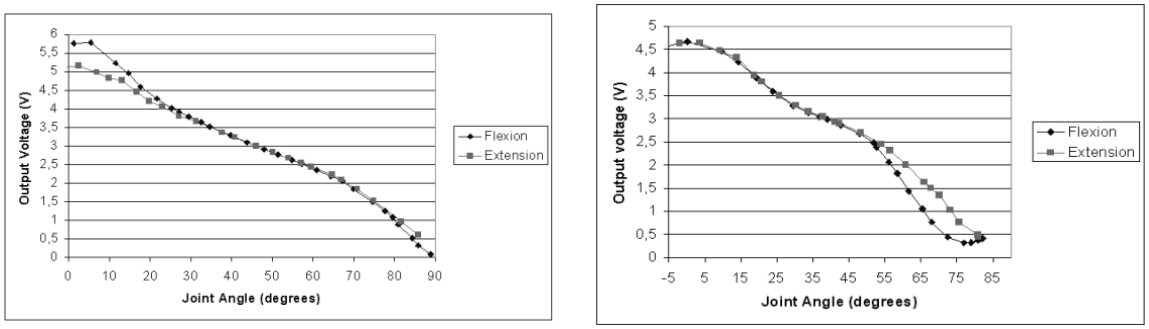

(a) MP joint

(b) PIP joint

Figure 5.18: Response curve for the MP and PIP joints (Output voltage versus Joint Angle).

Results are presented in Figure 5.18 for the sensor in the MP joints (Figure 5.18(a)) and in the PIP joints (Figure 5.18(b)), respectively. The flexion phase is indicated with small dark circles, while the extension is indicated with small light squares.

It is important to point out that both curves for both sensors generally present low hysteresis. The difference between the flexion and the extension curves is mainly due to the mechanical clearance of the sensorized slider.

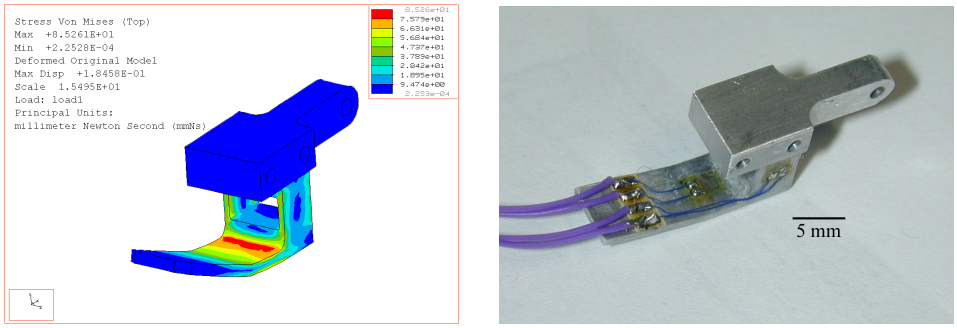

(a) Simulation (b) PIP joint

FIGURE 5.19: Results of the force sensor FEM simulation (left) and photograph of the sensor prototype (right).

5.4.3.2 Force sensor

A 2D force sensor, based on strain gauges technology, has been developed in order to sensorize the distal phalanx of index and middle fingers, and the thumb. The force sensor measures both normal and tangential forces. The sensor design has been optimized using the Pro/Mechanica Structure software (see Fig. 5.19).

The 2 strain gauges (Entran ESA–25-1000, §5.4.3.2.1) are put as a variable element in a Wheatstone bridge configuration. The characteristics of these strain gauges has already been presented in §5.4.3.2.1. The electronic board for the aquisition of these 2 signals is showed in Figure 5.20.

5.4.3.2.1 Entran ESU–025–1000 Strain Gauges The Entran ESU–025–1000 (Figure 5.21(a)) are semiconductor strain gauges (made by silicon, p-type), U-shaped, with a range of sensibility from 0 to 1000 $\mu\Sigma$, but they can resist to a deformation up to 3000 $\mu\Sigma$. The nominal resistance is 1000 Ω ($\pm$ 22%), tha Gauge factor is 155 ($\pm$ 5%), and the external dimension are very small, only 1.27×0.38mm. The characteristics of these strain gauges are summarized in table 5.11.

5.4.3.2.2 Characterization of 2D force sensor The force sensor was characterized using an INSTRON 4464 testing machine. A traction-compression loading cycle (0 N – 10 N – 0 N) was performed for each direction. Results are presented in Figure 5.22(a) and Figure 5.22(b), for the normal loading direction and the tangential loading direction, respectively. Diagrams show a linear behavior of the 2D force sensor.

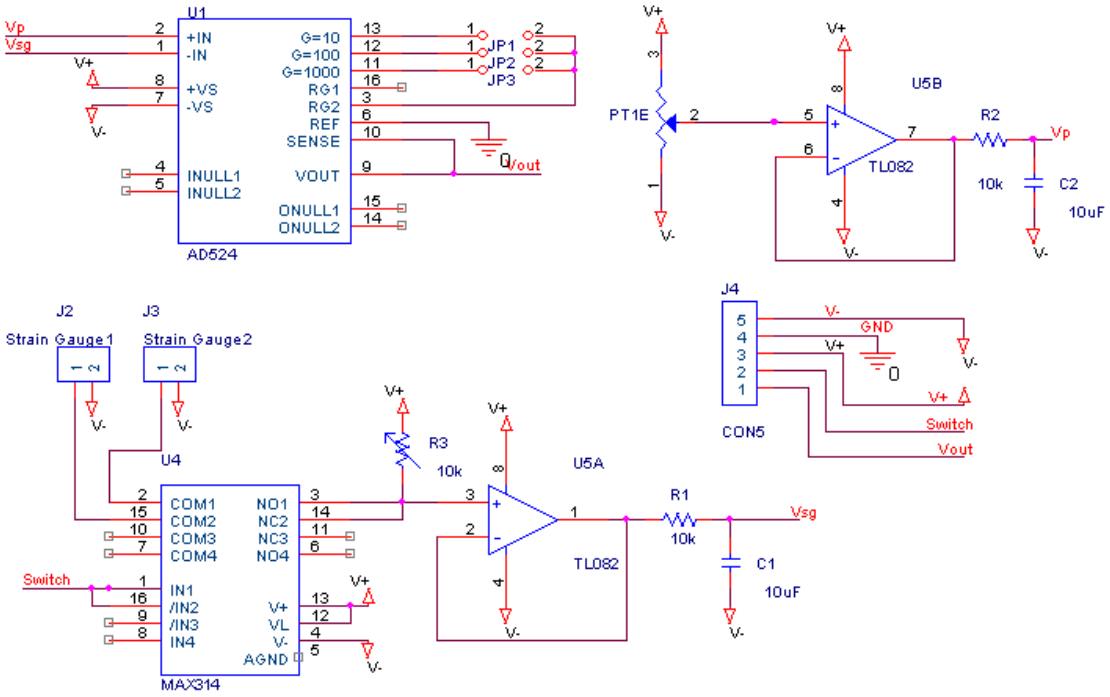

FIGURE 5.20: The schemadic diagram of the acquisition board for the 2D force sensor.

5.4.4 SFM - Sensory Feedback Module

The RTR1 prosthetic hand does not have any module for the sensory feedback to the user. As usual with current hand prostheses, the sensory feedback is given in an indirect form:

- visual feedback;
- proprioceptive sensation on the stump, due to the load of the graspoed object;
- change of the sound of the motors.

5.5 Discussion

In this chapter a novel approach to the design and fabrication of prosthetic hands, called *biomechatronic* design, has been presented. The biomechatronic design consists of integrating multiple DoFs finger mechanisms, multi-sensing capabilities, and distributed control in order to obtain human-like appearance, simple and direct controllability and low mass. The biomechatronic design approach can lead to the development of hand prostheses much more acceptable by the amputee than current prostheses, when combined with other important factors, such as low energy consumption for adequate autonomy (at least 8 hours

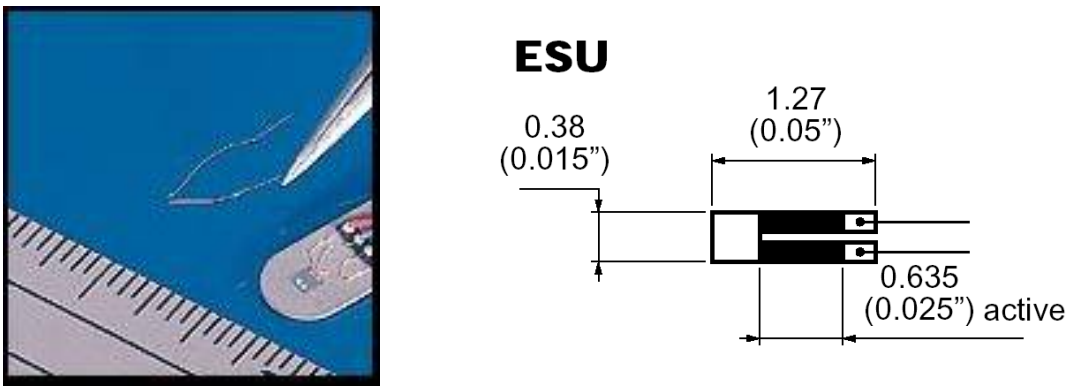

(a) Picture (b) Schematic drawings

FIGURE 5.21: Picture and schematic drawings of the esu–025–1000 Strain Gauges.

between recharges), noiseless operation for not disrupting social interactions, cost suitable for support by the health insurance system, and above all sensory feedback to the amputee through neural interfaces. A biomechatronic hand prototype with three fingers and a total of six independent DoFs has been designed and fabricated. The proposed hand is designed to augment the dexterity of traditional prosthetic hands while maintaining approximately the same dimension and weight.

This hand presents some advantages respect to the state of the art of the hand prosthesis:

- it has a better dexterity than traditional prostheses while maintaining approximately the same dimensions;
- the actuation system and the sensors are all enclosed within the hand;
- despite of the high number of DoFs, the hand is very light.

Anyhow, this hand presents also several drawbacks:

- the grasping force is extremely low, comparable to the force exerted by human fingers during fine manipulation.
- the micromotors are also quite noisy;
- the micromotors are very fragile;
- the RTR1 hand is slower than a conventional DC prosthesis;
- the power consumption of the 6 brushless motors is (in total) higher than the power consumption of a bulky DC motor.

MODELS	SHAPE	R RESISTANCE nom.	TCR /100°F (/55°C) nom.(Note 3)	GF - GAGE FACTOR nom.	TCGF /100°F (/55°C) nom. (Note 3)
ESU-025-500	U	500 Ω	+14%	+140	-15%
ESU-025-1000	U	1000 Ω	+22%	+155	-18%

QUANTITY OF GAGES IN PACK:	**Matched Sets of 4:** 4	**Unmatched sets of 10:** 10
MATCHING (R):	**Matched Sets of 4:** R within ±2% of each other	**Unmatched sets of 10:** R within ±10% of each other
R nom., 20°C (70F°):	**Matched Sets of 4:** Resistance in ohms, ±10%	**Unmatched sets of 10:** Resistance in ohms, ±20%
GF nom., 20°C (70F°):	Gage Factor, $\frac{\Delta R/R}{\Delta L/L}$ ±5%.	
TCR nom. (Note 3):	Thermal Coefficient of Resistance, $\frac{(\Delta R/R)\% \pm 3\%}{100°F}$, 70°F to 170° (20°C to 77°C).	
TCGF nom. (Note 3):	Thermal Coefficient of Gage Factor, $\frac{\Delta GF\% \pm 3\%}{100°F}$, 70°F to 170°F (20°C to 77°C).	
GAGE TYPE:	P-Type Silicon.	
STRAIN LEVEL (Note 1):	0-1000µstrain recommended, 0-3000µstrain maximum.	
WATTAGE RATING (per gage):	0-25milliwatt recommended, 50milliwatt maximum. Watts=(Voltage on Gage)²/(Gage Resistance).	
TEMPERATURE RANGE:	-100°F to +600°F (-73°C to 315°C).	
LEAD WIRES:	Gold, 0.0015" diameter x 0.25" length min. (0.038mm dia. x 6.35mm).	
YOUNG'S MODULUS:	E=27x10⁶psi (1.9x10⁶kg/cm²).	
SENSITIVITY, Vo (Note 2):	Voltage Out=1/4(No. Active Arms) (Gage Factor)(Strain Level) (Excitation Voltage). Example: Fully active 4 Arm Bridge, GF=130, 500µstrain, 5V Exc. Vo=1/4 (4) (130) (500x10⁻⁶) (5V)=325mV.	
BONDING:	Apply thin Epoxy precoat for electrical isolation. Then apply bonding coat to substrate, place gage (handling by its leads only) on wet epoxy and align. Gage is held in position by surface tension only, DO NOT apply weights or force, as this may damage the gage. Micro Measurements M-Bond 610 or equivalents are recommended.	

[1]µstrain = strain in inches/inch x 10⁻⁶. [2] Equations assume bridge with adjacent tension and compression arms for additive outputs. [3]The actual values of TCR and TCGF greatly depend upon excitation voltage, heat sinking, temperature of use, mounting and prestrain, and catalog values should not be used as absolute numbers for calculation of data for experimental or design use. TCR and TCGF, where important, must be calibrated after gage mounting.

Table 5.11: Characteristics of the esu–025–1000Strain Gauges.

- due to the high number of active DoFs, the hand needs a more complex control scheme in order to be used as a prosthesis.

The grasping force is low because of the limited torque generated by the miniature actuators used for the hand (which are among the best available on the market in that range of size). However, even if the force generated by the hand is low, a better distribution of contact areas between the three fingers and the grasped object can be obtained thanks to the novel kinematics. This result can partially compensate for the reduction in actuator force and ultimately allows to retain almost the same grasping stability as traditional prostheses when grasping objects of complex shape [22].

The presence of noise is typical of all the motors. Micromotors, in particular, moves at very high speed and are more noisy than conventional DC motors. At present no practical solution has been found to this problem, but some possible solutions could be foreseen. For example, one possible solution for reducing noise caused by motors activation is to adjust the acoustical impedance of the motors housing and of the external palm/finger structure.

The real problem with this hand is the presence of too many motors. Despite of their small dimension, the controllers for six motors is too bulky to fit on a hand prosthesis, so it cannot be used in clinical practice. Moreover, while the power consumption of a single micromotor is lower than the one of a bulky DC motor (150 mA vs. 1000 mA), the

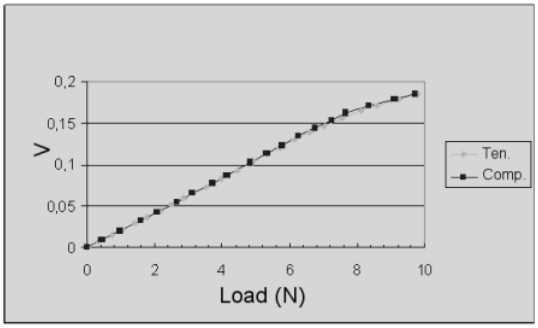

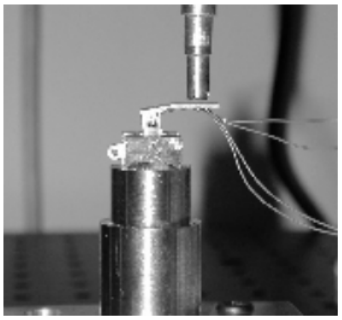

(a) Response curve of Force sensor - normal direction

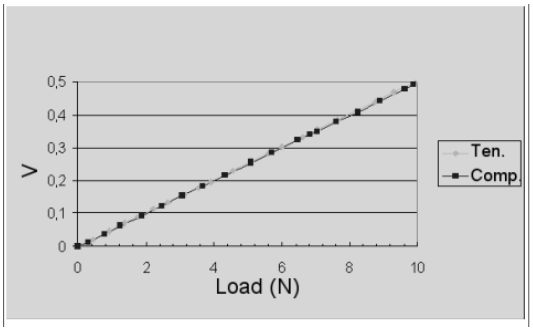

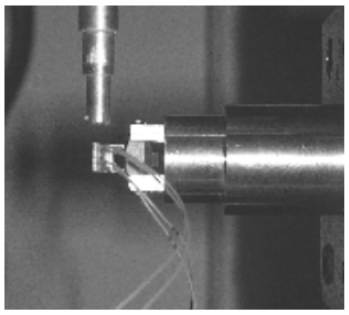

(b) Response curve of Force sensor - tangential direction

FIGURE 5.22: Response curve of Force sensor (voltage versus load) (left) for external forces along the normal (top) and tangential direction (bottom), and photograph of the prototype during tests (right).

presence of 6 motors reverts this proportion (150 mA×6 vs. 1000 mA). Last but not least, the duration of the closing and opening movements in the RTR1 hand is quite higher than in a conventional DC prosthesis (4.8 seconds vs. 2.2 seconds) .

For all these reasons the design approach based on microactuators is, at present, quite far from offering a valid alternative to standard design approach. In the next future, however, the realization of better component could permit the exploitation of this design strategy.

With the present technology, a valid design strategy, aimed at increasing the grasping force and reducing the control complexity of the hand, while retaining the main positive characteristics of previous designs, could be the adoption of underactuated mechanisms.

Six

An advanced prosthesis with thumb adduction/abduction

6.1 Introduction

As already seen in previous chapters, there are some main factors that cause the loss of interest for myoelectric hand prostheses. One possible solution to raise this interest could be to use smaller actuators (micro-actuators), addressing the objective of increasing DoFs [9]. Despite of the promising results, the design approach based on microactuators has, at present, too much drawbacks, mainly due to the lack of high torque micro-actuators and the difficulty to implement complex control scheme with a natural interface, in order to control all the DoFs. So, this strategy is at present quite far from offering a valid alternative to standard design approach (Chapter 5).

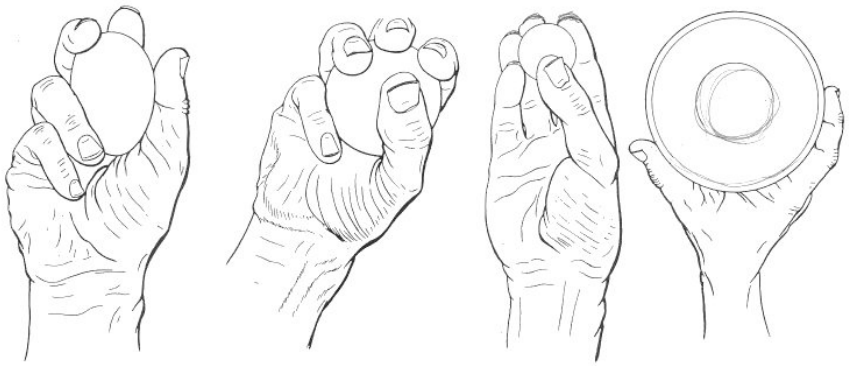

FIGURE 6.1: Adaptability of the human hand

It is important to point out that prosthetic hands are designed primarily for grasping tasks and not for manipulative tasks; manipulation, in fact, requires: high dexterity, advanced sensors, complex control strategies and natural interfaces [50],[42].

Commercial hand prostheses have one or two DoFs providing finger movements and thumb opposition; due to the lack of DoFs, such devices are characterized by a low grasping functionality, in fact, they do not allow adequate encirclement of objects, in comparison with the adaptability of the human hand (Figure 6.1); as a result object must be grasped accurately to be held securely [23].

In order to fit the myoelectric prostheses for different amputation levels, all the actuators have to be embedded in the hand structure (*intrinsic* actuation). The *intrinsic* actuation choice combined with the use of traditional electro-magnetic actuators leads to an extreme reduction of available DoFs (Figure 5.1). This approach produces artificial hands with a maximum of two DoFs, which are able to provide a pinch force of about 100 N; in this case, the motion of the phalanges is determined at the design stage and therefore no shape adaptation is possible [70]. These devices are simple and easy to build, but are not flexible enough to accommodate several objects. As listed above, they present the following limitations: low functionality, low cosmetics and, due to sensory lack, low controllability.

According to [14] the prosthesis has to perform a stable grasp with a wide variety of objects with complex shapes and to adopt simple control scheme. In order to enhance prosthesis flexibility by keeping the *intrinsic* actuation solution, and implementing simple control algorithms, a different approach should be used.

6.2 Underactuated Mechanical Hands

A mechanism is said to be underactuated when it has less actuators than degrees of freedom; traditional actuators (i.e. electro-magnetic motors) are replaced with passive elastic elements and mechanical stops. These elements can be considered as passive actuators, which cannot be controlled. They are small and simple and lead to a reduction of the number of DoFs.

When applied to mechanical hands, the underactuated mechanisms, lead to an *adaptive* grasp. Underactuated mechanisms allow the grasping of an object in a way that is closer to the human grasping than independent actuation [61].

6.2.1 Differential Mechanisms

The differential mechanism is the basis of an underactuated mechanism. Differential mechanism is a mechanism in which the amount of dynamical input from three ports acts in balance [36]. Fundamental examples of differential mechanism are shown in Figure 6.2.

These differential mechanisms can control multiple DoFs with a single actuator by combining it with elastic elements and mechanical stops; consequently, they are the main component of an underactuated mechanism.

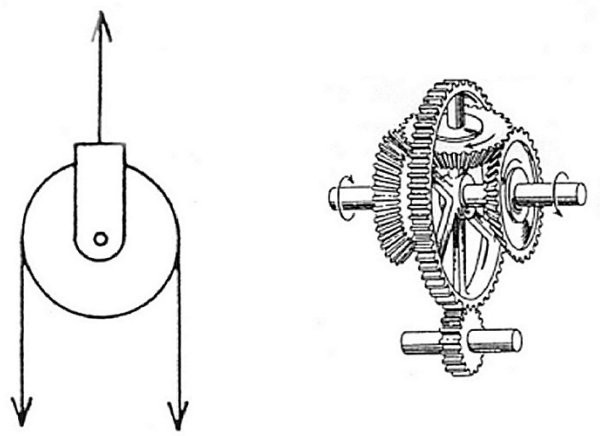

(a) movable pulley (b) differential gear mechanism

FIGURE 6.2: Differential mechanisms: (A) movable pulley, (B) differential gear mechanism.

6.2.2 Underactuated Mechanical Hands

The literature shows two different types of underactuated hands depending on the transmission system: underactuated hands based on tendon transmission [13, 64] and underactuated hands based on link transmission [3, 33, 85]; tendon systems are generally adopted in order to minimize transmission dimensions but are limited to small grasping forces, while link systems are preferred for applications in which large grasping forces are required.

This class of mechanical hands has been developed for industrial and space applications in order to augment the flexibility, without raising the mechanical complexity and their adoption in the prosthetic field is not suitable due to size and weight restrictions and to reliability requirements. These devices and their underactuated mechanisms are, in fact, too complex and too bulky compared to a prosthetic hand.

A few underactuated passive (body-powered) prosthetic hands have been proposed [22, 26]; in these references, however, the concept of underactuation is not analyzed in depth. In [23] an example of underactuated active (myoelectric) hand is presented. This device allows an adaptive grasping but only adaptation between fingers has been realized and no adaptation between phalanxes has been considered.

The RTR II hand has been created in an attempt to increase passive shape adaptation by addressing the problem of inter-phalanges adaptation.

6.3 Design and Development

The design approach based on underactuated mechanisms allows reproducing most of the grasping behaviors of the human hand without augmenting the mechanical and the control complexity.

In general, for an underactuated hand, the correct choice of the characteristic of the elastic elements and the correct placing of the mechanical stops allows a natural wrapping movement of the finger around the object. In order to achieve a correct finger movement the object should touch first the proximal phalanx (B), then the middle (C) and finally the distal phalanx (D) (Figure 6.3) [22].

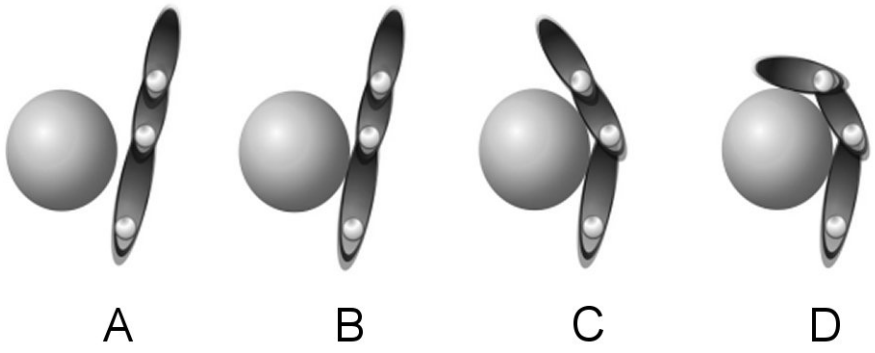

Figure 6.3: Natural finger movement.

During the grasping task the geometrical configuration of the finger is always determined by the external constraints related to the geometric characteristics of the object and the active coordination of the phalanges is not necessary. It is important to note that the sequence (A-D) showed in Figure 6.3 could occur with the continuous action of only one actuator. The underactuated prosthetic devices can perform an automatic finger wrapping around the object without the amputee intervention.

In this framework a first prototype of an underactuated prosthetic hand has been developed. The hand has three fingers: the middle, the index and the thumb. Underactuated mechanisms based on the Soft Gripper, proposed by Shigeo Hirose, have been applied to both fingers and thumb. The Soft Gripper model (Figure 6.4) has been developed in order to softly and gently conform to objects of any shape. It consists of N links (phalanges), which rotate freely about N axes. A pulley is fitted at each axis. The pulleys are coaxial to the axes and rotate freely about them. A wire runs from the tip to the root of the mechanism taking one turn about each pulley. N springs are fitted around each axes and iper-extension is prevented by N mechanical stops [37].

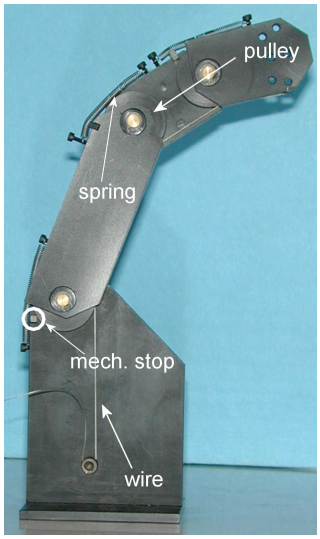

FIGURE 6.4: Soft Gripper model.

The force applied on the wire generates a moment in correspondence with each axis. These moments are proportional to the radius of the pulleys. The model in Figure 6.4 guarantees an adaptive behavior of the phalanges with respect to the grasped object, it has three DoFs and it is actuated by a single wire. It is possible to vary the force distribution on the grasped object and the kinematic behavior of the phalanges, setting the pulley diameters and the spring stiffness.

The RTR II adopts this model for the index, middle and the thumb. The hand has two motors (Figure 6.5): motor A for the flexion and extension movements of all the fingers and the thumb and motor B for the adduction and abduction movements of the thumb.

6.3.1 Finger design

Index and middle are identical, both fingers have three phalanges (Figure 6.6(a)). Pulley radii have been chosen in order to guarantee the static equilibrium during terminal grasps (involving only the distal phalanges). Pulleys can be easily changed in order to vary the kinematics behavior of the finger (§6.3.4).

The wire, fitted around every pulley, generates the flexion movement; the extension movement is realized by torsion springs. The two wires (respectively index and middle finger wires) are connected to the motor by means of an adaptive grasp mechanism based on a linear slider and two compression springs (§6.3.2), and the slider is connected to the motor through a leadscrew transmission.

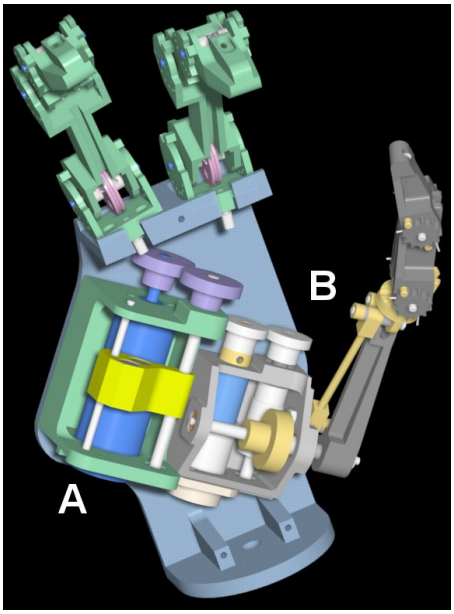

Figure 6.5: Solid model of the prosthetic hand.

6.3.2 Adaptive grasp mechanism design

In order to perform an adaptive grasp between the fingers, an adaptive grasp system has been designed. The system is based on compression springs: both finger wires are connected to a linear slider, through two compression springs (Figure 6.7). During a general grasp, index and middle fingers may not come in contact with the grasped object at the same time, one of the fingers and the thumb will come into contact first. When this occurs, in a conventional prosthesis, the other finger will no longer be able to reach the object to improve the grasp stability. Thank to the adoption of the compression springs this problem can be solved: when the first finger (e.g. middle finger) comes in contact with the object, the relative spring starts to compress, the slider is now free to continue its motion and the second (e.g. index finger) can flex, reaching the object.

When high forces are required, compression springs behave as a rigid link and all force is transmitted from the slider to the fingers. Note that the thumb wire is directly connected to the linear slider; this is the main advantage of using compression springs instead of extension spring.

6.3.3 Thumb design

The thumb has two phalanges, it is able to flex and extend using the soft gripper mechanism. The thumb wire is directly connected to the linear slider; it is also able to adduct and abduct. The complete thumb assembly is shown in Figure 6.6(b).

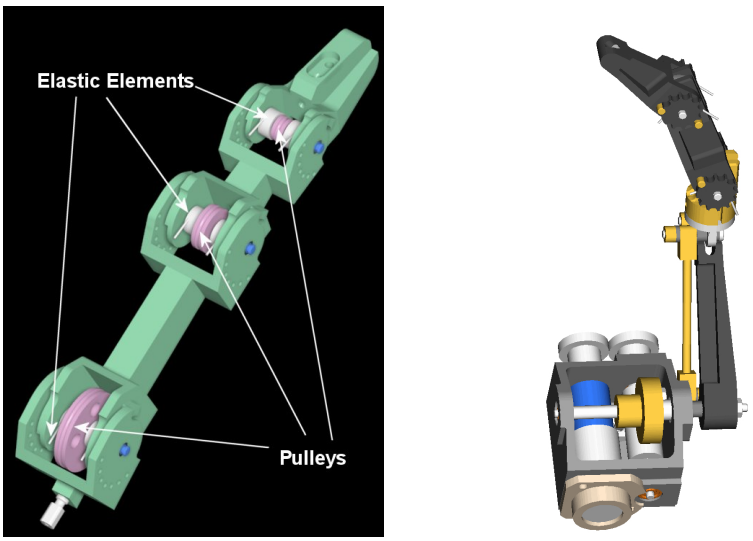

(a) Index/middle finger model (b) Thumb model

FIGURE 6.6: 3D models of the index and middle fingers (left), and of the thumb (right).

The adduction and abduction movements are realized by means of a four bar link mechanism. The four bar link has been introduced in order to mimic the adduction and abduction movements of the human thumb, varying the rotational axis of the thumb during its movement. By designing the thumb able to adduct and abduct, the hand can perform more grasping patterns, increasing the prosthesis flexibility [23].

6.3.4 Finger kinematics

We started the kinematics analysis considering one finger (e.g. index finger) as in Figure 6.4 and we analyzed the reaching phase of the object; only unconstrained movements of the finger are considered.

Our goal is to find the relation between the angular position of the motor θ_m and the angular position of every phalanx θ_i with $i = 1, 2, 3$. Due to the finger design, the wire position y_s is related to the actuator angular position θ_m through the relation:

$$y_s = \frac{\theta_m \, p}{\tau_m} + c \tag{6.1}$$

where p = pitch of the lead screw transmission of the slider, τ_m = gear ratio of the motor, and c = constant related to system geometry and wire length. Note that the presence of the compression spring for the adaptive mechanism is neglected in this model.

Starting from the wire inextensibility and from the following condition:

$$T \geq 0 \tag{6.2}$$

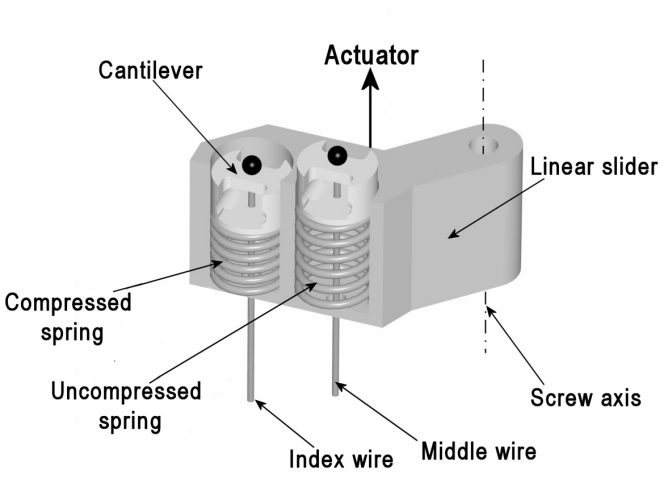

Figure 6.7: Adaptive grasp mechanism schematization.

where T is the cable tension, the kinematics relation can be written as:

$$\begin{cases} \theta_3 = c_0 + c_1\theta_1 + c_2\theta_2 + c_3 y_s \\ \dot{\theta}_3 = c_1\dot{\theta}_1 + c_2\dot{\theta}_2 + c_3\dot{y}_s \\ \ddot{\theta}_3 = c_1\ddot{\theta}_1 + c_2\ddot{\theta}_2 + c_3\ddot{y}_s \end{cases} \tag{6.3}$$

with c_1, $c_{2,}c_3$ constants related to system geometry and wire length.

To solve the kinematics problem and predict the movement of the unconstrained finger we need two more relations. These two equations can be found solving the finger dynamic.

6.3.5 Finger dynamic model

In order to evaluate the finger dynamic behavior during the reaching phase to the object, a bidimensional mathematical model has been developed. The model input is the wire position while the model outputs are the wire tension and the motion law of the lagrangian coordinates.

The finger model consists of three links; the geometric and inertial characteristics are computed starting from the solid model shown in Figure 6.6(a). The inertial effects due to the pulleys, the pins and the torsional springs are neglected. The wire is supposed to be inextensible and all the friction and gravity effects are neglected.

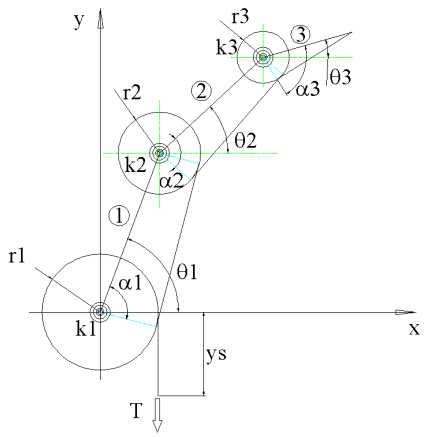

FIGURE 6.8: Finger schematization.

The dynamic equations can be written starting from the Lagrangian formulation:

$$\frac{d}{dt}\left(\frac{\partial L}{\partial \dot{q}_r}\right) - \frac{\partial L}{\partial q_r} = F_r \qquad r = 1, 2, \ldots n \tag{6.4}$$

where $L = E - U$, E= kinetic energy of the system, U= potential energy of the system, q_r= Lagrangian coordinate, F_r= generalized force associated with q_r, and n= number of DoFs of the system. In this model $n = 3$ and the lagrangian coordinates are θ_1, θ_2 and y_s which represents the slider position (see Figure 6.8). θ_3 is a linear function of previous coordinates. Assigning:

- geometrical variables:
  - l_1, l_2, l_3= link length
  - dg_1, dg_2, dg_3= C.G. position
- inertial variables:
  - m_1, m_2, m_3= link mass
  - I_{O1}= moment of inertia of the link 1 with respect to the origin
  - I_{G2}, I_{G3}= moment of inertia of links 2, 3 with respect to C.G.
- elastic variables:
  - k_1, k_2, k_3= stiffness spring constant

and writing the Lagrangian equations we obtain a highly non linear second order system with these variables: θ_1, θ_2 and T.

The input is $y_s(t)$, while the outputs are $\theta_1(t)$, $\theta_2(t)$ and $T(t)$. The system non-linearity arises from the kinetic and potential energy expressions:

$$\begin{cases} E = \frac{1}{2}A_1\dot{\theta}_1^2 + \frac{1}{2}A_2\dot{\theta}_2^2 + \frac{1}{2}A_3\dot{\theta}_3^2 + \\ A_4\dot{\theta}_1\dot{\theta}_2\cos(\theta_1 - \theta_2) + A_5\dot{\theta}_2\dot{\theta}_3\cos(\theta_2 - \theta_3) + \\ A_6\dot{\theta}_1\dot{\theta}_3\cos(\theta_1 - \theta_3) \end{cases} \tag{6.5}$$

where:

$$\begin{cases} A_1 = I_{O_1} + m_2 l_1^2 + m_3 l_1^2; \\ A_2 = I_{G_2} + m_3 l_2^2 + m_2 d_{G_2}^2; \\ A_3 = I_{G_3} + m_3 d_{G_3}^2; \\ A_4 = m_2 l_1 d_{G_2} + m_3 l_1 l_2; \\ A_5 = m_3 l_2 d_{G_3}; \\ A_6 = m_3 l_1 d_{G_3}; \\ U = \frac{1}{2}k_1\left(\frac{\pi}{2} - \theta_1\right)^2 + \frac{1}{2}k_2\left(\theta_1 - \theta_2\right)^2 + \\ \qquad \frac{1}{2}k_3\left(\theta_2 - \theta_3\right)^2. \end{cases} \tag{6.6}$$

where θ_3 has been replaced with the kinematic equation shown in eq. 6.3, which represents the holonomic constraints of the finger model.

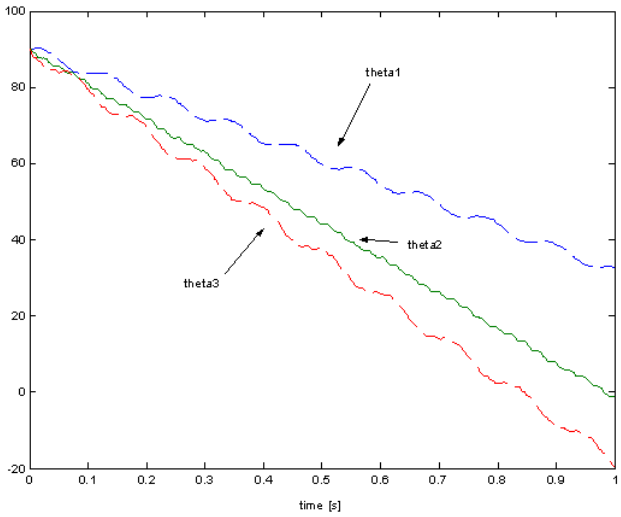

Figure 6.9: Angular position of the three phalanxes (linear input: ys(t) = 138.45 + 10 t).

The system solution (Figure 6.9) has been achieved using the SIMULINK package associated with MATLAB™. Pulley radii and spring stiffness affect the dynamic behavior

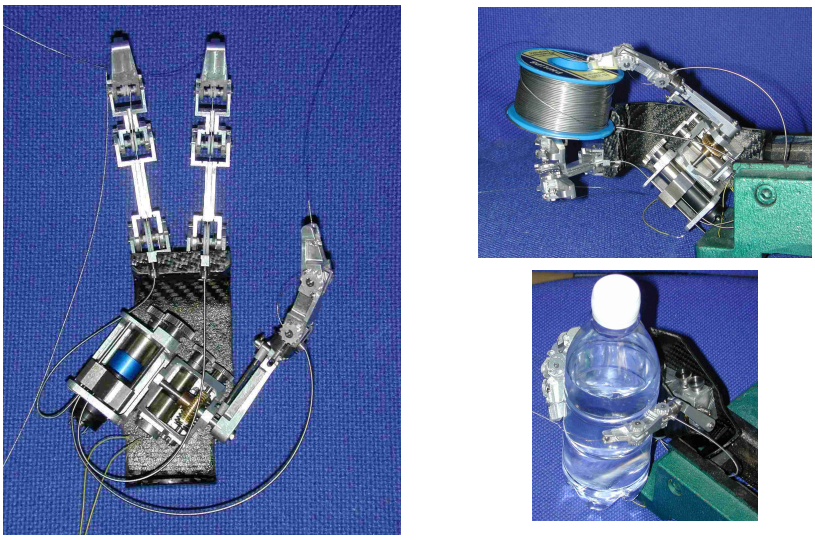

(a) The first prototype

(b) Lateral and cylindrical grasping

FIGURE 6.10: A picture of the first prototype of the RTR II prosthetic hand.

of the finger model. So, this tool can be useful to define these parameters in order to mimic the human finger movements. According to the results showed above, the finger bends, tracking the linear movement of the slider, with little vibrations whose amplitude depends on the link inertia.

6.3.6 Prosthesis development

Following the design principle described above, a first prototype of an underactuated hand has been designed and fabricated (Figure 6.10). This hand is capable of cylindrical grasping and lateral grasping (Figure 6.10(b)).

6.4 The control of the RTR II hand

The exchange of data between the user and the real world, according to the formal scheme presented in §4.3, is showed in Figure 6.11. In the next subsections the 4 control modules will be described in details.

In order to simplify the development and testing of the control algorithms, the TCM and LCM have been developed using LabView 6.1. The configuration of the analog inputs and of the digital outputs of the NI6025E for the control of the hand are shown in Table 6.1.

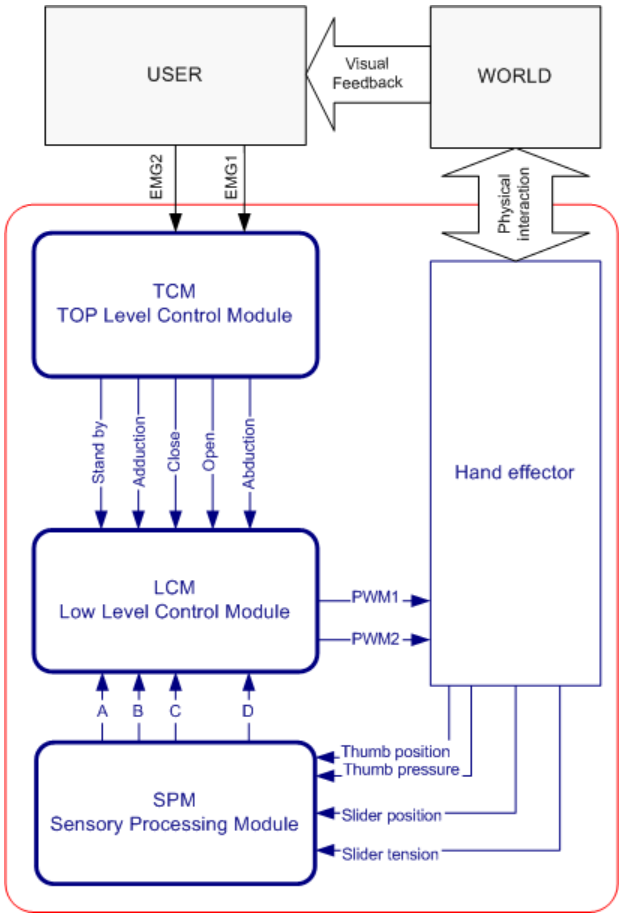

Figure 6.11: Schematic diagram of the exchange of data from the user to the real world and vice versa, passing through the prosthetic device.

6.4.1 Top level Control Module - TCM

The control scheme for the RTR II hand is a direct derivation of the control scheme used for the RTR I hand. Two EMG electrodes (Delsys DE2.3) have been used to acquire two EMG signals from the user, in order to control the opening/closing of the hand and the thumb adduction/abduction. The first electrode is placed on the *extensor carpii radialis*, and the second on the *flexor carpii radialis*.

6.4.1.1 Signal Processing

The two EMG signals are sampled at 1000 Hz (channels 0 and 1 of the National Instruments NI6025E acquisition board), and the variance of the EMG is extracted by using

Ch. #	type	Signal
0	A	EMG 1
1	A	EMG 2
2	A	Tensiometer
3	A	FSR
4	A	Slider position
5	A	Thumb position
6	A	-
7	A	-
8	A	R_{sens} Thumb
9	A	R_{sens} Slider
10	A	-
11	A	PWM
12	A	-
13	A	-
14	A	-
15	A	-

(a) Analog inputs

Channel #	Type	Signal
0	D	MOT 1 - Power
1	D	MOT 2 - Power
2	D	Direction
3	D	
4	D	
5	D	
6	D	
7	D	
GPCTR0 OUT	Counter	PWM

(b) Digital outputs

TABLE 6.1: The configuration of the analog inputs and of the digital outputs of the NI6025E for the control of the RTR2 prosthetic hand.

equation 5.5. A simple threshold classification has been chosen in order to detect the activation of the hand.

6.4.1.2 User training

A software for the training of the user has been developed by using LabVIEW. This software is directly derived from the software already used for the RTR 1 hand (Figure 5.13). By using this software, the user is trained to contract the *extensor carpii radialis* and *flexor carpii radialis*, in order to generate the control signals. The visual representation of the EMG signal and its variance help the user to learn how to control the hand.

The user training protocol is divided into several phases, as follows:

1. the user is asked to contract the two antagonist muscles, in random sequence, for a variable period of time, ranging from $t_{\text{training}_0} = 2$ minutes (experienced user) to $t_{\text{training}_0} = 10$ minutes (new user). During this training period the position of the electrodes is adjusted in order to get the best signals;

2. in order to determine the dynamic range of the EMG signals, the user is asked to contract the *extensor carpii radialis* for $t_{\text{ext}} = 5$ seconds at maximum contraction level. The variance of the signal in the last part of this contraction (100 ms) is the signal the the user could reproduce without problems for the whole day during normal activities.
   This value σ_{ext} is normalized to 1, thus setting the gain of Channel 1 ($G_{\text{extension}}$).

3. the user is asked to contract the *flexor carpii radialis* for $t_{\text{flex}} = 5$ seconds at maximum contraction level. The variance of the signal in the last part of this contraction is the signal the the user could reproduce without problems for the whole day during normal activities.
   This value σ_{flex} is normalized to 1, thus setting the gain of Channel 2 (G_{flexion}).

4. the user is then asked to move the arm with the electrodes for $t_{\text{baseline}} = 5$ seconds without commanding the opening or the closure of the hand. In this way the baselines of the 2 EMG channels are recorded, thus setting the 2 activation thresholds. The variance of the 2 channels are recorded, and the 2 thresholds are set as the mean value μ of the variance of the EMG signal during t_{baseline} plus its variance, i.e. $\tau_{\text{ext}} = \mu(\sigma_{\text{ext}}) + \sigma(\sigma_{\text{ext}})$, $\tau_{\text{flex}} = \mu(\sigma_{\text{flex}}) + \sigma(\sigma_{\text{flex}})$.

5. the user is then asked to generate the control signals for the adduction and abduction of the thumb. In particular:

   a) the user is asked to switch from the lateral grasping configuration to the cylindrical grasping configuration by generating a short contraction ($t_{\text{short}} = 50$ ms) of the *extensor carpii radialis*, followed by a longer contraction ($t_{\text{long}} \geq 100$ ms) of the *flexor carpii radialis*.

   b) the user is asked to switch from the cylindrical grasping configuration to the lateral grasping configuration by generating a short contraction ($t_{\text{short}} = 50$ ms) of the *flexor carpii radialis*, followed by a longer contraction ($t_{\text{long}} \geq 100$ ms) of the *extensor carpii radialis*.

   c) the above 2 steps are repeated 5 times.

6. the uses is asked to move the hand and to contract the muscles and generate control commands, in order to verify that the above parameters suit the user needs.

7. the above steps are repeated until the user reaches a satisfactory ability in generating the commands to the hand.

6.4.2 Low level Control Module - LCM

The Low level Control Module receives as input the following signals:

- from the Top Level Control Module:

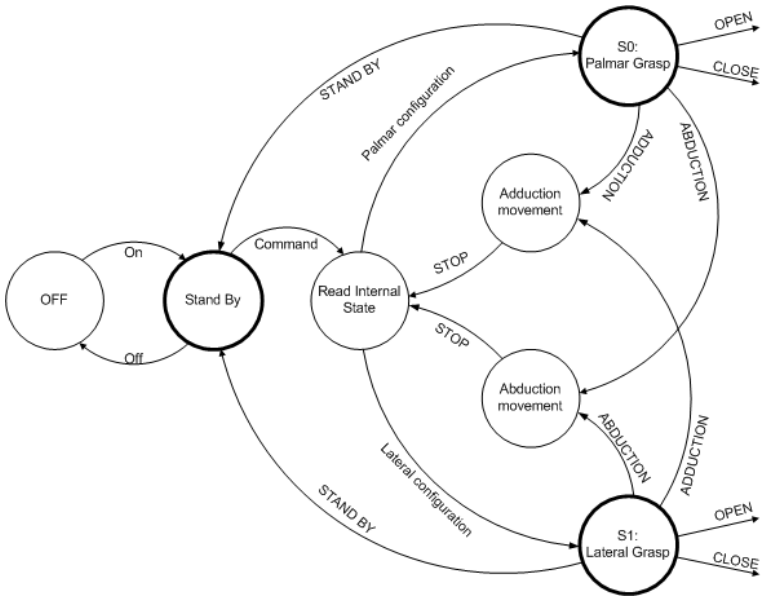

(a) Part I

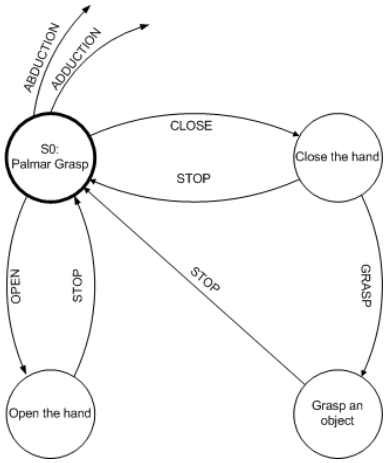

(b) Part II

FIGURE 6.12: Schematic description of the behavior of the Low level Control Module.

– Stop;
– Open the hand;
– Close the hand;
– Thumb abduction;
– Thumb adduction.

- from the Sensory Processing Module:
  - Thumb angular position;
  - Slider position;
  - Thumb pressure;
  - Tension on the cable;
  - Mean current in the thumb motor;
  - Mean current in the slider motor.

These signals are used to control the behavior of the prosthetic hand according to the commands coming from the TCM.
In particular, the LCM operates as follows:

- When the system is turned on, it goes in the **Stand By** state (Figure 6.12), waiting for any command coming from the TCM.
- Once a command is generated from the TCM, the LCM reads its internal state.
- Depending on the position of the thumb, the LCM goes into **S0: palmar grasp** (if the rotation of the thumb is over a determined threshold th_{rotation}) or in **S1: lateral grasp** (if the rotation of the thumb is below a determined threshold th_{rotation}).
- In both of these internal states (S0 or S1) the hand executes the command arrived from the TCM. As said before, the possible commands coming from the TCM are:

  hand opening (Figure 6.12(a)): the hand opens until it receives a STOP command (i.e., no more commands) or it reaches the maximum extension (determined by the slider sensor). The speed of the movement depends on the amplitude of the OPEN command

  hand closing (Figure 6.12(a)): the hand closes until it receives a STOP command (i.e., no more commands), or if it reaches the maximum flexion (determined by the slider sensor), or if a contact with an object is detected. The speed of the movement depends on the amplitude of the CLOSE command.
  In case a contact is detected, the hand goes into the **Grasp state**, in which it grasp the object with a force determined by the amplitude of the CLOSE command. If the starting state is **S0: palmar grasp** both the tensiometer on the slider and the pressure sensor on the thumb are used to control the force. Otherwise, if the starting state is **S1: lateral grasp**, only the pressure sensor is used.

  thumb abduction (Figure 6.12(b)): In both S0 and S1 the thumb abducts. Once the movement stops, the hand reads its internal state and, according to the position of the thumb respect to the threshold th_{rotation} goes into S0 or S1. The speed of the movement depend on the amplitude of the ABDUCT command.

thumb adduction (Figure 6.12(b)): In both S0 and S1 the thumb abducts. Once the movement stops, the hand reads its internal state and, according to the position of the thumb respect to the threshold th_{rotation} goes into S0 or S1. The speed of the movement depend on the amplitude of the ABDUCT command.

STOP: the STOP command is issued both by the user (if s/he wants to stop the current movement) or automatically by the LCM (in case the hand has reached the desired level of grasping force, or the end of the active stroke of the slider or of the thumb, or there is an obstacle).

- In case no commands arrive to the hand within $t_{\text{stand-by}}$ the hand goes to the **Stand by** state.

6.4.3 Sensory Processing Module - SPM

The artificial sensory system is the core of the hand control system, and has a twofold function: first, it provides input signals for the low-level control loop of the grasping phase, thus enabling local and autonomous control of the grasp without requiring user's attention and reaction to incipient slippage. Moreover, it generates sensory signals that could be transmitted to the user through an appropriate neural interface. The aim of the sensors design is to be able to integrate in the artificial hand a great number of different sensors in order to confer to the hand the functionality as close as possible as that of the human.

The hand sensory system is necessary to enable automatic control of grasping tasks without requiring special attention and efforts to the hand user. In addition the sensory system is studied to enable a first set of experiments intended to investigate the feasibility of providing the amputee with cognitive feedback about the grasping task that is performed.

For these reasons, the artificial sensory system is inspired at replicating the natural sensory system providing both proprioceptive and exteroceptive sensing abilities.

In synthesis the sensory system is composed of different sensors, both proprioceptive and exteroceptive. In particular, the current prototype is provided with position sensors for the thumb and the fingers, a tensiometer on the cable that drives the index finger and a force sensor on the tip of the thumb.

In the following subsections the sensory system will be described in details.

6.4.3.1 Slider position sensor

A qualitative measurement of phalanges positions is obtained by detecting the displacement of the slider where a Hall effect sensor (model SS496B, Honeywell Inc, Freeport, Il, USA) is mounted. This sensor detects the position of the slider along his stroke during the flexion/extension movements of the fingers, like the physiological angular sensors in the joint capsules KANDEL.

The main problem encountered when developing this position sensor was to cover the entire slider's stroke (about 20 mm) which is large compared to the normal working range

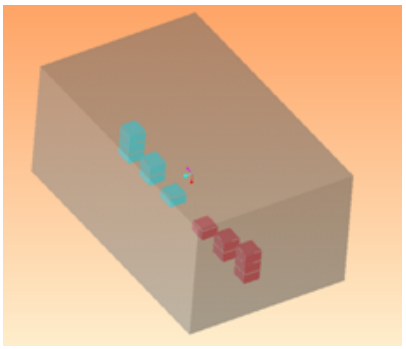

(a) Ansys model

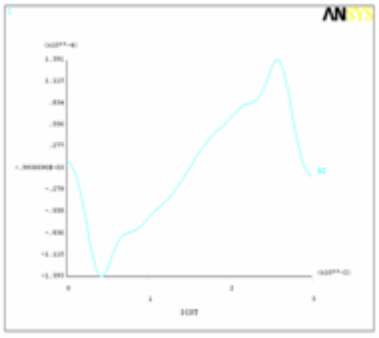

(b) simulation (gap = 0.5mm)

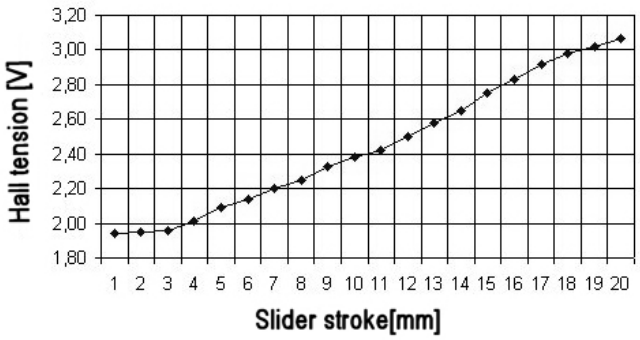

(c) Hall tension versus linear slider's stroke (gap = 2mm)

Figure 6.13: The Ansys model of the slider position sensor and its simulated output (top). Hall tension versus linear slider's stroke (bottom). Hall tension trend is monotonic and quite linear over the entire slider's stroke.

of Hall effect sensors; for this reason we have simulated and compared a number of different magnets configurations by means of the software Ansys® Multiphysics (ANSYS Inc. Corporate, Canonsburg, PA, USA). A specific optimal configuration has been experimentally found by using 12 Honeywell International Inc. 103MG5 magnets (Figure 6.13).

The Hall electrical tension generated in this configuration is able to cover the entire slider's stroke and its trend is monotonic and quite linear, as shown in Figure 6.13. A Matlab®(The MathWorks, Inc., Natick, MA, USA) model, described in MASSA-ICRA2002, has been developed to correlate the slider position with the joints angles: through this model is possible to estimate the position of the joints during an opening-closure motion.

The experimental analysis has assessed the simulation and the final calibration on board (Figure 6.13(c)) has provided good linearity and repeatability (enhanced by reducing the machining and assembling tolerances) MASSA-ICRA2002. With a power supply of 5V,

the output of the sensor could be approximated by:

$$V_{out} = 0.0643 \cdot x_{slider} + 1.8371, \qquad R^2 = 0.9901 \tag{6.7}$$

where R^2 is defined as:

$$R^2 = 1 - \frac{\sum (y_j - \hat{y}_j)^2}{\sum (y_j)^2 - \sum (\hat{y}_j)^2} \tag{6.8}$$

6.4.3.2 Thumb position sensor

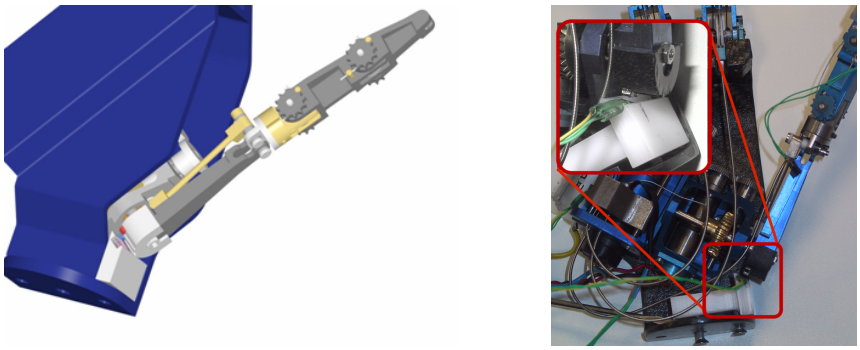

(a) CAD model (b) Photograph

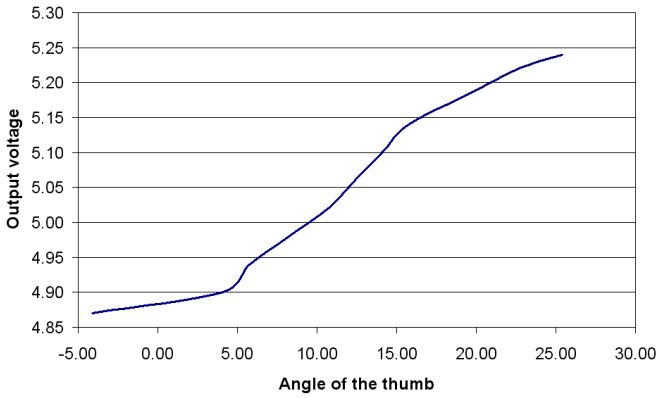

(c) Hall tension versus thumb position.

FIGURE 6.14: The CAD model of the thumb position sensor, the picture of the prototype and the output of the sensor. Hall tension trend is monotonic and quite linear over the entire slider's stroke.

A round-shaped cap with two magnets has been assembled at the base of the thumb, at the center of rotation of the four bar link mechanism providing abduction/adduction capabilities to the thumb. A Hall effect sensor (model SS496B, Honeywell Inc, Freeport, Il, USA), located in front of the cap, determines the angle displacement of thumb metacarpus when performing the thumb adduction/abduction movements, thus behaving like the physiological angular joint sensors in the joint capsules [41].

The output of the position sensor V_{out} is related to the angular position of the thumb θ_{thumb} by the following equation:

$$V_{out} = 131.1 \cdot \theta_{thumb} - 319.76, \qquad R^2 = 0.9575 \tag{6.9}$$

The sensor has an operative range of 30 $^\circ$ and has shown good sensitivity, and repeatability performance (Figure 6.14(c)).

6.4.3.3 Slider tensiometer

In the RTR II hand, the transmission cables are fixed on one end to the index and middle distal phalanges and, on the other end, they are connected to the linear slider through the two compression springs of the differential mechanism. The cables act directly on two mobile elements, which compress the springs during the adaptive grasp of an object of irregular shape. The force sensor is obtained by sensorizing an elastic element acting as a mechanical stop for the cables.

The tendon tensiometer is based on strain gauges sensors (model ESU-025-1000, Entran Device Inc, Fairfield, NJ, USA). The micromechanical structure has been fabricated to obtain a deformable cantilever (Figure 6.15), in order to continuously monitor the cable tension applied by the motors, as the Golgi tendon organ in series with a muscle [41].

The calibration has been performed with an INSTRONR4464 test machine (Instron Corporation, Canton, Massachusetts, USA) with a static load cell working in the range of ± 1 KN. A cone-shaped tip, fixed to the load cell, has been used to apply the load, as shown in Figure 6.16(a). A Wheatstone bridge, followed by a low pass RC filter with $f_t = 100\ Hz$ and a signal amplifier, has been used to detect the variation of the resistance of the two strain gauges. Then, the strain gage sensors signal has been acquired through an acquisition board (National Instruments^{TM} DAQ Card 1200), and finally processed by a custom LabVIEW^{TM} interface to visualize in real time its output (Volts) versus the applied load (N). The output of the tensiometer V_{out} is related to the applied tension T_{cable} by the following equation (Figure 6.16(b)):

$$V_{out} = 26.349 \cdot T_{cable} - 0.3732, \qquad R^2 = 0.9996 \tag{6.10}$$

The sensing device has shown good dynamic, sensitivity and repeatability performance; a little hysteresis and time delay have been detected due to the differential mechanism of the hand (there is a spring under the strained component) [59].

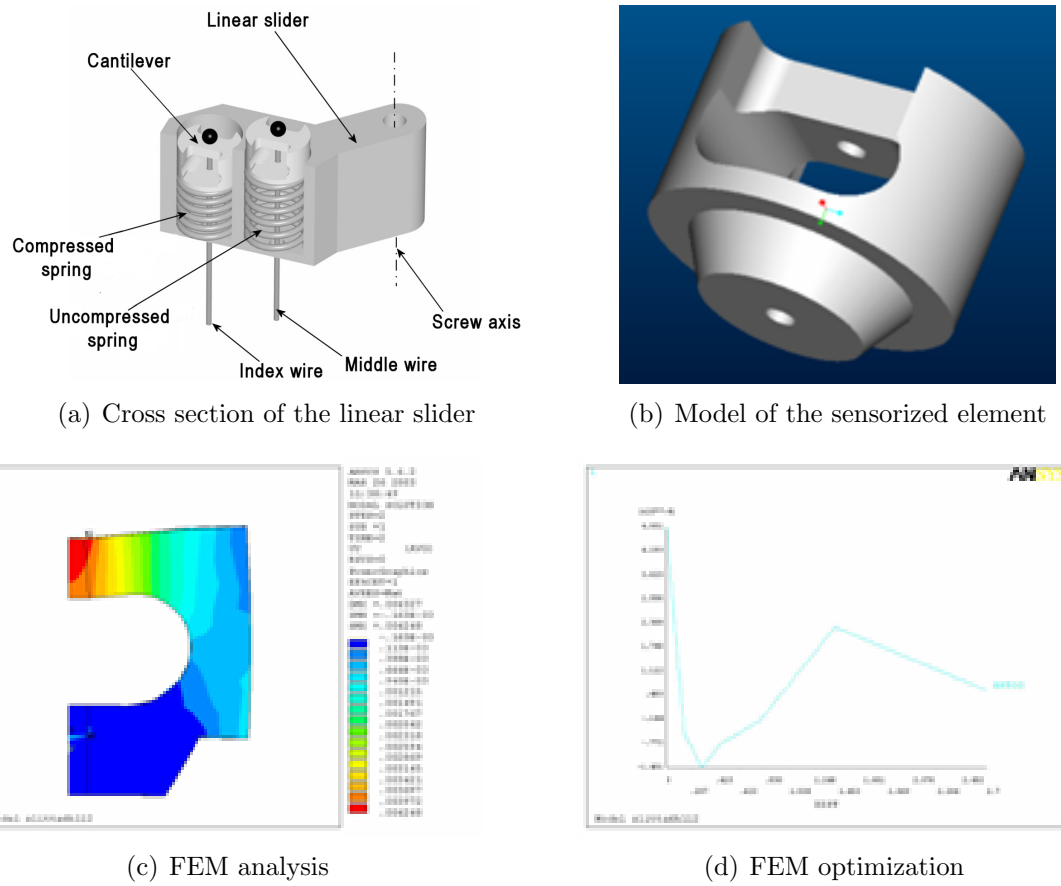

(a) Cross section of the linear slider

(b) Model of the sensorized element

(c) FEM analysis

(d) FEM optimization

FIGURE 6.15: Realization of the sensorized element. The value of cable tension is estimated through the measurement of the elastic deformation of the cantilevers realized on the mobile elements.

6.4.3.4 Thumb pressure sensor

An artificial mechanoreceptor is obtained by means of a FSR pressure sensor (part #400, Interlink Electronics, Camarillo, Ca, USA), 5 mm in diameter and 0.3 mm of nominal thickness, embedded at the thumb tip: the whole distal phalange, with the FSR at the volar side, has been immersed in a thumb shaped shell containing melted silicone (Figure 6.17(a)). When the silicone polymerization has been over, a force sensitive thumb tip has been obtained. The force sensor has been applied only on the thumb tip that is significantly involved in all the functional grasping tasks [87].

The hand was locked with the force sensor facing upwards, and a cylinder (5 mm in diameter), fixed to the load cell of the testing machine, has been used to apply the load.

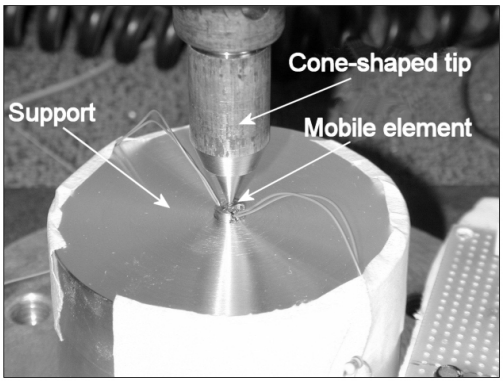

(a) Cone-shaped tip

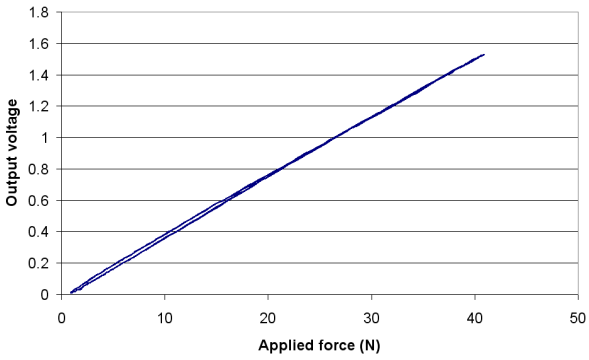

(b) Output response of the tensiometer

Figure 6.16: The cone-shaped tip used for the calibration (left), and output of the sensor (right).

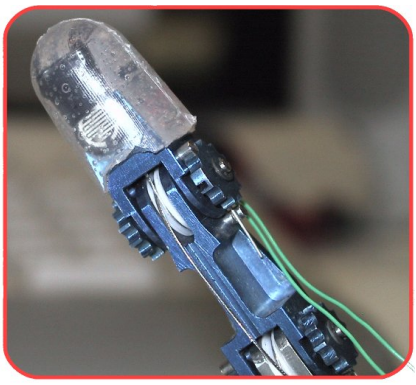

(a) Picture of the pressure sensor

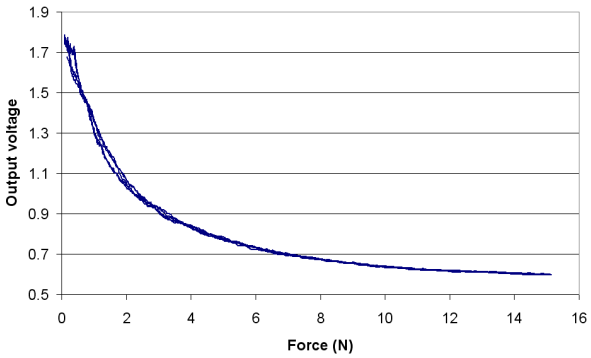

(b) Output response

Figure 6.17: Picture of the thumb pressure sensor and output response.

The output of the FSR force sensor V_{out} is related to the applied force F_{FSR} by the following equation (Figure 6.17(b)):

$$V_{out} = -0.2887 \cdot Ln(F_{FSR}) + 1.2867, \qquad R^2 = 0.9754 \tag{6.11}$$

The sensor gives information on the static pressure on a large area, more than 5 mm (Figure 6.17), and it has shown good dynamic characteristics. As a consequence, the

developed force sensor could be likened to some features of the FA II and SA II physiological mechanoreceptors [41, 90].

6.4.3.5 Current limitations

Two power resistances ($R_{sens} = 0.330\Omega$) are put in series with the two motors in order to sense the mean current in the motors. These resistances, namely R_{sens_T} and R_{sens_S}, are used in order to limit the power consumption during active grasping or in case the movement of the hand is obstructed by an external obstacle. In particular, R_{sens_S} limits the current in the thumb adduction/abduction motor to 0.5 A, while R_{sens_T} limits the maximum current in the slider motor to 1 A.

Once the hand has grasped the object, in fact, the unbackdrivable mechanism maintains the grasping force without requiring any additional power supply. In this way the charge of the batteries can be saved, thus increasing the number of active grasps that could be realized with a single charge.

6.4.4 Sensory Feedback Module - SFM

The RTR2 hand has no explicit Sensory Feedback Module. As usual with current hand prostheses, the sensory feedback is given in an indirect form:

- visual feedback;
- proprioceptive sensation on the stump, due to the load of the grasped object;
- change of the sound of the motors during grasping.

6.5 Discussion

The design approach based on underactuated mechanism has been proposed and applied to the prosthetic field with the aim of rising the prosthesis flexibility while maintaining the intrinsic actuation solution and implementing simple control algorithm. The proposed dynamic model represents a useful tool for simulating the expected grasping capabilities. It is important to note that the tendon transmission structure applied in the RTR II hand is observed with human finger. In the human hand the *flexor digitorum profundus* acts in the same way as the wire transmission in the Soft Gripper.

This hand presents some advantages respect to the state of the art of the hand prosthesis:

- it has 9 DoFs instead of just 1, while maintaining approximately the same dimensions of commercial prosthetic devices;
- the actuation system and the sensors are all enclosed within the hand;

- the control board and sensory processing board could be easily integrated within the palm;
- the hand is very light, it weights less than 320 grams;
- the underactuation allows a better encirclement of the objects, while maintaining a simple control system;
- the adduction/abduction DoF of the thumb allows also the lateral grasping.

Anyhow, the RTR2 hand presents several drawbacks:

- the maximum grasping force is lower than the grasping force of a conventional myoelectric prosthesis (16N vs. $\simeq$ 100N);
- the tendon-based transmission system requires more maintenance;
- the RTR2 hand is slower than a conventional DC prosthesis;
- the RTR2 hand is a little bit bigger than the human hand, and it does not fit in conventional cosmetic gloves;
- the adduction/abduction movement is difficult to be controlled by using EMG signal.

The RTR2 hand presents several improvements respect to the RTR1 hand and respect to commercial myoelectric prosthesis. By using only two DC motors, one for the thumb abduction/adduction, and the other one for the opening and closing of the 3 fingers, the underactuated mechanisms allows a very good encirclement of objects of any shape, without requiring any additional effort to the user. The hands automatically and passively adapts to the object, thus increasing the stability of the grasping.

The opening and closing of the hand are easily controlled by the user by contracting the *extensor carpii radialis* and *flexor carpii radialis*, respectively. Anyhow, due to the slowness of the movement (it takes more than 2 seconds for a complete flexion of the fingers), a direct EMG control of the opening and closing movements, even if feasible, is not recommended.

Moreover, the adduction/abduction movement is difficult to be controlled by using EMG signal, as it should be coded in an unnatural way. In order to be successfully controlled, this movement requires a long period of user training and, in any case, the user is forced to keep a continuous attention to the movement.

With the above considerations in mind, a new prosthetic device could be realized.

Seven

A hand prosthesis with one DoF: the SPRING hand

7.1 Introduction

The RTR II prosthetic hand, presented in the previous chapter, has shown a good adaptability the the shape of the objects to be grasped. Moreover, this prosthesis has the possibility to realize both cylindrical and lateral grasping. However, it turned out that the control of the thumb position with the EMG signal is feasible, but quite discomfortable, in particular during ADLs.

In order to enhance the performance of current prosthetic device, while maintaining the self-adaptability obtained thanks to the underactuation, a new prosthetic device, called SPRING hand, has been developed.

7.2 Finger Mechanism

In order to realize a self-adaptive grasp, an innovative underactuated mechanism based on cable transmission has been conceived and developed. The mechanism includes the three cables (one for each phalange) and two compression springs (one in the proximal phalange and one in the interphalangeal one) as shown in Figure 7.1. These springs allow the adaptive behavior of each phalange and guarantee the shape adaptation to the grasped object. The choice of the springs constant is due to a compromise: this constant must be as low as possible in order to reduce power consumption, and it must be sufficiently high in order to prevent compression before the contact with the object. Each cable is fixed to the corresponding phalange; the three cables are pulled in unison by means of a linear slider. The movement of the slider produces the rotations of the three joints, as indicated by the arrows in Figure 7.1. The first cable is fixed to the distal phalange and is wound around the metacarpophalangeal (MP) and the proximal interphalangeal (PIP) joints on its way to the linear slider. The second cable is fixed to the intermediate phalange through

a compression spring. It is also wound around the MP joint and then attached to the slider. The third cable is fixed to the proximal phalange through a second compression spring and attached to the linear slider.

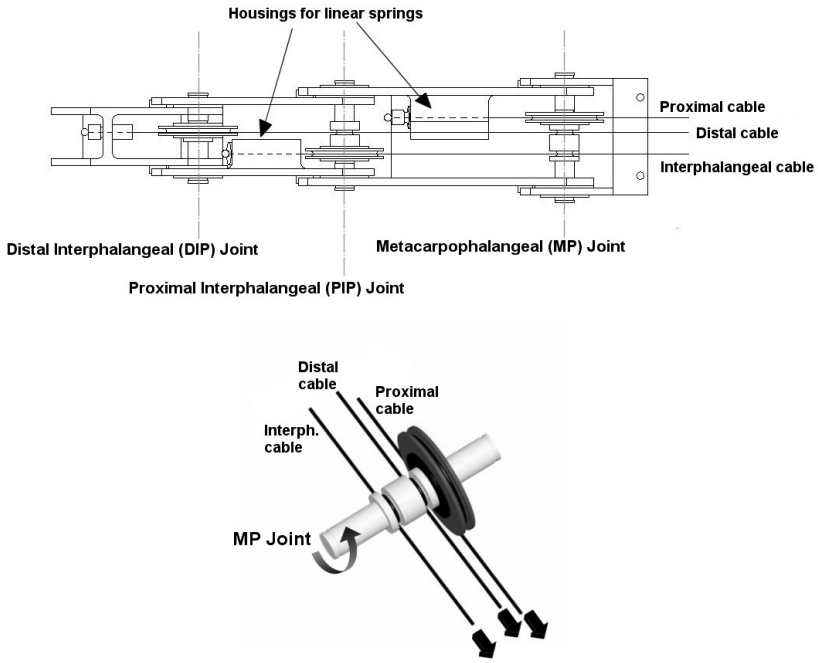

Figure 7.1: Top view of the finger prototype showing cable transmission with springs (upper) and detail drawing of the Metacarpophalangeal (MP) joint (lower).

At the beginning of the grasp the finger is in the fully extended position (a). When the proximal link comes into contact with an object to realize a power grasp, the continuous movement of the slider produces compression of the linear spring fixed on the proximal cable (b). This compression allows the intermediate and distal links to continue bending. When the intermediate link touches the object, the corresponding spring starts to compress, allowing the distal phalange to continue flexing (c). The grasping task is completed (d) since the distal cable is directly fixed to the slider without any compression spring (see Figure 7.2 for the entire sequence)

7.3 Finger kinematics

In the following, θ, α, and β indicate the proximal, intermediate and distal phalange rotations respectively, R is the pulley radius and r is the joint radius around which the cables winds (see Figure 7.3 and Table 7.1) and x is the slider displacement.

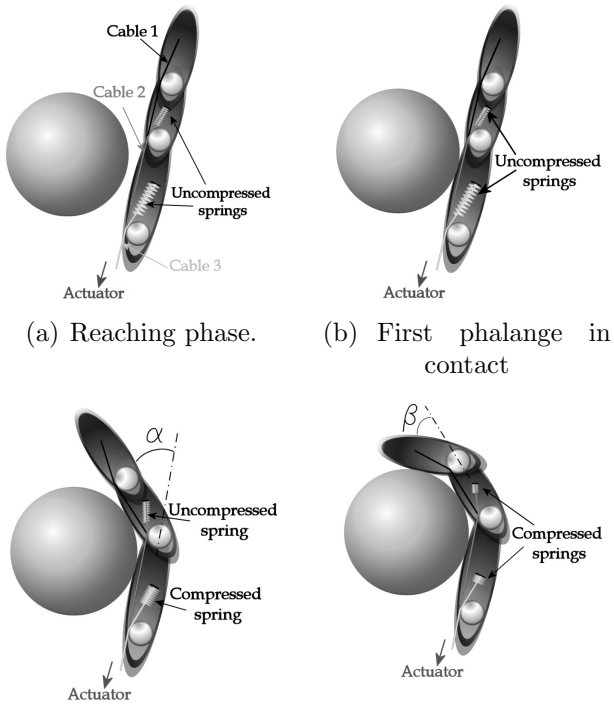

(a) Reaching phase.

(b) First phalange in contact

(c) Compression of the first spring

(d) Encirclement of the object.

FIGURE 7.2: Grasping sequence: (a) reaching phase, (b) first phalange in contact, (c) the compression of the first spring allows the flexion of the PIP joint, (d) after the contact with the second phalange, the compression of the spring allows the flexion of the DIP joint and the encirclement of the object.

As the slider starts to pull the three cables, the rotation of the proximal phalange around the MP joint has two consequences:

1. the cable fixed to the intermediate phalange unwinds from the MP joint;
2. the cable fixed to the distal phalange unwinds from the MP and PIP joints.

These rotations determine the orientations that the distal phalanges take with respect to the proximal phalange. It is possible to get the rotations of the three joints (α), (β) and (θ) corresponding to the slider displacement, x, taking into account the compensation due to the cables unrolling originated by pulley rotations. In particular, L_1 is the compensation length of the intermediate cable on the MP joint due to the proximal rotation; L_2 is the compensation length of the distal cable on the PIP joint due to the intermediate rotation. Consequently, it is possible to calculate the values of the angles corresponding to this compensation respectively on the intermediate and distal pulleys, here called C_1 and C_2,

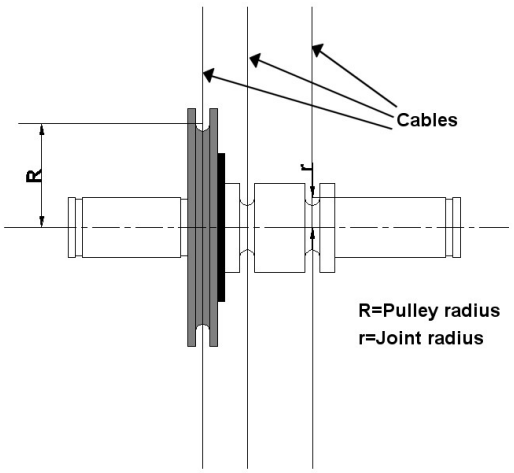

FIGURE 7.3: View of the MP joint showing pulley and joint radii. The pulley is free to rotate relatively to the joint.

and to get the real rotations around the PIP and DIP joints, as shown in Equations (7.4),(7.7).

$$\theta(x) = \frac{x}{R} \tag{7.1}$$
$$L_1(x) = r\,\theta(x) \tag{7.2}$$
$$C_1(x) = \frac{L_1(x)}{R} \tag{7.3}$$
$$\alpha(x) = \theta(x) - C_1(x) \tag{7.4}$$
$$L_2(x) = r\,\alpha(x) \tag{7.5}$$
$$C_2(x) = \frac{L_2(x)}{R} \tag{7.6}$$
$$\beta(x) = \theta(x) - C_1(x) - C_2(x) \tag{7.7}$$

The curves describing the angles α, β, θ versus the slider displacement x are straight lines as shown in Figure 7.4(a), the inclination of the lines depends on the value of pulleys and joints radii.

In the first SPRING prototype the value of the pulley radius, R, has been fixed to $7mm$. This is the maximum value that fits within the height of the phalanges, in order to get the highest possible torque during grasping tasks. As mentioned before, the value of the joint radius, r, affects the rotational angles during the closing sequence: it has been chosen equal to $3mm$ to obtain an anthropomorphous closure movement.

For example, according to the selected geometrical parameters, if a movement of the slider $5.5mm$ backwards is hypothesized, it turns out that the rotation around the MP

Name	Description
θ	Proximal Phalange Rotation
α	Intermediate Phalange Rotation
β	Distal Phalange Rotation
R	Pulley Radius
r	Joint Radius
x	Slider Movement

TABLE 7.1: Parameter for the description of the finger kinematics.

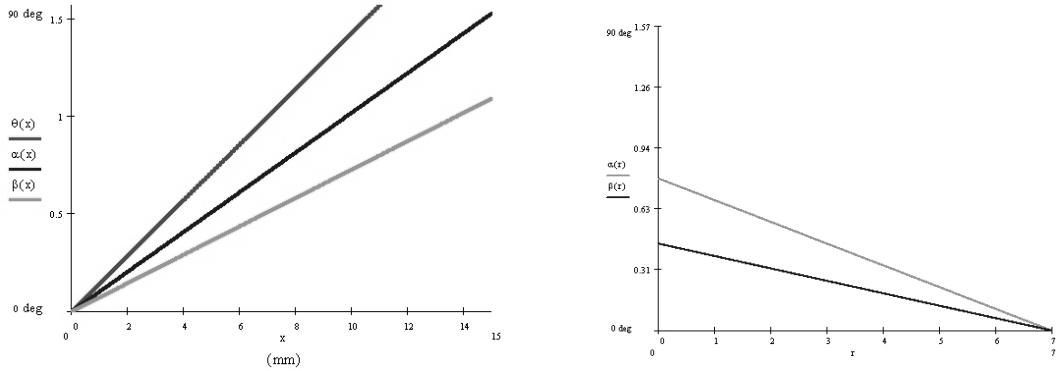

(a) (b)

FIGURE 7.4: The direct proportionality between the angles of rotation α, β, θ and the movement of the slider x (left). The angles α and β in function of the joint radius r on the proximal interphalangeal (PIP) joint (right).

joint is $\theta = 45°$, the rotation of the intermediate link (α) is equal to 25.4° and the rotation (β) of the distal link is 15.5°. These angle values provide a natural flexion-extension of the fingers, as described in Figure **??**.

It is necessary to use the smallest radii of the joints to get α and β always smaller but closer to the value of the proximal link, in order to obtain "a natural" flexion of the finger. Figure 7.4(b) shows angles α, β versus the radius r on the PIP joint. Every cable is wound in the same direction in order to contribute positively to the flexing torque. The torque values at each joint can be calculated from the cables tensions according to the following Equations:

$$\text{MP joint:} \quad T_{Proximal} = T_1\, R + T_2\, r + T_3\, r \tag{7.8}$$

$$\text{PIP joint:} \quad T_{Intermediate} = T_2\, R + T_3\, r \tag{7.9}$$

$$\text{DIP joint:} \quad T_{Distal} = T_3\, R \tag{7.10}$$

where R is still the radius of the pulley fixed on the joint, r is the radius of the joints on which the cables are wound and T_i (i=1,3) are the tensions in the three cables.

A high value of the pulley radius R is favorable because it increases the flexing torque, as shown in Equations (**??**),(**??**) and (**??**). It is important to find a correct compromise between a low value of the joint radius r, that guarantees an anthropomorphous closing sequence according to Figure 7.4(a), and a high value that gives a good contribution to the flexing torques as shown in Equations (**??**) and (**??**).

7.4 The SPRING Hand

The Spring hand implements the finger mechanism described above on three fingers: index and middle fingers and a thumb in opposition. The hand is underactuated: the DoFs of the hand are eight, but the hand has only one motor that drives all the DoFs. A DC Minimotor has been selected to obtain a 10 N pinch force at the finger tip. The specifications of the actuator are showed in Table 7.2.

MOTOR DATA (2224 006 SR)					GEAR DATA (20/1)		
Nominal voltage	Un	6	Volt		Housing material	all steel	
Terminal resistance	R	1,94	Ω		Geartrain material	metal	
Output power	P2 max	4,55	W		Recommended input speed	5000	rpm
Efficiency	η max	82	%				
					Reduction ratio	**3,71:1**	
No-load speed	n0	8200	rpm				
No load current	I0	0,029	A		weight w/o motor	28	g
Stall torque	**Mh**	**21,2**	**mNm**		lenght w/o motor	18,35	mm
Friction torque	Mr	0,2	mNm		lenght with motor	42,55	mm
Speed constant	Kn	1380	rpm/V		output torque contunuous op	500	mNm
Back-EMF constant	Ke	0,725	mV/rpm		output torque intermitent op	700	mNm
Torque constant	Km	6,92	mNm/A				
Current constant	Kl	0,144	A/mNm		**Efficiency**	**88**	**%**
Weight		46	g				
Torque up to	M0 max	5	mNm				
Current up to	I0 max	1,2	A				

Table 7.2: Motor and gear data.

The following equation has been used to calculate the global tension in the cables:

$$F = \frac{T_e}{0.5\, d_m \dfrac{(f\,\pi\, d_m) + L\,(cos\alpha_n)}{(\pi\, d_m\, cos\alpha_n) - f\, L}} \tag{7.11}$$

where F is the global tension in the cables, T_e is the motor torque, d_m is the screw medium diameter, f is the friction coefficient between screw and leadscrew, L is the screw pitch, and α_n is the screw angle measured on the normal plane.

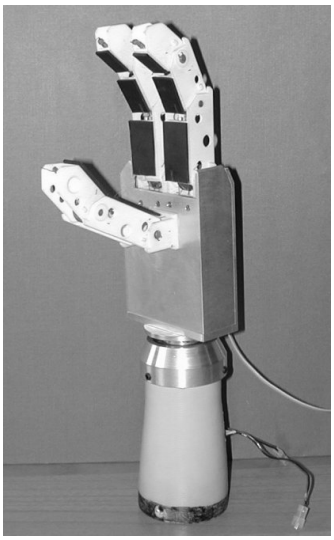

FIGURE 7.5: The first prototype of the SPRING hand

The SPRING hand prototype, integrated with a prosthetic wrist providing one additional DOF, is showed in Figure 7.5. The index and middle fingers are composed of a base, fixed to the palm, and by three phalanges connected by rotational joints. The thumb has a base fixed to the palm too, but it is composed of only two phalanges, as in the human hand. The palm is the center of the actuation and transmission systems, which will be described in detail.

7.4.1 Transmission system

According to prosthetics requirements, the actuator and the transmission system are integrated in the palm, as shown in Figure 7.6(a). The system is composed of an independent structure fixed to a central wall within the palm by means of small bolts. The transmission system is composed of:

- Slider

- Differential mechanism
- Belt and pulleys
- Guides

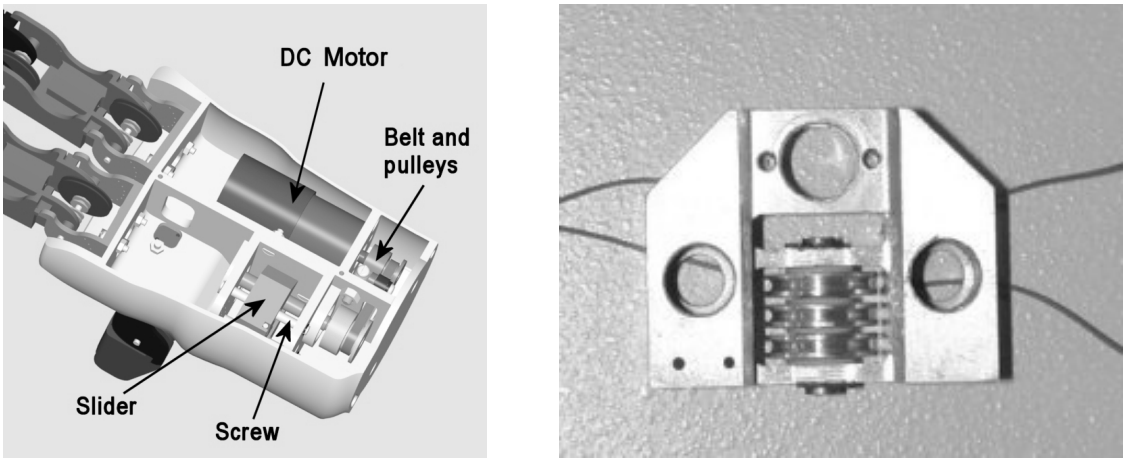

(a) Actuation and transmission system (b) The slider

Figure 7.6: The actuation and transmission systems are placed inside the palm. The slider is the core of the transmission system.

The slider is the fundamental element of the transmission system: in fact it is possible to get the flexion and the extension of the fingers thanks to its two-way linear motion. The slider pulls all the eight cables for the flexion movement of the index, middle fingers and the thumb. In order to facilitate the slider's stroke on the two guides, two linear ball bearings have been implemented; their housings are visible in Figure 7.6(b). In the upper central part of the slider, a housing has been realized for a threaded element in order to join the screw. The differential mechanism is composed of three simple independent pulleys, separated by Teflon spacers, on which the three cables run. Each cable, fixed to a phalange of the index finger, runs around the differential mechanism to the respective phalange of the middle finger.

The differential mechanisms allow to control the movement of multiple degrees of freedom using only one actuator, and to branch the energy flux without the help of a dedicated electronic unit [36]. The differential mechanism used in the SPRING hand is based on compression springs and allows the adaptability between the index and middle finger. In this way, when the hand is grasping an object of irregular shape, (see Figure 7.7), the index and middle fingers can stop their flexion at different rotation angles in order to increase contact areas between fingers and object and to provide a stable grasp.

Commercial belt and pulleys have been used to transmit the motion from the actuator to the screw. This solution allows to compensate possible backlash between the screw and the motor axis, in addition, timing belt and pulleys are less noisy than other transmissions, such as spur gears. The guides are simple cylindrical elements that transform the rotational screw motion in the linear one of the slider

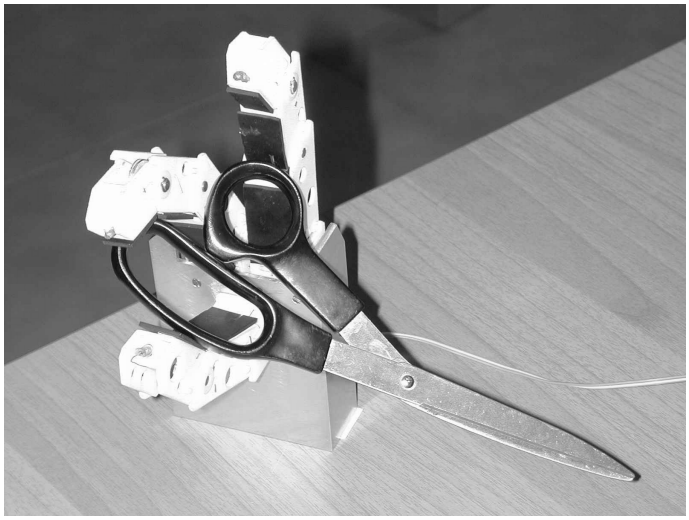

FIGURE 7.7: The differential mechanism used in the SPRING hand allows the adaptability between the index and middle finger

7.5 The control of the SPRING hand

The exchange of data between the user and the real world, according to the formal scheme presented in §4.3, is showed in Figure 7.8. In the next subsections the 4 control modules will be described in details.

In order to simplify the development and testing of the control algorithms, the TCM and LCM have been developed using LabView 6.1. The configuration of the analog inputs and of the digital outputs of the NI6025E for the control of the hand are shown in Table 7.3.

7.5.1 Top level Control Module - TCM

The control scheme for the RTR II hand is a direct derivation of the control scheme used for the RTR I hand. Two EMG electrodes (Delsys DE2.3) have been used to acquire two EMG signals from the user, in order to control the opening/closing of the hand and the thumb adduction/abduction. The first electrode is placed on the *extensor carpii radialis*, and the second on the *flexor carpii radialis*.

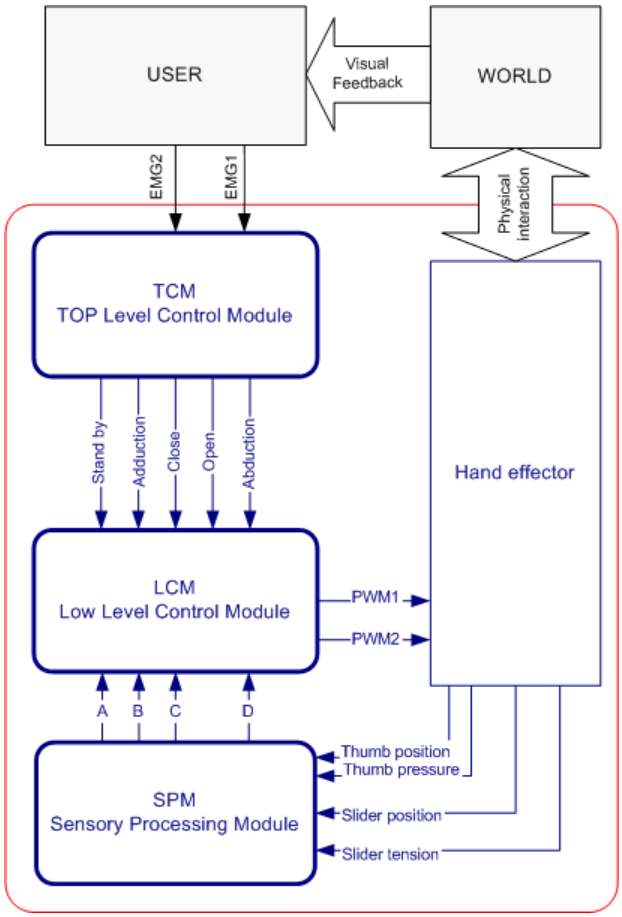

Figure 7.8: Schematic diagram of the exchange of data from the user to the real world and vice versa, passing through the prosthetic device.

7.5.1.1 Signal Processing

The two EMG signals are sampled at 1000 Hz (channels 0 and 1 of the National Instruments NI6025E acquisition board), and the variance of the EMG is extracted by using equation 5.5. A simple threshold classification has been chosen in order to detect the activation of the hand.

7.5.1.2 User training

A software for the training of the user has been developed by using LabVIEW. This software is directly derived from the software already used for the RTR 1 hand (Figure 5.13). By using this software, the user is trained to contract the *extensor carpii radialis* and *flexor*

Ch. #	type	Signal
0	A	EMG 1
1	A	EMG 2
2	A	-
3	A	-
4	A	-
5	A	-
6	A	-
7	A	-
8	A	R_{sens}
9	A	-
10	A	-
11	A	PWM
12	A	-
13	A	-
14	A	-
15	A	-

(a) Analog inputs

Channel #	Type	Signal
0	D	MOT 1 - Power
1	D	-
2	D	Direction
3	D	-
4	D	-
5	D	-
6	D	-
7	D	-
GPCTR0 OUT	Counter	PWM

(b) Digital outputs

TABLE 7.3: The configuration of the analog inputs and of the digital outputs of the NI6025E for the control of the RTR2 prosthetic hand.

carpii radialis, in order to generate the control signals. The visual representation of the EMG signal and its variance help the user to learn how to control the hand.

The training protocol is the same already described in §5.4.1.2.

7.5.2 Low level Control Module - LCM

The Low level Control Module receives as input the following signals:

- from the Top Level Control Module:
  - Stop;
  - Open the hand;
  - Close the hand;
  - Thumb abduction;
  - Thumb adduction.

- from the Sensory Processing Module:
  - Thumb angular position;
  - Slider position;
  - Thumb pressure;
  - Tension on the cable;
  - Mean current in the thumb motor;
  - Mean current in the slider motor.

These signals are used to control the behavior of the prosthetic hand according to the commands coming from the TCM.

The hand operates as follows (Figure 7.9):

- When the system is turned on, it goes in the **Stand By** state, waiting for any command coming from the TCM.
- Once a command is generated from the TCM, the LCM reads its internal state, and goes into **S0: wait**, in which the hand executes the command arrived from the TCM. As said before, the possible commands coming from the TCM are:

  hand opening: the hand opens until it receives a STOP command (i.e., no more commands) or it reaches the maximum extension (determined by the slider sensor). The speed of the movement depends on the amplitude of the OPEN command

  hand closing: the hand closes until it receives a STOP command (i.e., no more commands), or if it reaches the maximum flexion/extension, or if a contact with an object is detected. The speed of the movement depends on the amplitude of the CLOSE command.
  In case a contact is detected, the hand goes into the **Grasp state**, in which it grasp the object with a force determined by the amplitude of the CLOSE command.

  STOP: the STOP command is issued both by the user (if s/he wants to stop the current movement) or automatically by the LCM (in case the hand has reached the desired level of grasping force, or the end of the active stroke of the slider or of the thumb, or there is an obstacle).

- In case no commands arrive to the hand within $t_{\text{stand-by}}$ the hand goes to the **Stand by** state.

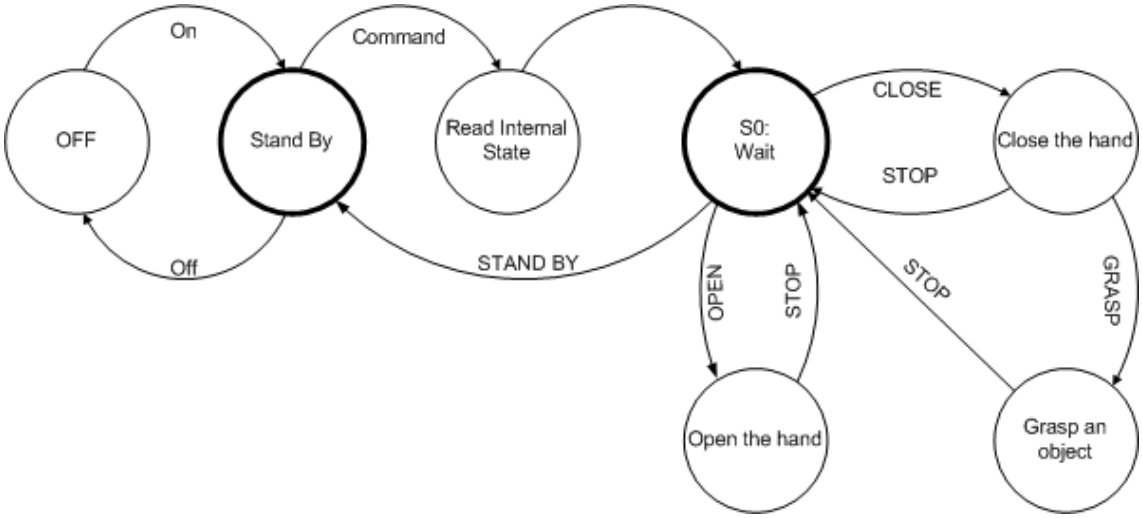

FIGURE 7.9: The control scheme for the SPRING prosthetic hand.

7.5.3 Sensory Processing Module - SPM

The hand sensory system is necessary to enable automatic control of grasping tasks without requiring special attention and efforts to the hand user. The SPRING hand is equipped with:

- Cable tensiometer;
- End of stroke sensor on the slider;
- Current limitation.

7.5.3.1 Cable Tensiometer

The slider of the transmission system has been sensorized to evaluate the global grasping force of the SPRING hand. Two strain gages have been mounted on the cantilevers where the differential mechanism is fixed. The two active gages are in the adjacent arms of a Wheatstone bridge in a half-bridge configuration. In this way a double output signal will be obtained and resistance changes, caused by thermal effects, will be compensated.

The sensorised slider has been designed according to the results of the stress and strain simulation obtained with a finite element method (software ANSYS 5.7). A calibration of the force sensor has been made with an external sensor, in order to correlate the real grasping force of the SPRING hand with the internal sensor output. The calibration has been performed with an INSTRON 4464 test machine with a static load cell working in the range of $\pm$ 1 KN. The tests have been performed in a quasi-static way, because the

speed of the load cell is $0.1mm/s$. The output data were acquired through a LabView PCI 6025E acquisition board.

Figure 7.10 shows the strain gages output (Volt) versus the applied load (Newton). The sensor output is linear in the whole operating range.

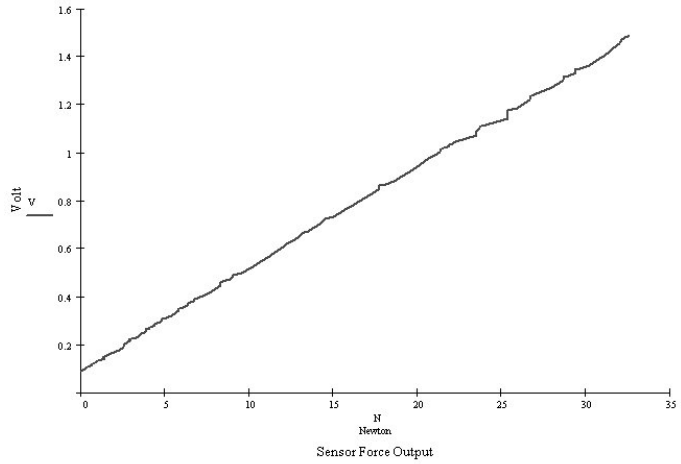

Figure 7.10: Data obtained during sensor calibration. Output voltage of the internal sensor versus force measured with an external sensor.

7.5.3.2 End of stroke sensor

A position sensor based on Hall effect sensors (Honeywell SS496A) has been designed and integrated in the hand prototype. This sensor is used to avoid any damage to the slider, preventing the hand to open over the maximum operating range.

7.5.3.3 Current limitations

A power resistance ($R_{sens} = 0.330\Omega$) is put in series with the motor in order to sense the mean current. This resistancesis used in order to limit the power consumption during active grasping or in case the movement of the hand is obstructed by an external obstacle. In particular, R_{sens} limits the maximum current in the slider motor to 1 A.

Once the hand has grasped the object, in fact, the unbackdrivable mechanism maintains the grasping force without requiring any additional power supply. In this way the charge of the batteries can be saved, thus increasing the number of active grasps that could be realized with a single charge.

7.5.4 Sensory Feedback Module - SFM

The SPRING hand has no explicit Sensory Feedback Module. As usual with current hand prostheses, the sensory feedback is given in an indirect form:

- visual feedback;
- proprioceptive sensation on the stump, due to the load of the grasped object;
- change of the sound of the motor during grasping.

7.6 Discussion

In order to obtain an acceptable and useful prosthetic hand the following main criteria must be addressed: grasping functionality, cosmetics and controllability. For this reason, an innovative design approach, aimed to enhance the ability of a prosthetic hand to perform a stable grasp with wide variety of objects, without augmenting the actuator power, has been followed.

A three fingered underactuated hand prosthesis, called the SPRING hand, has been investigated and developed in order to achieve good grasping functionality keeping a simple control. This has been achieved by exploiting an innovative design based on a differential mechanism inserted in the hand cable transmission. The hand mechanisms have been designed in order to obtain a natural flexion of the fingers, and a good flexing torque.

This hand presents some advantages respect to the state of the art of the hand prosthesis:

- the SPRING hand has 8 DoFs and only one motor that drives three polyarticulated fingers (index, medium and thumb). A differential mechanism allows the adaptability among the fingers and among the phalanges of each finger, thus enabling the grasp of irregular shaped objects;
- the ability of the SPRING hand to adapt to the shape of the grasped object allows to augment the number of contact points between the phalanges and the object, and, as a consequence, the contact areas;
- the control board and sensory processing board could be easily integrated within the palm;
- the movements of the hand are quite fast, in particular compared to the speed of the RTR2 hand. This makes the SPRING hand much more controllable by the user;
- the hand is very light, it weights less than 400 grams.

Anyhow, the SPRING hand still presents some drawbacks:

1. it's bigger than the human hand, and it does not fit inside a standard cosmetic glove;
2. the maximum grasping force ($5 \div 10N$, depending on the configuration of the hand) is not sufficient for ADLs.

Eight

Conclusions and future work

8.1 Conclusions

The replication of the human hand is a continuous challenge for scientists and engineers. During the last two decades several robotic and anthropomorphic hands has been developed. All these hands have a high number of DoFs (up to 16), and have a dexterity comparable to that of the human hand (§3.4.2). On the contrary, current commercial prosthetic hands, aimed at replicating the natural system, are unable to provide enough grasping functionality and to deliver sensory-motor information to the user [1, 15, 49]. Commercially available prosthetic devices (§3.3), such as Otto Bock SensorHand [70], as well as multifunctional hand designs (§3.4) are far from providing the manipulation capabilities of the human hand [17]. Moreover, they require a great deal of training and of concentration in order to be effectively used.

In the previous chapters three innovative prototypes of prosthetic hand, aimed at increasing the performance of hand prostheses, have been presented. A summary of the main characteristics of these hands is presented in Table 8.1. These hands has been developed starting from a detailed analysis of the state of the art of artificial hands in prosthetics and robotics (Chapter 3). By comparing the characteristics of these hands with the natural model, the human hand (Chapter 2), some important design goals has been defined (Chapter 4).

Two different approaches has been followed. The first prototype, called RTR1 hand (Chapter 5), is a three-fingered artificial hand that embeds 6 micromotors into the structure of the fingers, thus maintaining a dimension comparable to that of the human hand. The hand is also equipped with position and force sensors. The second artificial hand, called RTR2 hand (Chapter 6), exploits a different design approach, based on underactuated mechanisms. This hand has 3 fingers, 9 DoFs in total but just 2 DC motors, one for the thumb abduction/adduction and the other one for opening and closing the hand. The last hand prototype, named SPRING hand (Chapter 7), exploits the underactuation by using a different solution.

For all these three hands a common control scheme, based on EMG signal processing,

Hands	♯ of fingers	DOFs	Size/Human Hand Size	♯ of actuators	Weight [Kg]	Force [N]
RTR I	3	6	1	6	∼0.25	1 (tip)
RTR II	3	9	1.2	2	∼0.32	16
SPRING	3	8	1.2	1	∼0.4	10

Table 8.1: RTR Hands: analysis of the performance.

has been developed and applied, in order to understand if and how they could be used as hand prosthesis in clinical practice (§5.4, §6.4, and §7.5).

8.2 Future works

All these hands have their own advantages and drawbacks, but actually none of them could be used as a prosthesis in clinical practice, because of their performance and because of their dimension (§5.5, §6.5, and §7.6). Anyhow, the tests on these hands provided some useful guidelines for the future development of innovative and high performing artificial hands.

In particular, two different approaches could be devised (see also Figure 3.19). On the one hand, EMG-controlled prostheses could represent a "cheap" solution (i.e., low cost and non invasive) for the restoration (even if partial) of some hand functions. On the other hand, a multifunctional "cybernetic" hand prosthesis with ENG-based control will be a more sophisticated solution:

EMG-based hand prosthesis: In the last thirty years many research efforts have been carried out in the myoelectric control field. Several techniques have been developed in order to control multifunctional prosthetic devices, and many of them showed promising results. Moreover, these techniques could be also applied in other fields, not only in the control of myoelectric prostheses. For example, algorithms for the detection of the activation of the muscles are quite useful also in gait analysis [6]. However, despite of all these efforts, EMG signal analysis seems to be quite limited in the number of possible functions that could be restored by using a few electrodes. Moreover, the EMG signal cannot provide any feedback to the user [95].
A EMG-based hand prosthesis should posses a single active DoF, but the fingers could exploit the concept of the underactuation, thus realizing a more performing device.

ENG-based hand prosthesis: a possible solution to overcome the limits of the EMG-based approach could be the realization of an interface between the Peripheral Nervous System (PNS) and the artificial device (i.e., a "natural" Neural Interface (NI)) to record and stimulate the PNS in a selective way[21, 62, 74, 88]. Recent developments in the technology of electronic implants and in the understanding of nerve

> functions, in fact, have made it possible to fabricate selective neural interfaces that work by interchanging information between the nervous system and computerized artificial instruments. A biocompatible neural interface can restore some sensory feedback to the user by stimulating in an appropriate way her/his afferent nerves, and can allow the motor control of the prosthesis based on a "natural" ENG-based control. This will be possible by focusing appropriate research efforts on the technological development of the neural interface and on the characterization of the PNS afferent signals in response to mechanical and proprioceptive stimuli. When the patient receives sensory feedback from the stimulation of her/his afferent nerves, and the prosthetic device is controlled directly through the efferent nerves, she/he will be able to "feel" again the hand as part of her/his body.

It is worth noting that this situation is already present in the field of neuroprostheses, where we can find the "non invasive" solution, e.g., the Handmaster system[91] (which comprises a hand-forearm orthosis containing an array of electrodes, connected to a portable electronic microprocessor-controlled unit, and which is designed for simple and independent positioning by the patient), and the "invasive" solution, e.g., the Freehand system[83] (which consists of a pacemaker-like stimulator implanted in the chest, that sends electrical impulses from an external control/power source through lead wires to 8 electrodes implanted in the muscles of the forearm and hand).

Some projects that will exploit these two roads will be presented in the next subsections.

8.2.1 RTR4 prosthetic hand

The current state of the art of micro DC motor does not allow sufficiently small gearhead-motors and transmissions able to provide adequate torque or stall torque in actuators. By augmenting the number of active motors, the complexity of the control and of the sensor equipments increases. Thus, more components mean more cost, more maintenance charges, more assembling charges, more backlash and less reliability. Moreover, the unbackdrivable transmissions reduce the system efficiency.

A new design approach, based on compliant materials and joints, is currently being investigated for the realization of a truly prosthetic device. The design concept of this new hand, called RTR4, is showed in Figure 8.1.

This new hand will be a modification of the Ottobock prosthetic hand. The fingers of the Ottobock hand will be substituted by compliant fingers, made by carbon fiber or silicone. One DC actuator, located in the palm, will command three active and two passive fingers. In total, the three active fingers will have 8 DoFs, not all of them are directly drivable in under-actuation concept.

The control scheme will be the same already developed for the RTR1 and for the SPRING hands (§5.4 and §7.5, respectively). The user will be able to control the opening and closing of the hand in a natural and simple way, while the hands will adapt automatically to the shape of the grasped object.

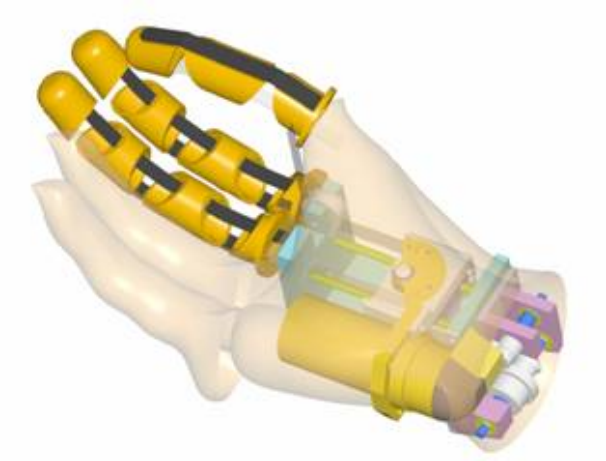

Figure 8.1: Design concept of the RTR4 prosthetic hand.

8.2.2 The PALOMA hand and the CYBERHAND Prosthesis

The design concept developed with the RTR2 hand will be exploited for the realization of two hands, called respectively PALOMA [71] and CYBERHAND [19]. A schematic picture of the PALOMA hand, mounted on the Dexter arm, is showed in Figure 8.2(a), and the design concept of the CYBERHAND prosthesis is shown in Figure 8.2(b).

Both projects will share the same hand, that will try to mimic as much as possible the natural hand, in terms of performance but moreover in terms of sensors. The hand will have:

- 10 DoFs total, but 4 degrees of motion (DoMs) in total;
- Underactuated fingers, each driven by a single cable actuated by a motor;
- 4 DoMs, one for each finger (flexion/extension) + one for thumb positioning (adduction/abduction);
- 9 Hall effect sensors, one for each finger joint;
- 4 DC 6V motors, and Encoders;
- 3 Force Tension cable/tendon sensors;
- 3 components force sensors based on strain gages integrated in the fingertips;
- Distributed on/off contact sensors: 44 sensitive areas for each finger (21 on the distal phalange, 11 on the intermediate phalange, 12 on the proximal phalange), 10 sensitive areas on the palm, and 4 sensitive areas on the dorsum.

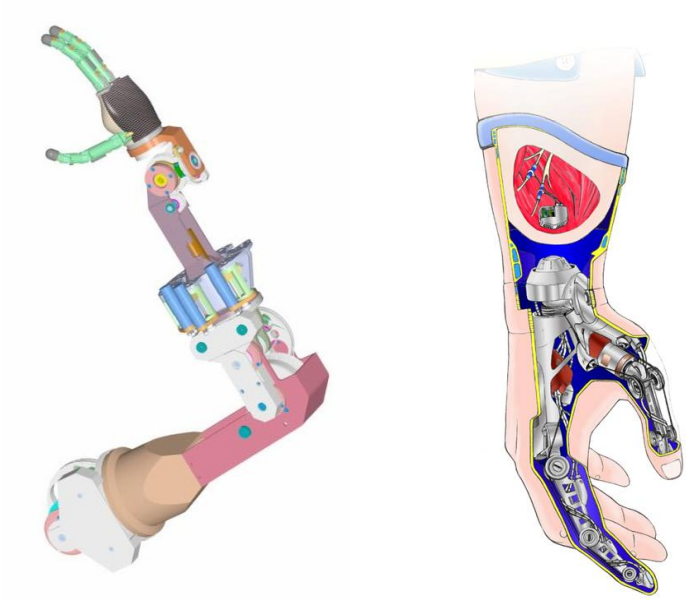

(a) The PALOMA hand mounted on the Dexter arm.

(b) the CYBERHAND prosthesis.

FIGURE 8.2: Future work: the PALOMA hand and the CYBERHAND Prosthesis.

The PALOMA project aims at the development of a human-like robotic manipulation platform for implementing neuro-physiological models of sensory-motor coordination in human grasping. The proposed robotic system originates from requirements imposed by neurophysiological knowledge about the corresponding human system. Hence, it is composed of sensors and actuators replicating some level of anthropomorphism, in the physical structure and/or in the functionality. Software modules implement human-like basic mechanisms of perception and learning, on which more complex architectures are developed. The system is integrated so as to be as modular as possible and to be re-arranged for validating different hypotheses [20].

The CYBERHAND project, instead, aims at increasing the basic knowledge of neural regeneration, and sensory-motor control of the hand in humans and to exploit this knowledge to develop a new kind of hand prosthesis which will overcome some of the drawbacks of current systems. This new prosthesis will:

1. be felt by an amputee as the lost natural limb delivering her/him a natural sensory feedback by means of the stimulation of some specific afferent nerves;

2. be controlled in a very natural way by processing the efferent neural signals coming from the central nervous system (reducing the discomfort of the current EMG-based control prosthesis).

Bibliography

[1] P.J. Agnew. Functional effectiveness of a myoelectric prosthesis compared with a functional split hook prosthesis: A single subject experiment. *Prost. & Orth. Int.*, 5: 92–96, 1981.

[2] S.-E. Baek, S.-H. Lee, and J.-H. Chang. Design and control of a robotic finger for prosthetic hands. In *Proc. Int. Conf. Intelligent Robots and Systems, IROS '99*, pages 113–117, Kyongjou, Korea, October 17–21 1999.

[3] S. J. Bartholet. Reconfigurable end effector, 198x. US patent #5108140.

[4] G. A. Bekey, R. Tomovic, and I. Zeljkovic. *Control Architecture for the Belgrade/USC Hand*. Dextrous Robot Hands. SpringerVerlag,, NY, 1990.

[5] G.A. Bekey, Huan Liu, R. Tomovic, and W.J. Karplus. Knowledge-based control of grasping in robot hands using heuristics from human motor skills. *IEEE Transactions on Robotics and Automation*, 9(6):709–722, 1993.

[6] P. Bonato. Recent advancements in the analysis of dynamic EMG data. *IEEE Engineering and Medicine in Biology*, 20(6):29–32, 2001.

[7] J. Butterfaß M. Grebenstein, H. Liu, and G. Hirzinger. DLR-hand II: Next generation of a dextrous robot hand. In *ICRA International Conference on Robotics & Automation*, pages 109–114, Seoul, Korea, May 21-26 2001.

[8] M.C. Carrozza, B. Massa, P. Dario, R. Lazzarini, M. Zecca, S. Micera, and P. Pastacaldi. A two DOF finger for a biomechatronic artificial hand. *Technology & Health Care*, 10(2):77–89, 2002.

[9] M.C. Carrozza, B. Massa, S. Micera, R. Lazzarini, M. Zecca, and P. Dario. The development of a novel prosthetic hand — ongoing research and preliminary results. *IEEE/ASME Transaction on Mechatronics*, 7(2):108–114, June 2002.

[10] E.Y.S. Chao, K. An, W.P. Cooney III, and R.L. Linschied. *Biomechanics of the Hand*. World Scientific, 1989.

[11] D. S. Childress and R. F. Weir. Quantitative assessment of direct muscle attachment to act as a control input for externally powered prostheses. In *Proc. 8th World Congr. Int. Soc. Prosthetics Orthotics*, page 101, Melbourne, Australia, April 2–7 1995.

[12] W. Craelius, R. L. Abboudi, and N. A. Newby. Control of a muli-finger prosthetic hand. In *ICORR'99: Int Conf Rehab Rob*, pages 255–260, Stanford University, Stanford, California, USA, July 1-2 1999.

[13] J. D. Crisman. Robot arm end effector, 199x. US patent #5570920.

[14] J. D. Crisman, C. Kanojia, and I. Zeid. Graspar: A flexible, easily controllable robotic hand. *IEEE Robotics & Automation Magazine*, 3(2):32–38, 1996.

[15] M. E. Cupo and S. J. Sheredos. Clinical evaluation of a new, above elbow, body powered prosthetic arm: A final report. *J. Rehab. Res. Dev.*, 35:431–444, 1998.

[16] D. J. Curcie, J. A: Flint, and W. Craelius. Biomimetic finger control by filtering of distributed forelimb pressures. *IEEE Trans Neural Systems and Rehabilitation Engineering*, 9(1):69–75, 2001.

[17] M. R. Cutkosky. *Robotic Grasping and Fine Manipulation*. Kluwer Academic Publishers, Boston, 1985.

[18] M. R. Cutkosky. On grasp choice, grasp models, and the design of hands for manufacturing tasks. *IEEE Transactions on Robotics and Automation*, 5(3):269–279, 1989.

[19] CYBERHAND. Development of a cybernetic hand, 2001. IST-FET Project #2001-35094.

[20] P. Dario, C. Laschi, A. Menciassi, E. Guglielmelli, M. C. Carrozza, L. Zollo, G. Teti, L. Beccai, F. Vecchi, and S. Roccella. A human-like robotic manipulation system implementing human models of sensory-motor coordination. In *IARP 2002*, 2002.

[21] Paolo Dario, Paolo Garzella, Maurizio Toro, Silvestro Micera, Mani Alavi, Uwe Meyer, Elena Valderrama, Laura Sebastiani, Brunello Ghelarducci, Cristina Mazzoni, and Paolo Pastacaldi. Neural interfaces for regenerated nerve stimulation and recording. *IEEE Transactions on Rehabilitation Engineering*, 6(4):353–363, 1998.

[22] H. de Visser and J. L. Herder. Force directed design of a voluntary closing hand prosthesis. *Journal of Rehabilitation Research and Development*, 37(3):261–271, 2000.

[23] N. Dechev and S. Cleghorn, W.L.and Naumann. Multiple finger, passive adaptive grasp prosthetic hand. *Mechanism Machine Theory*, 36(10):1157–1173, 2001.

[24] J. A. Doeringer and N. Hogan. Performance of above elbow body-powered prostheses in visually guided unconstrained motion task. *IEEE Trans. Rehab. Eng.*, 42:621–631, 1995.

[25] D. Dorcas and R. N. Scott. A three state myoelectric control. *Med. Biol. Eng.*, 4: 367–372, 1966.

[26] R. Doshi, C. Yeh, and M. LeBlanc. The design and development of a gloveless endoskeletal prosthetic hand. *J. Rehab. Res. Dev.*, 35:388–395, 1998.

[27] K. Englehart, B. Hudgins, and P. A. Parker. A wavelet-based continuos classification scheme for multifunction myoelectric control. *IEEE Trans Biomed Eng*, 48(3):302–311, 2001.

[28] A. G. Erdman and G. N. Sandor. *Mechanism Design*. Prentice Hall International, Inc., 3rd edition, 1997.

[29] L. Eriksson, F. Sebelius, and C. Balkenius. Neural control of a virtual prosthesis. In L. Niklasson, L. Bodén, and T. Ziemke, editors, *ICANN 98, Perspectives in Neural Computing*. Skövde, Sweden, September 2-4 1998.

[30] K. A. Farry, I. D. Walker, and R. G. Baraniuk. Myoelectric teleoperation of a complex roboitic hand. *IEEE Trans Rob Autom*, 12(5):775–788, 1996.

[31] S. Fujii, D. Nishikawa, and H. Yoko. *Development of a Prosthetic Hand Using Adaptable Control Method for Human Characteristics*, volume 5, pages 360–376. IOS Press, Amsterdam, The Netherlands, 1998.

[32] O. Fukuda, T. Tsuji, A. Ohtsuka, and M. Kaneko. EMG-based human-robot interface for rehabilitation aid. In *Proc 1998 IEEE Int. Conf. Rob. Autom.*, pages 3492–3497, Leuven, Belgium, May 16-20 1998.

[33] C. M. Gosselin. Underactuated mechanical finger with return actuation, 199x. US patent #5762390.

[34] D. Graupe and W. K. Cline. Functional separation of EMG signals via ARMA identification methods for prosthesis control purposes. *IEEE Transactions on System, Man and Cybernetics*, 2:252–258, 1975.

[35] D. Graupe, J. Salahi, and K. H. Kohn. Multifunctional prosthesis and orthosis control via microcomputer identification of temporal pattern differences in single-site myoelectric signals. *J. Biomed. Eng*, 4:17–22, 1982.

[36] S. Hirose. Connected differential mechanism and its applications. In *Proceedings of the 1985 IEEE International Conference on Advanced Robotics*, pages 319–326, 1985.

[37] S. Hirose and Y. Umetami. The development of soft gripper for the versatile robot hand. *Mechanism and Machine Theory*, 13:351–359, 1977.

[38] Han-Pang Huang and Chung-Ying Chiang. DSP-based controller for a multi-degree prosthetic hand. In *IEEE ICRA 2000*, pages 1378–1383, San Francisco, CA, USA, April 24–28 2000.

[39] B. Hudgins, P. Parker, and R. N. Scott. A new strategy for multifunction myoelectric control. *IEEE Transaction on Biomedical Engineering*, 40:82–94, 1993.

[40] T. Iberall, G. Sukhatme, D. Beattie, and G. Bekey. Control philosophy and simulation of a robotic hand as a model for prosthetic hands. In *Proceedings of the 1993 IEEE/RSJ International Conference on Intelligent Robots and Systems, IROS '93*, pages 824–831, 26–30 Jul 1993.

[41] E. R. Kandel, J. H. Schwartz, and T. M. Jessel. *Principles of Neural Science*. McGraw Hill, New York, USA, 4$^{\text{th}}$ edition, 2000.

[42] M. Kaneko, T. Shirai, K. Harada, and T. Tsuji. Analysis on detaching assist motion (DAM). In *IEEE Conf. On Robotics and Automation*, pages 3028–.3033, 2001.

[43] I. A. Kapandji. *The Physiology of the Joints. Volume One. Upper Limb.* Churchill Livingstone, Edinburgh, 1982.

[44] M. F. Kelly, P. A. Parker, and R. N. Scott. Myoelectric signal analysis using neural networks. *IEEE Eng Med Biol*, 9(1):61–64, 1990.

[45] L.P.J. Kenney, I. Lisitsa, P. Bowker, G.H. Heath, and D. Howard. Dimensional change in muscle as a control signal for powered upper limb prostheses: A pilot study. *Medical Engineering & Physics*, 21:589–597, 1999.

[46] T. Kuiken. Neuromuscular reorganization to improve the control of myoelectric prostheses. In *9^{ht} World Congress of the International Society for Prosthetics and Orthotics (ISPO)*, Amsterdam, The Nederlands, 1998.

[47] P. J. Kyberd and M. Evans. Intelligent control of a prosthetic hand. In *4th European Conference for the Advancement of Assistive Technology AAATE'97*, Thessaloniki, Greece, September 29 - October 2 1997.

[48] P. J. Kyberd, M. Evans, and S. Winkel. An intelligent anthropomorphic hand, with automatic grasp. *Robotica*, 16:531–536, 1998.

[49] P. J. Kyberd, O. E. Holland, P. H. Chappel, S. Smith, R. Tregidgoi, P. J. Bagwell, and M. Snaith. MARCUS: A two degree of freedom hand prosthesis with hierarchical grip control. *IEEE Trans Rehab Eng*, 3(1):70–76, 1995.

[50] T. Laliberté and C. M. Gosselin. Simulation and design of underactuated mechanical hands. *Mechanism and Machine Theory*, 33(1):39–57, 1998.

[51] M. P. LaPlante and D. Carlson. *Disability Statistics Report*, chapter Disability in the United States: Prevalence and Causes. National Institute on Disability and Rehabilitation Research, 7 edition, 1996.

[52] C. M. Light and P. H. Chappell. The development of an advanced multi-axis myoprosthesis and controller. In *MEC99*, pages 70–76, 1999.

[53] C. M. Light and P. H. Chappell. Development of a lightweight and adaptable multpleaxis hand prosthesis. *Medical Engineering & Physics*, 22:679–684, 2000.

[54] Li-Ren Lin and Han-Pang Huang. Mechanism design of a new multifingered robot hand. In *IEEE IEEE International Conference on Robotics and Automation*, pages 1471–1476, Minneapolis, MN, USA, April 22–28 1996.

[55] C. S. Lovchik and M. A. Diftler. The robonaut hand: A dexterous robot hand for space. In *IEEE International Conference on Robotics & Automation*, pages 907–912, Detroit, Michigan, May 10-15 1999.

[56] G. Lundborg, B. Rosén, and S. Lindberg. Hearing as substitution for sensation: A new principle for artificial sensibility. *Journal of Hand Surgery [Am]*, 24(2):219–224, 1999.

[57] G. Lundborg, B. Rosén, K. Lindström, and S. Lindberg. Artificial sensibility based on the use of piezoresistive sensors. *Journal of Hand Surgery [Br]*, 23B(5):620–626, 1998.

[58] M.T. Mason and J.K. Salisbury. *Robot Hands and the Mechanics of Manipulation*. MIT Press, Cambridge, MA, USA, 1985.

[59] B. Massa, S. Roccella, M. C. Carrozza, and P. Dario. Design and development of an underactuated prosthetic hand. In *International Conference on Robotics and Automation ICRA 2002*, pages 3374–3379. IEEE, Washington D.C., USA, May 11–15 2002.

[60] R. H. Meier and D. J. Atkins. *Comprehensive Management of the Upper Limb Amputee*. Springer-Verlag, New York, 1989.

[61] S. Montambault and C. M. Gosselin. Analysis of underactuated mechanical grippers. *ASME Journal of Mechanical Design*, to be published.

[62] L. Montelius, F. Sebelius, L. Erikssson, H. Holmberg, J. Shouenbourg, N. Danielsen, L. Wallman, T. Laurell, and C. Balkenius. Pattern recognition of nerve signals using an artificial neural network. In *Proceedings of the 18th Annual International Conference of the IEEE Engineering in Medicine and Biology Society*, pages 1502–1503, Amsterdam, Netherlands, October 31- November 3 1996.

[63] S. Morita, T. Kondo, and K. Ito. Estimation of forearm movement from EMG signal and application to prosthetic hand control. In *IEEE ICRA*, pages 3692–3697, Seoul, South Korea, May 21–26 2001.

[64] J. F. Mullen. Mechanical hand, 199x. US patent #3694021.

[65] K. Nagai, Y. Eto, D. Asai, and M. Yazaki. Development of a three-fingered robotic hand-wrist for compliant motion. In *Proc. Int. Conf. Intelligent Robots and Systems, IROS 1998*, pages 476–481, Victoria B.C., Canada, October 13–17 1998.

[66] National Amputee Statistical Database (NASDAB). Amputee Statistical Database for the United Kingdom, 1999/00. Document found at `http://www.show.scot.nhs.uk/isd/amputee/`.

[67] D. Nishikawa, Y. Ishikawa, W. Yu, M. Maruishi, I. Watanabe, H. Yokoi, Y. Mano, and Y. Kakazu. On-line learning based EMG prosthetic hand. In *Electrophysiology and Kinesiology*, pages 575–580, 2000.

[68] D. Nishikawa, W. Yu, H. Yokoi, and Y. Kakazu. Analyzing and discriminatin EMG signals using wavelet transform and real-time learning method. In *Artificial Neural Networks In Engineering Conference (ANNIE'99)*, pages 281–286, St.Louis, USA, November 7–10 1999.

[69] D. Nishikawa, W. Yu, H. Yokoi, and Y. Kakazu. EMG prosthetic hand controller discriminating ten motions using real-time learning method. In *IEEE IROS '99*, pages 1592–1597, Kyongju, South Korea, October 17–21 1999.

[70] Otto Bock HealthCare GmbH. *http://www.ottobock.com*. Duderstadt (DE), 2002.

[71] PALOMA. Progressive and Adaptive Learning for Object MAnipulation: a biologically inspired multinetwork architecture, 2001. IST-FET Project ♯2001-33073.

[72] D.T.V. Pawlock and R.D.Howe. Dynamic contact of the human fingerpad against a flat surface. *ASME J Biomech Eng*, 121:605–611, 1999.

[73] R. Reiter. Eine neue elecktrokunsthand. *Grenzgebiete der Medizin*, 4:183, 1948.

[74] R. R. Riso. Strategies for providing upper extremity amputees with tactile and hand position feedback - moving closer the bionic arm. *Technology and Health Care*, 7(6): 401–409, 1999.

[75] M. E. Rosheim. *Robot Evolution – The Development of Anthrorobotics*. John Wiley & Sons Inc., 1994.

[76] F. Routhier, D. Rancourt, and C. M. Gosselin. Design of a hand prosthesis based on kinematic principles. In *Proceedings of the Myoelectric Controls Powered Prosthesis Symposium*, pages 53–56, Fredericton, NB, 1995.

[77] G. N. Saridis and T. P. Gootee. EMG pattern analysis and classification for a prosthetic arm. *IEEE Trans Biomed Eng*, 29(6):403–412, 1982.

[78] S. Schulz, C. Pylatiuk, and G. Bretthauer. A new ultralight antropomorphic hand. In *IEEE Conf. On Robotics and Automation ICRA 2001*, pages 2437–2441, Seoul, South Korea, May 21-26 2001.

[79] R. N. Scott and P. A. Parker. Myoelectric prostheses: State of the art. *Journal of Medical Engineering & Technology*, 12(4):143–151, 1988.

[80] MICRO SWITCH Sensing and Control. *Hall Effect Sensing and Application*. Honeywell Inc., West Spring Street, Freeport, Illinois 61032, 2003. `http://www.honeywell.com/sensing`.

[81] D. H. Silcox, M. D. Rooks, R. R. Vogel, and L. L. Fleming. Myoelectric prostheses. *J. Bone & Joint Surg.*, 75:1781–89, 1993.

[82] D. C. Simpson. The choice of control system for multimovement prostheses: Extended physiological proprioception (EPP). In P. Herberts *et al.*, editor, *The Control of Upper-Extremity Prostheses and Orthoses*, 1975.

[83] B. Smith, Z. Tang, M.W.J.S. Pourmehdi, M.M. Gazdik, J.R. Buckett, and P.H. Peckham. An externally powered, multichannel, implantable, stimulator-telemeter for control of paralyzed muscle. *IEEE Trans Biom Eng*, 45:463–175, 1998.

[84] T. H. Speeter. Primitive based control of the Utah/MIT dextrous hand. In *International Conference on Robotics & Automation*, pages 866–877, Sacramento, CA, USA, April 9-11 1991.

[85] W. T. Townsend. The barrett-hand grasper, programmably flexible part handling and assembly. *Industrial Robots*, 27(3):181–188, 2000.

[86] Raoul Tubiana. *The Hand*. W. B. Saunders Company, West Washington Square, Philadelphia, PA 19105, 1981.

[87] F. Vecchi, C. Freschi, S. Micera, A. M. Sabatini, and P. Dario. Experimental evaluation of two commercial force sensors for applications biomechanics and motor control. In *5th Annual Conference of the International Functional Electrical Stimulation Sociaty (IFESS 2000)*, Aalborg (DK), June 17–24, 2000 2000.

[88] P. H. Veltink. Sensory feedback in artificial control of human mobility. *Technology and Health Care*, 7(6):383–391, 1999.

[89] R. Vinet, Y. Lozac'h, N. Beaundry, and G. Drouin. Design methodology for a multifunctional hand prosthesis. *, J. Rehab. Res. Dev.*, 32:316–324, 1995.

[90] J. G. Webster. *Tactile Sensors for Robotics and Medicine*. John Wiley & Sons, New York, 1988.

[91] H. Weingarden, G. Zeilig, R. Heruti, Y. Shemesh, A. Ohry, A. Dar, D. Katz, R. Nathan, and A. Smith. Hybrid functional electrical stimulation orthosis system for the upper limb: Effects on spasticity in chronic stable hemiplegia. *Am J Phys Med Rehabil*, 77(4):276–281, 1998.

[92] R.F. Weir, C.W. Heckathorne, and D. S. Childress. Cineplasty as a control input for externally powered prosthetic components. *Journal of rehabilitation Research and Development*, 38(4):357–363, 2001.

[93] Walley T. Williams. One-muscle infant's myoelectric control. *Journal of the Association of Children's Prosthetic-Orthotic Clinics*, 24(2), 1989.

[94] W. Yu, H. Yokoi, Y. Kakazu, and D. Nishikawa. Electromiograohic (EMG) pattern recognition by reiforcement learning method for prosthetic arm control. In *ANNIE'97*, 1997.

[95] M. Zecca, S. Micera, M.C. Carrozza, and P. Dario. On the control of multifunctional prosthetic hands by processing the electromyographic signal. *Critical Reviews in Biomedical Engineering*, 2003 (accepted).